The Thesis Committee for Josiah Marie Sananda

Certifies that this is the approved version of the following Thesis:

Sr isotope and elemental variations in bald cypress tree rings as tracers of water composition through time in urban and rural streams

APPROVED BY

SUPERVISING COMMITTEE:

Jay Banner, Supervisor

Ashley Matheny

Jose Abella-Gutiérrez

Sr isotope and elemental variations in bald cypress tree rings as tracers of water composition through time in urban and rural streams

by

Josiah Marie Sananda

Thesis

Presented to the Faculty of the Graduate School of

The University of Texas at Austin

in Partial Fulfillment

of the Requirements

for the Degree of

Master of Science in Geological Sciences

The University of Texas at Austin

December 2023

Acknowledgements

I extend my gratitude to my mentors in the Department of Earth and Planetary Sciences- Jay Banner, Jose Abella-Gutiérrez, Staci Loewy, Aaron Satkoski, Ashley Matheny, and Nathan Miller. Their unwavering dedication and countless hours invested in my academic and scientific journey have been instrumental in propelling me toward realizing my full potential. In the face of seemingly insurmountable challenges, these mentors provided guidance that was essential to the successful completion of the research project.

Thanks to Bryan Black at the University of Arizona for his invaluable research guidance and for introducing me to the world of dendrochronology. Gratitude is also extended to the collaborative efforts of the students in the Banner Research Group, whose assistance in the field and lab significantly contributed to this project’s success. Thank you to Daniella Rempe and Bayani Cardenas of the Jackson School of Geosciences for also being fantastic mentors and giving me the opportunity to take my field skills to the next level with Hydro Field Camp.

I am eternally grateful to the lifelong friends I have made during my time at the Jackson School of Geosciences. I express deep appreciation to Jackie Epperson, Kayla White, Allysa Dallmann, Evan King, and Nicole Ferrie for their consistent, daily support. Their encouragement played a pivotal role in my successful journey. To my family, I am thankful for your limitless support, uplifting advice, guidance, and unconditional love.

Abstract

Sr isotope and elemental variations in bald cypress tree rings as tracers of water composition through time in urban and rural streams

Josiah Sananda, M.S. Geo. Sci.

The University of Texas at Austin, 2023

Supervisor: Jay Banner

As urbanization in Central Texas rapidly expands, municipal water leaking from infrastructure poses an increasing threat to water quality and potentially enhances climate resilience in riparian zones through more consistent baseflow. Strontium isotopes ($^{87}Sr/^{86}Sr$) are effective tracers of sources of dissolved ions in Central Texas streams, indicating a significant fraction of municipal water contributing to baseflow in urban streams. In the extensively urbanized Waller Creek, a significant municipal water contribution to streamflow is reflected in the stream's high $^{87}Sr/^{86}Sr$ values, while rural Onion Creek streamwater exhibits a relatively low $^{87}Sr/^{86}Sr$ signature. Tree ring chronologies from Waller and Onion Creeks reveal significant differences related to the input of municipal water, and suggest that trees from Waller Creek watershed may have recorded the changes that urbanization has induced in water quality. To track the history of infrastructure degradation and its impact on streamwater, we reconstruct a time series of water composition in two distinct watersheds using $^{87}Sr/^{86}Sr$ ratios in rings of riparian bald cypress trees. We identify contaminants introduced to tree cores through traditional methods of core preparation for

dendrochronology and optimize new methods to avoid contamination. Wood digestion methods are also optimized to yield high reproducibility of $^{87}Sr/^{86}Sr$. Bald cypress trees, dating back to the 1840s in Onion Creek and the 1940s in Waller Creek, record their environmental conditions, as reflected in the $^{87}Sr/^{86}Sr$ values of their rings. Results from this study demonstrate that bald cypress growth rings record $^{87}Sr/^{86}Sr$ values from the streamwater in which they grow. Based on the $^{87}Sr/^{86}Sr$ record in tree rings, we conclude that the water compositions of both Onion Creek and Waller Creek have remained largely unchanged over the lives of our sampled trees. This suggests that the extent to which urban infrastructure in Waller Creek has been degraded and has contributed to Waller Creek baseflow has been occurring since at least the 1940s.We constrain the effects of translocation to determine the precision of our dendrochemical record, concluding that translocation is not an important factor in the overall variability of the $^{87}Sr/^{86}Sr$ record through time.

Table of Contents

List of Tables

List of Figures

1. Introduction

As urbanization and population accelerate globally, a comprehensive understanding of the temporal dynamics of urban stream quality increases in importance. The United Nations (2018) World Urbanization Prospects reported that in 1930, approximately 30% of the world's population lived in urban areas. By 2018, this number had increased to 55%, and it is projected to continue rising to 68% by the year 2050 (United Nations, 2018). Understanding the evolving relationship between urban development and natural hydrologic systems is essential for the preservation of freshwater resources. Global climate change has resulted in heightened climatic extremes, which promote the urgency to increase the resiliency of freshwater resources to extreme weather conditions (Nielson-Gammon et al., 2020). Anthropogenic impacts on watersheds include alterations to the riparian zone, nutrient loading, degraded water quality over time, and flashy discharge during storms. This combination of hydrologic impacts has been termed "urban stream syndrome" (Paul and Meyer, 2001; Meyer et al., 2005; Walsh et al., 2005). The mechanisms that produce the symptoms of urban stream syndrome are often numerous and difficult to identify at a point source. Runoff, enhanced by increased impervious surface cover, is a large transporter of pollution into surface and groundwaters (Muller et al., 2020). Point sources altering surface water quality and quantity may be traced to irrigation and leakage from the age-related failure of infrastructure (Garcia-Fresca and Sharp 2005; Beal et al., 2020; Mauceri and Banner, 2023; Banner et al., 2024). Non-revenue water (NRW) describes the volume of water that is unaccounted for out of the total volume distributed to the city from water supply companies (tap water). This is water that was never charged to customers (Frauendorfer, 2010). Wastewater and NRW will together be referred to as "municipal water" hereafter. Municipal water escapes the infrastructure network by leakage and may enter streams, resulting in alterations to baseflow (Reynolds and Barrett, 2003; Tang et al., 2004; Pu et al., 2014; Banner et al., 2024). The addition of flow and nutrients through municipal water entering surface waters has been shown, in some cases, to increase stream resilience to drought and the productivity of vegetation (Banner et al., 2024; Hesse et al., 1998).

Dendrochemistry (i.e., the chemical analysis of tree rings) has been used to reconstruct time series of contamination events and environmental conditions across the world. Symeonides (1979) reconstructed the history of copper and lead pollution from a nearby smelting complex using tree rings. Kagawa et al. (2002) found abnormally high concentrations of ^{90}Sr in rings from 1945 in Hiroshima Japanese cedar and attributed it to nuclear fallout. $^{87}Sr/^{86}Sr$ signatures in tree rings have been used by English et al. (2001) to trace the origins of conifers used in prehistoric buildings, by Åberg et al. (1990) to reconstruct soil acidification in Sweden, and by Miller et al. (2014) to trace sources of dust over time in the Wasatch Mountains. Chloride concentrations in *Taxodium distichum* have aided in providing evidence for saltwater intrusion in North Carolina, where flood mitigation is now promoted (Yanosky et al., 1995). High concentrations of heavy metals in Louisiana bald cypress tree rings were successfully correlated with the commencement of petroleum refineries and dredging (Latimer et al., 1996). The mobilization of elements between tree rings, referred to as "translocation", is species-specific and crucial to understanding and interpreting dendrochemical data. Dendrochemical results in the form of temporal reconstructions of environmental conditions are often presented in the dendrochemistry literature without acknowledgment or investigation of translocation processes. For example, English et al. (2001) claim to use $^{87}Sr/^{86}Sr$ as a proxy due to its lack of mass fractionation or translocation in trees, but offer no analysis of or citation behind the claim. Åberg et al. (1990) equate the behavior of Ca and Sr in natural systems and use decreasing Ca concentrations in soils over time as evidence of soil impoverishment without mention of translocation processes. Miller et al. (2014) discount the translocation of strontium in spruce trees based on a literature review including Legge et al. (1984)'s argument that conifers record environmental signals more accurately than hardwood and Rediske and Selders (1953)'s analysis of kidney bean plants. The presentation of dendrochemisty results without addressing the evidence for or against translocation processes is an oversight that should be addressed.

There are studies that justify dendrochemistry results with an analysis of translocation. For example, Symeonides (1979) reported data to show evidence for lateral translocation of zinc and cadmium through their studied trees, but not for copper or lead. Kagawa et al. (2002) found significant concentrations of ^{137}Cs in rings formed before the Hiroshima atomic bomb, indicating lateral translocation of the element. However, Strontium-90 was, as expected, at its highest levels in 1945, the year the bomb was dropped. Kagawa et al. (2002) refer to Sr as relatively immobile when compared with Cs. Padilla and Anderson (2002) argue that element mobility in trees is confined to the active xylem, which the study presents as "the last 1-7" years. However, the number of active sapwood rings in a tree is dependent on a multitude of factors, both genetic and environmental, and the range is at least as wide as 1 to 50 annual rings (Miles, 2013).

Texas is projected to experience a population increase of 73% between 2020 and 2070, totaling 51.5 million residents (TWDB, 2022). The Central Texas region is expected to receive the bulk of this influx, bringing with it impending rapid land use change, primarily within and around cities. Understanding the mechanisms contributing to hydrologic systems in this region has the potential to help advance sustainable development. Significant financial and political focus is placed on the development of new infrastructure and urban expansion. Maintenance and replacement of already existing infrastructure are not included in the state water plan and are often overlooked (TWDB, 2022), even though water-related infrastructure, including wastewater treatment plants, were developed starting in the early 1920s. Central Texas faces a heightened risk of drought and flooding, a challenge that is expected to intensify with the impacts of climate change (TWDB, 2022; Nielson-Gammon, et al., 2020). This problem will be further compounded as the region experiences a population surge, leading to increased water demand, while freshwater availability decreases.

In Austin-area watersheds, municipal water has been determined to compose up to 90% of baseflow at times (Beal et al., 2020). Studies describe the mechanisms by which municipal water enters and interacts with hydrologic systems, but these studies are limited in terms of duration and sample frequency (Christian et al., 2011; Senison et al., 2013; DeMott, 2006; Reynolds and Barrett, 2003; Pu et al., 2014; Beal et al., 2020; Manlove, 2020). Developing a historical record of streamwater quality is essential for pinpointing the timing and magnitude of any deviations from natural hydrologic patterns. Having such a timeline of impacts on water composition can serve a crucial role in guiding policy decisions and generating public interest in the preservation of local freshwater quality. Additionally, a temporal reconstruction of water chemistry can enhance the understanding of geochemical evolution processes and mechanisms of the hydrologic system. This would help to inform future research in hydrologic sciences and guide solutions to urban water quality problems potentially not yet identified by modern studies. Here we seek to extend the historical record of streamwater composition beyond that established by water sampling and analysis over the past 22 years within two central Texas watersheds using elemental concentrations and isotopic compositions found within tree rings.

This study focuses on two endmember watersheds in the Austin, Texas area: Waller Creek and Onion Creek. Variation in land use within these watersheds serves as endmembers with respect to impervious surface cover, population density, and urbanization extent (Fig. 1; Table 1). Their respective streamwaters are geochemical endmembers based on their distinct elemental and isotopic ($^{87}Sr/^{86}Sr$) compositions. In this study, trace element and $^{87}Sr/^{86}Sr$ data for stream water, municipal water, soils, bedrock, and tree rings are assessed to determine the historic to present interactions between municipal water and the hydrologic system. Strontium (Sr) isotopes (expressed as the $^{87}Sr/^{86}Sr$ ratio) have been used as tracers of sources of dissolved ions in waters (Musgrove and Banner, 2004; Banner et al., 1994; Christian et al., 2011; Beal et al., 2020; DeMott et al., 2006; Mauceri and Banner, 2023). This isotopic tracer is made possible by the distinct high and low $^{87}Sr/^{86}Sr$ signatures of municipal water and carbonate-influenced "natural" waters in the region, respectively. Christian et al. (2011) found that streamwater from eight Austin-area watersheds had $^{87}Sr/^{86}Sr$ ratios that strongly correlated with the watersheds' population densities ($R^2 = 0.93$) (Christian et al., 2011; Beal et al., 2020; Fig. 2). Trace element concentrations, element ratios, and $^{87}Sr/^{86}Sr$ ratios in streamwaters have been used to understand geochemical mixing between bedrock, soils, wastewater, and municipal sources (Beal et al., 2020; Christian et al., 2011, Mauceri and Banner, 2023). Anthropogenically-derived trace elements found in streamwaters come from nutrients in fertilizers and wastewater, and environmental contaminants such as heavy metals. In the present study, trace element concentrations are analyzed in trees and streamwaters to 1) aid $^{87}Sr/^{86}Sr$ data in determining the ability of bald cypress trees to record the chemistry of their environments through time, and 2) determine variation within and between trees in Waller and Onion Creek watersheds.

Bald cypress (*Taxodium distichum*) is a species that often grows along streams, sometimes with its root system fully submerged. This species has been used to reconstruct climatic conditions across the southeastern U.S., where they can be found growing in wetlands, lowlands, and riparian zones (Cleaveland et al., 2011; Stahle and Cleaveland, 1992; Stahle et al., 1988, 1998, 2019; Little, 1971). This species grows naturally along the banks of Onion Creek where individual trees have been dated back to 1840. Bald cypress trees were planted along Waller Creek in the 1930s to enhance campus aesthetic and work alongside a series of weirs in Waller Creek toward flood mitigation and reduction of bank erosion. 71 bald cypress trees span the mile of Waller Creek running through the University of Texas at Austin campus. Many of these trees are offspring of their parent trees, which were transplanted from a local nursery (UT-Austin, 2022). Ring widths and chronologies of bald cypress growing in the riparian zones of Waller and Onion Creeks highlight the positive unintended impacts of municipal input (or lack thereof) in these streams (Banner et al., 2024). Waller Creek tree ring growth histories lack the strong climate correlation that is present in the ring growth histories of trees in Onion Creek ($p < 0.01$) (Banner et al., 2024; Fig. 3). This indicates that flow is at least partially maintained via infrastructure leakage and/or irrigation run-off to streams, allowing vegetation to continue growing and buffering the impacts of drought (Banner et al., 2024).

This study presents a novel approach to using $^{87}Sr/^{86}Sr$ signatures and trace element concentrations in bald cypress tree rings as indicators of water quality in urban streams within the Austin area. Our hypothesis posits that these trees' annual rings will preserve the $^{87}Sr/^{86}Sr$ ratio and elemental composition of the streamwater such that a temporal record of streamwater quality may be constructed. The success of this method depends upon the assumptions that 1) the selected trees primarily rely on streamwater for their water supply, and 2) translocation of the ions of interest is either negligible or quantifiable. We seek to (1) determine the extent to which bald cypress trees chemically reflect their hydrogeologic setting, (2) assess the preservation or translocation of elements within and between growth rings, and (3) determine the utility of bald cypress trees in reconstructing time series of historical water quality.

2. Study Area

2.1. Regional and spatial setting

Waller Creek and Onion Creek watersheds lie at opposite ends of Austin's urbanization spectrum. The Waller Creek watershed, which is the urban endmember in this study, runs from north to south and is covered by approximately 60% impervious surface (Table 1). The catchment area (15 km^2) for this stream runs through the University of Texas campus and into the Colorado River in the heart of downtown Austin (Fig. 1). The congestion and development both in and around Waller Creek's fragile riparian zone have led to critical water quality and riparian ecological issues for this stream. Waller Creek streamwater is significantly influenced by municipal water input, runoff, and irrigation, and its flow is often maintained during drought conditions (Manlove, 2020; Mauceri and Banner, 2023; Banner et al., 2024). The Onion Creek watershed, while significantly larger (547 km^2), contains only about 10% impervious surface cover and is largely undeveloped (Table 1). Onion Creek flows west to east and is often dry during peak drought conditions. Development within the watershed is concentrated around two main municipalities: Driftwood and Buda, and the Austin-Bergstrom International Airport. Slaughter Creek and Bear Creek are tributaries that join with Onion Creek at approximately 7 km and 15 km upstream of our sampled tree stands, respectively. Slaughter Creek watershed contained about 19.4% impervious cover as of 2013 and Bear Creek contained about 8.2% (AustinTexas.gov, 2017). Streamwater from these creeks has potentially impacted the chemistry of trees and streamwaters of Onion Creek watershed. The majority of Onion Creek runs through the northern half of Hays County, which is within the reaches of the Lower Colorado River Authority water distribution plan (LCRA, 2022). Thus, urban development in the Onion Creek watershed also relies primarily on the Colorado River as its source of municipal water, with some groundwater contribution from the Edwards and Trinity aquifers.

2.2. Hydrogeologic setting

In addition to the anthropogenic processes altering our study watersheds, the underlying bedrock may influence the chemical compositions of streamwaters, soils, and trees. The Onion Creek and Waller Creek watersheds are largely composed of Lower Cretaceous marine carbonates, which interact with streamwaters through dissolution and recrystallization processes (Beal et al., 2020; Manlove, 2020). Waller Creek discharges from and primarily flows over the Lower Cretaceous Austin Chalk. The bedrock of this watershed also has small contributions of Quaternary gravel deposits formed from previous channel deposits of the Colorado River (Fig. 4; Young, 1977). The Austin Chalk, a biomicritic chalk composed mostly of coccoliths (Pearson, 2012), is characterized by extensive fractures (7,100 – 286,000 mD; Stowell, 2000) and low matrix permeability (0.03 – 1.27 mD; Hovorka, 1998). Waller Creek flows through the second-oldest member of the Austin Chalk, the Vinson, starting at 47th Street until it merges with the Colorado River. All Waller Creek trees selected for this study grow within this Vinson Member (Fig. 4). Samples from the Austin Chalk, collected from the Shoal Creek and the Waller Creek watersheds (n = 7), had an average $^{87}Sr/^{86}Sr$ ratio of 0.70741 and a standard deviation of ($\pm$0.00001 SD) (Christian et al., 2011; Manlove, 2020, Beal et al., 2020). Fractionation of the $^{87}Sr/^{86}Sr$ ratio is negligible during mineral precipitation and other geologic and biological processes (Graustein, 1989).

Similarly to Waller Creek, the Onion Creek watershed is dominated by Lower Cretaceous carbonates, with the creek's baseflow sustained by springs discharging from the Trinity Aquifer (Hunt et al., 2016). Onion Creek flows through the Lower Cretaceous Glen Rose Limestone in the western portion of the watershed and moves east into the Edwards Limestone where its flow recharges the Edwards aquifer (Hunt et al., 2016). Just upstream of the city of Buda, the underlying bedrock stratigraphy becomes increasingly younger (within the Lower Cretaceous). Downstream of Buda, the bedrock is dominated by the Ozan Formation and Terrace deposits (Fig. 4). Most of the Onion Creek trees analyzed in this study (n = 11 out of 16) are within McKinney Falls State Park, where Onion Creek flows over the McKown Formation, a calcarenitic limestone facies of the Austin Chalk (Young, 1977). Limestone (n = 6) and dolomite (n = 1) samples collected from the Onion Creek watershed contained an average $^{87}Sr/^{86}Sr$ ratio of 0.70772 with a standard deviation of ($\pm$0.00026 SD) (Christian et al., 2011). Other Onion Creek watershed trees used in this study were approximately 3.4 km upstream of McKinney Falls State Park where sand, silt, clay, and gravel Terrace deposits dominate the bedrock (United States Geological Survey, 1993).

The Colorado River, the source of Austin's municipal water for the recorded history of the city, is influenced by the relatively high $^{87}Sr/^{86}Sr$ signature that is characteristic of the age, mineralogy, and Rb/Sr ratio of its underlying silicates upstream of Austin (Harrington and Herczeg, 2003). The high $^{87}Sr/^{86}Sr$ ratio of Austin's municipal water assists in water source tracing as it differs significantly from the carbonate bedrock units in Austin watersheds that display $^{87}Sr/^{86}Sr$ values that reflect lower Cretaceous seawater (mean seawater = 0.7076; Christian et al., 2011; Musgrove and Banner, 2004). These marine carbonate bedrock units influence the $^{87}Sr/^{86}Sr$ signature of soils and stream waters found in Austin watersheds. Manlove (2020) and Beal et al. (2020) used water-rock interaction models applied to $^{87}Sr/^{86}Sr$ vs Sr/Ca and streamwater data to examine the dissolution and recrystallization processes of carbonate rocks within Austin-area watersheds. The low matrix permeability Austin Chalk of

Waller Creek was inferred to host municipal or natural water for a relatively short time compared to the higher-permeability Glen Rose and Edwards limestones of Onion Creek. This can account for the relatively limited geochemical evolution of Waller Creek waters, via calcite dissolution compared with waters from Onion Creek that appear to have evolved via carbonate mineral recrystallization (Manlove, 2020; Beal et al., 2020).

3. Methods

3.1. Sample collection and core preparation for geochemical analysis

Streamwater samples (*n* = 54) were collected bimonthly from two streams, Waller Creek and Onion Creek, over a two-year period from 2021 to 2023. This monitoring continues a historical record of water quality at these sample sites dating back to 2001. In total, seven sites along Waller Creek and four sites along Onion Creek were selected for monitoring, to produce a representative spatial distribution within the watersheds that encompassed the range of tree stands selected for this study. Streamwater samples were collected under baseflow conditions, following protocols outlined by the United States Geological Survey (USGS, 2016). A minimum of five days was required to pass after a rain event before obtaining a baseflow sample. Precleaned HDPE Nalgene bottles were used for sample collection. Samples were filtered from the collection bottle into precleaned 15 ml bottles for anion analysis (using 0.22-micron syringe filters to exclude microbial contaminants) and acid-cleaned bottles for cation and $^{87}Sr/^{86}Sr$ analysis (using 0.45-micron syringe filters). Syringes and filters used for cation and Sr isotope samples were acid-cleaned, while those used for anion analyses were only purged with sample water prior to sample capture. Filtered to unfiltered sample comparisons for major cation concentrations (*n* = 9) show that 90% of the samples are within a 5% difference, and all analyses are within 14% (Table 2). Three filtered samples from April 2022 were omitted from all datasets due to their anomalously high concentrations (>500 ppb) of boron, aluminum, barium, and zinc. This apparently resulted from contamination via 0.45-micron syringe filters when a cleaning step was overlooked. Samples designated for cation and $^{87}Sr/^{86}Sr$ isotopes were all acidified to a 1% concentration of HNO_3 using ultrapure concentrated HNO_3 before analysis or storage.

Bald cypress tree stands were selected within each watershed based on tree abundance, accessibility, and size. Within each stand, individual trees were carefully selected, considering factors such as their overall health, estimated age (measured, for instance, by circumference), the presence of a significant portion of their roots extending into the streambed, and minimal buttressing. In 2018, 21 bald cypress trees from Waller Creek and 16 from Onion Creek were cored for this project. When possible, two or more cores were extracted from the same tree, 180 degrees apart, on the stream side and the bank side of the tree. Multiple cores were taken from 9 of the Onion Creek trees and 19 of the Waller Creek trees. Cores were extracted at breast height (~1.37m) using both 18-inch and 39-inch Haglof increment borers. Plastic straws were used to transport the cores from the field. Cores were mounted with adhesive, sanded, and polished, following standard practice in preparation for dendrochronology (Cook and Kairiukstis, 2013; Phipps, 1985). Trees were visually crossdated and then ring widths were measured using CooRecorder software (Larsson, 2013), after which crossdating was statistically checked using the program COFECHA (Holmes, 1983). Prior to dendrochemical analysis, an investigation into the core preparation method was conducted. The Elmer's School Glue adhesive was analyzed for its $^{87}Sr/^{86}Sr$ ratio ($^{87}Sr/^{86}Sr = 0.71420$). The reproducibility of samples that had been mounted using glue was compared to the reproducibility of samples that had never been mounted. Additional details are presented in the *Sample preparation for dendrochronology and dendrochemistry* section of this thesis.

From 2022 to 2023, a subset of the original trees was re-cored and prepared for analysis with a new, cleaner method. These new cores from Waller Creek trees ($n = 10$) and Onion Creek trees ($n = 8$) were extracted within 2-3 inches of the borehole left in 2018. Borers were cleaned between each tree using only ethyl alcohol, reducing contamination from the previous cleaning method, which used WD-40 or mineral oil. Core preparation procedures were also optimized to minimize contamination. Within 24 hours, cores were removed from the field sampling straws and soaked in ultrapure water for 48 hours to engender the mobilization and thus removal of elements in interstitial water held within the xylem sap and pore space (Sheppard and Thompson, 2000). Cores were also ultrasonicated for 2 hours to further promote this process. To retain their shape while drying, cores were tied into pre-cut mounts from Rocky Mountain Tree-Ring Research, Inc. using string. Once dry, we develop a vise-like holder used to secure cores in place while a stainless-steel razor blade, pre-cleaned with ethanol, was used to plane and expose the rings, replacing the need for sanding and polishing (Supp. Figs. 1 and 2). Dendrochronology was completed using the same methods and programs as used for the 2018 cores. Cores selected for chemical analyses were divided into 5-year increments lengthwise using stainless-steel razor blades, preserving half of each core as an archive.

3.2. Sample preparation for dendrochronology and dendrochemistry

Traditional methods of core preparation for dendrochronology involve sanding, polishing, and application of adhesives for mounting. Handling and preparation can introduce contaminants that penetrate wood pores. Typically, samples are glued into grooved wooden blocks to stabilize them while the exposed surface is sanded, polished, and dated. Sanding is done using progressively graded sandpaper, ranging from 80 to 600 grit. We investigated the adhesive used for mounting our core samples, Elmer's School Glue, to assess its potential for contamination. This adhesive, which was used to mount core samples collected in 2018, was analyzed to determine its influence on wood. The translation of the glue's relatively high ratio ($^{87}Sr/^{86}Sr$ = 0.71420) into the wood cellulose was tested by analyzing corresponding rings of a tree core segment split down the middle, where one half was glued into a mount and the other half was not (Fig. 5a). The two halves were analyzed separately for $^{87}Sr/^{86}Sr$ and compared (Fig. 5b).

Prior to analysis, the glued samples used in the experiment above were soaked in deionized water for 24 hours in an effort to remove the glue. The high ratio from the mounting of the cores was retained in the glued, soaked samples, but the concentration of major cations decreased significantly after soaking. We hypothesized that elements held in the pore space (i.e., interstitial water), could be mobilized when soaked and ultimately purged from the pore space, accounting for the concentration decreases observed in soaked cores. This was examined using three fresh bald cypress core segments. The three segments (designated A, B, and C) were divided into halves and each half was assigned the number 1 or 2 (Fig. 6). Segments A1, B1, and C1 were analyzed for trace elements without further treatment prior to digestion. Segments A2, B2, and C2 were soaked for 24 hours in deionized water prior to analysis. Elemental concentrations were reduced up to 777% in soaked cores, indicating the potential for significant overprint of elementals held in modern interstitial water if cores are not soaked in preparation for dendrochemistry.

From 2022 to 2023, a subset of the original trees was re-cored and prepared for analysis with a new method. These new cores from Waller Creek trees (n = 10) and Onion Creek trees (n = 8) were extracted within 2-3 inches of the borehole left in 2018. Preparation methods developed in this study were designed to minimize contamination by replacing sanding, polishing, and adhering with effective, sanitary alternatives. Sanding was replaced with slicing of the cores using ethanol-cleaned, stainless steel razor blades, which revealed a flat surface that could be dated using dendrochronology (Fig. 7). Dendrochronology was performed on Waller Creek trees (n = 21) and Onion Creek trees (n = 13) in 2018 and is detailed in Banner et al. (2023). Waller

Creek bald cypress trees have an average age of 66.3 years of growth, which is consistent with documented planting events. Onion Creek bald cypress trees naturally grow bankside and are 132 years old on average (Banner et al., 2024). Chronologies were updated for the subset of trees cored in 2022-2023 for this study (Table 1).

3.3. Digestion methods

Two methods of wood digestion were compared for efficiency, contamination, and reproducibility- the microwave method and the ashing method. The microwave method used an Anton Paar Multiwave 7000 microwave digestion system on the Organic High program. Dry wood segments were microwaved using 2 ml of concentrated, double-distilled HNO_3. Complete dissolution was achieved for all samples after one run (1 hour). The maximum sample size tested was 400 mg (n = 41). The ashing method was developed using a muffle furnace before the microwave became available for regular use. Wood samples were ashed in the furnace at 260^{o}C for 3 hours. Low contamination conditions are indicated by Sr blank results by Thermal Ionization Mass Spectrometry (TIMS) and using quartz crucibles for digestion (<15 pg Sr; typical sample:blank ratio = 1200). Ashed samples were heated to 130^{o}C for 12 hours in double-distilled 7N HNO_3, dried, and brought to full digestion in an additional 2 ml of 7N HNO_3. Replicate samples by ashing reproduced within ±0.00004 for $^{87}Sr/^{86}Sr$ on TIMS. When comparing the two methods (i.e., microwaving and ashing), the same samples again reproduced within ±0.00005 for $^{87}Sr/^{86}Sr$ (Fig. 8). Given that the two methods produced similar blanks and replication, results by the two methods are used interchangeably and are documented for each sample in Table 3.

3.4. Streamwater and wood analyses for trace elements and $^{87}Sr/^{86}Sr$ ratios

Streamwater samples collected from Onion Creek (n = 20) and Waller Creek (n = 34) were analyzed for cation and anion concentrations. A subset of these streamwater samples from Onion Creek (n = 3) and Waller Creek (n = 4) were analyzed for $^{87}Sr/^{86}Sr$ ratios. Wood samples (n = 76) were analyzed for cation concentrations and most (n = 60) were also analyzed for $^{87}Sr/^{86}Sr$ ratios. Five-year increments from the oldest, middle, and youngest portions of each core were analyzed. One full core from each watershed was analyzed in 5-year increments (10-year increments were analyzed in Onion Creek tree OC3 from 1840 to 1940) from pith to bark. These 5-year segments ranged from 18 to 400 mg. Chemical analyses of streamwaters and wood were conducted at the University of Texas at Austin, Department of Earth and Planetary Sciences. Cation concentrations were analyzed using an Agilent 7500ce Quadrupole Inductively Coupled Plasma Mass Spectrometer (ICP-Q-MS). For Ca, Mg, Na, and Sr, the percent difference between replicate analyses (n = 9) averaged <1%. 93% of replicate data were within 4% (Table 4). Anion concentrations for streamwaters were analyzed using ion chromatography (IC) at the UT Department of Civil, Architectural, and Environmental Engineering from 2021 through 2022 and at the Department of Earth and Planetary Sciences in 2023. In both departments, seven anion concentrations were analyzed, including F, Cl, NO_2, Br, NO_3, SO_4, and PO_4. Thermo Scientific Dionex Seven Anion Standard II was used with each analysis. Alkalinity titrations were completed manually and using an S M Titrino 702 autotitrator on 25 ml of sample. Titrations were performed within 48 hours of sample collection, to an endpoint pH of 4.5 using 0.1N H_2SO_4. Two-sigma analytical uncertainty for most anions, including alkalinity, was better than 5%. 80% of replicate anion data is within a 5% difference of each other. 92% of data is within 13%, and 3 outlier differences between replicates for NO_3, HCO_3, and SO_4 are 22%, 32%, and 62% different, respectively (Table 5). The limits of detection for reported cations and major anions Cl and SO_4 were 1 to 10 orders of magnitude below sample concentrations (Table 4 and Table 5). Charge balances in streamwater samples show that 67% of the samples lie within ±5% of neutral and 100% of samples lie within ±10% of neutral. The average charge balance for Waller Creek water samples is ±5% while the average for Onion Creek waters is ±4%. Field blanks were collected on streamwater sampling trips (*n* = 7) and analyzed for cations and anions. In all but two blanks, all anion concentrations fell below detection limits (Table 6a). In those two samples, the only detectable anion was SO_4, in concentrations of 0.3 and 3.1 ppm. The sample-to-blank ratios for the two SO_4 concentrations were between 44 and 273, indicating a negligible contribution to the sample concentration (Table 6b). Field blank cation concentrations for major cations including Na, Mg, K, Ca, and Sr are presented in Table 7a. The sample-to-blank ratios for the cations detected in the blanks ranged from 5 to 1,365 (Table 7b).

Stream water samples (*n* = 7) and wood samples (*n* = 60) were analyzed for $^{87}Sr/^{86}Sr$ ratios (Table 8). Twenty-two of these analyses (21 wood samples and 1 streamwater sample) were done using a Thermo Scientific Triton Thermal Ionization Mass Spectrometer (TIMS). The remaining 6 water samples and 39 wood samples were analyzed for $^{87}Sr/^{86}Sr$ using a Nu Plasma 3D multicollector inductively coupled plasma mass spectrometer (MC-ICP-MS) with a DSN desolvating nebulizer. Both laboratories are in the Department of Earth and Planetary Sciences and each sample analysis is adjusted for the value obtained for the NIST SRM-987 standard. Strontium was isolated from samples using standard column chromatography methods with BioRad Sr Specific resin in 70 µl columns and nitric acid. TIMS samples were loaded on rhenium filaments with tantalum fluoride slurry and analyzed in static mode, 160 measurements of 8 seconds each. For the MC-ICP-MS, samples are dissolved in 2% HNO_3 and analyzed in static mode for 80 measurements of 3 seconds each. Sample analyses were bracketed by replicate analysis of NIST SRM-987 before and after every analysis. For both analytical methods mass bias was corrected using an exponential fractionation factor and $^{88}Sr/^{86}Sr$ = 8.270309. Mass 87 was corrected for ^{87}Rb using measured ^{85}Rb and $^{87}Rb/^{85}Rb$ = 0.3860. For TIMS NIST SRM-987 measurements averaged 0.710250 across all sample runs (63 analyses over 11 months). Reported data are normalized to the accepted $^{87}Sr/^{86}Sr$ ratio for NIST SRM-987 (0.710428) based on the average measured $^{87}Sr/^{86}Sr$ ratio for NIST SRM-987 per analytical session. The analytical uncertainty for $^{87}Sr/^{86}Sr$, based on 2-sigma standard deviation of the population of NIST SRM-987 is ±0.000017 for most samples. Smaller samples, which yield less Sr, have slightly larger analytical uncertainty (±0.000040). Sample replicates (*n* = 8) reproduce within ±0.00006 (Table 9; n = 4 replicate pairs). Full procedural blanks as determined by isotope dilution over the time period of the study were 15, 1, 7, and 15 . 32, 36, 45, 50, and 100 pg Sr. The wood sample with the lowest amount of Sr (120 ng) contains 1,200 times more Sr than the highest blank (0.1 ng). Thus, the blank sizes are negligible for the samples analyzed.

4. Results

4.1. Quantifying contamination in tree cores

In analyzing and quantifying the contamination of tree cores from traditional mounting processes, unmounted bald cypress samples were 12 - 25 times more reproducible than their corresponding halves that were mounted with Elmer's School Glue. Additionally, the $^{87}Sr/^{86}Sr$ values of the mounted samples were consistently higher than the values of the same rings without glue (Fig. 5b). The Sr isotope reproducibility of the edge pieces of mounted samples (i.e., core portions in most direct contact with the glue; $n = 6$), was ±0.00174. The center pieces of the glued half ($n = 3$) were reproducible to within ±0.00025. The unglued half of the core was analyzed in three increments, which yielded a reproducibility of ±0.00002. A separate segment of the same core, unglued, was divided vertically into four sub-samples and analyzed for $^{87}Sr/^{86}Sr$. The reproducibility of these four replicates was within ±0.00007. While the $^{87}Sr/^{86}Sr$ value of Elmer's School Glue was significantly higher than the ratio of any bald cypress wood samples ($^{87}Sr/^{86}Sr = 0.71420$), according to mass balance calculations, the concentration of Sr in the glue (0.09 ppm) was not high enough to alone account for the change in $^{87}Sr/^{86}Sr$ of the mounted wood samples. Cores in contact with glue (i.e., all cores collected in 2018) were ultimately determined to be unusable for chemical analyses of trace elements or $^{87}Sr/^{86}Sr$ ratios. Trace element results of the wood samples soaked in deionized water prior to analysis revealed significantly lower concentrations of major cations including K, Fe, Na, and Mg when compared to concentrations of samples that were not soaked (Fig. 6). Potassium had the largest decline in concentration of the soaked half with differences ranging from 387 to 777%. Concentration decreases were also observed in A2, B2, and C2 for Na, Mg, and Fe. Calcium and strontium decreased in concentration within the soaked half for segments A and C, but higher concentrations of both elements were observed in the soaked B segment (Fig. 6). The consistent decrease in concentration of major cations after soaking the cores indicated that residual water was mobilized out of the core. Wood extractives (non-structural components of tree anatomy), xylem sap, and residual water often contain elements that have the potential to obscure environmental temporal signals (Sheppard & Thompson, 2000; Cutter & Guyette, 1993; Galicki et al., 2008). Our results led to the implementation of a 48-hour soaking period in deionized water immediately after the collection of each core, prior to drying.

4.2. $^{87}Sr/^{86}Sr$ in bald cypress trees and streamwaters

$^{87}Sr/^{86}Sr$ values in Waller Creek and Onion Creek trees were analyzed in 5-year growth increments (*n* = 46). For all 23 Onion Creek samples, $^{87}Sr/^{86}Sr$ ratios range from 0.70793 to 0.708140 (Fig. 9). $^{87}Sr/^{86}Sr$ values in individual Onion Creek core analyses (*n* = 23) vary by up to 0.00017 over time. Onion Creek tree OC3 has the most significant ratio change over time (0.00017). Between the 3 samples analyzed in tree core OC3 from 1840 to 1890, the $^{87}Sr/^{86}Sr$ ratio is significantly lower than the ratios within the remaining 11 samples (variation = 0.00006; Fig. 9). The set of Waller Creek core analyses (*n* = 37) display a significantly higher range of $^{87}Sr/^{86}Sr$ from 0.708555 to 0.708943 (Fig. 10). Individual trees vary up to 0.000137. There is no overall significant linear temporal trend in $^{87}Sr/^{86}Sr$ ratios from cores from Waller Creek watershed. For trees in both watersheds, $^{87}Sr/^{86}Sr$ values coincide with the $^{87}Sr/^{86}Sr$ ranges found in streamwaters and soils in each corresponding watershed (Figs. 11 and 12). Onion Creek streamwater, influenced by the Cretaceous carbonate bedrock from which it flows, has a mean $^{87}Sr/^{86}Sr$ of 0.7080 (Fig. 11; n = 44; Christian et al., 2011; Beal et al., 2020). Waller Creek streamwaters spanning the same time interval average 0.7088 (Figs. 10 and 11; n = 110; Christian et al., 2011; Beal et al., 2020. Onion Creek trees display $^{87}Sr/^{86}Sr$ values significantly lower and more similar to the values found in Austin-area Cretaceous carbonate bedrock (mean = 0.7076; Beal et al., 2020; Christian et al., 2011) when compared with the values found in Waller Creek cores, municipal supply, and wastewater (mean municipal supply and wastewater $^{87}Sr/^{86}Sr$ mean = 0.7091, Christian et al., 2011).

Christian et al. (2011) monitored the same site in Waller Creek, each week for 42 consecutive weeks from August 2001 to September 2002 (mean = 0.70885; Christian et al., 2011; average is represented by the red square in Fig. 10). The standard deviation of this dataset is shown using error bars and is 0.00051. This indicates the observed stream fluctuations within one year of data from the same site along Waller Creek. For all Waller Creek trees, excluding two (4171 and 4036), this variability (i.e., the standard deviation of streamwater within one year, 0.00051) is greater than the variability across individual tree core $^{87}Sr/^{86}Sr$ analyses.

Two cores from the same tree (Waller Creek 3924A and B) were analyzed for $^{87}Sr/^{86}Sr$ (Fig. 13). Values differ outside of the analytical uncertainty (±0.000017). The differences between the two cores' $^{87}Sr/^{86}Sr$ ratios of the youngest, middle, and oldest increments are 0.000088, 0.000111, and 0.000083, respectively. Core 'A' was taken from the downstream-facing side of the tree while Core 'B' was taken from the upstream-facing side of the tree. The resolvable isotopic differences (i.e., higher $^{87}Sr/^{86}Sr$ values within the core taken from the downstream side) may be due to contribution from the pipes that, if flowing, would deliver water directly to the surface roots extended outward from the southwest (downstream) side of the tree (Fig. 13a). The pipes have not been observed to flow throughout the duration of this study. If these pipes have historically dispensed municipal water with higher $^{87}Sr/^{86}Sr$ than that of the water flowing from upstream of the tree, then this could account for the difference in $^{87}Sr/^{86}Sr$ values.

One core from Waller Creek (tree 4171) was analyzed for $^{87}Sr/^{86}Sr$ and trace elements in 5-year increments from pith to bark (Fig. 14). The temporal trend from 1945 to present varied by 0.000108 and ranged from 0.708576 to 0.708685 with the highest ratio found in the oldest segment. These values fall at the lower end of, but still within, the Waller Creek streamwater data spread. There is a significant downward trend in $^{87}Sr/^{86}Sr$ ratios from 0.70869 in 1945-1949 to 0.70858 in 1967-1971 (R^2 = 0.798). That trend is immediately followed by an abrupt $^{87}Sr/^{86}Sr$ increase peaking at 0.70864 in the 1989-1993 segment (R^2 = 0.9343) (Fig. 14).

4.3. Trace elements in bald cypress trees and streamwaters

Trace elements were analyzed from the same Waller Creek and Onion Creek cores as were analyzed for $^{87}Sr/^{86}Sr$. The temporal trends for major cations of interest (i.e., Sr, Ca, Mg, Na, P, and K) are presented in Figure 15. In Waller Creek trees, elements including Mg and Na display a significant temporal decrease in concentration. In Onion Creek trees, Mg follows the same trend. In all Waller Creek and Onion Creek trees, the concentration of P significantly increases in rings formed after 1985 (R^2 = 0.647 in Waller Creek trees and R^2 = 0.653 in Onion Creek trees). The temporal trends for Ca and Sr are similar within and between trees in each watershed. One core was selected from each watershed to be analyzed for $^{87}Sr/^{86}Sr$ and trace elements, in 5-year increments, continuously from pith to bark. In Waller Creek watershed, tree 4171 was analyzed, and in Onion Creek watershed, tree OC3 was chosen to analyze continuously. Elemental trends over time are consistent, in most cases, between all cores in Waller Creek watershed. The three temporal data points captured by the 5-year increments are consistent with the longer temporal record presented by tree 4171. Two outliers for Ca, tree 4172 and tree 4164, increase in concentration in the 2017-2023 segment, unlike the rest of the cores which all experience a nearly identical concentration decrease to less than 1000 ppm Ca. The pith-to-bark consecutive analyses for Onion Creek core OC3 matches closely with the 5-year increments from the youngest, middle, and oldest 5-year increments (Fig. 15). All major elemental concentrations are decreasing moving from pith to bark in all excluding P and K. These elements are significantly more concentrated in the trees than in the streamwaters from their corresponding watersheds. The average Sr concentration in Waller Creek waters is 0.4 ppm and in Onion Creek the average is 0.6 ppm (Fig. 16). The trees average 10.8 ppm Sr from Waller Creek and 11.4 ppm from Onion Creek, consistent with the difference in concentration observed in the streamwaters between the watersheds (Fig. 17). Removing the Onion Creek outlier point at 35 ppm Sr causes the R^2 to drop to 0.275. Densely urbanized Austin watersheds (i.e. Waller Creek and Shoal Creek) are dominated by the dissolution of the Austin Chalk and their waters evolve along a relatively steep positive linear relationship between Sr and Ca (R^2 = 0.866; Fig. 16) Onion Creek and other semi-urbanized Austin watersheds have a much less positively correlated Sr/Ca relationship (R^2 = 0.071), and Sr concentrations increase with the dissolution and recrystallization of limestone (Fig. 16; Manlove, 2020). The Sr and Ca concentrations within bald cypress trees in this study all co-vary along a positive linear trendline, with Onion Creek trees having an R^2 of 0.782 and Waller Creek trees having an R^2 of 0.360 (Fig. 17 and Supp. Fig. 3). The concentrations of trace elements found in our bald cypress trees are consistent with observations in studies of other species (Watmough, 2014).

4.4. Translocation

Translocation is the transport of water and elements within a tree over a distance that crosses growth rings (Swanson, 1957). A high heartwood moisture content and a large number of sapwood rings in bald cypress trees may promote ease of translocation, but the low heartwood permeability may reduce it (Cutter and Guyette, 1993). Some tree species will translocate essential elements (such as K, P, Mg, and Mn) toward the sapwood and cambial layer for use in new growth rings. This increases concentrations of these elements in the sapwood. Toxic or disruptive elements (such as metals and radioactive isotopes, including ^{90}Sr; Smith and Shortle, 1996) may be pushed toward the heartwood, infilling old xylem and increasing concentrations (Cutter & Guyette, 1993). Translocation is investigated in the present study using statistical differences between the concentrations of cations across the heartwood-sapwood boundary. The heartwood-sapwood boundary was identified in each core using the clear change in the coloration of the rings (Table 10; Fig. 8; Supp. Figs. 6 and 7). The average heartwood-sapwood boundary transition among Onion Creek trees was 1977 and the average among Waller Creek trees was 2001 (black dashed lines in Fig. 15). For each element, concentrations in rings before and after the heartwood-sapwood boundary (total number of concentration data points for each element = 75) were separated and two types of tests were performed on the datasets to determine whether there was a statistically significant difference between the heartwood and the sapwood. The same tests were performed for Sr isotope ratios ($n = 60$). For the t-tests, each element's average concentration and standard deviation were found for the heartwood and for the sapwood. These were used to determine the coefficients of variance, which informed the type of t-test used (Table 11Table 11). P-values are shown in Table 11 and are 0.001, 0.023, 0.224, 0.000, 0.027, and 0.000 for Sr, Ca, K, Mg, Na, and P, respectively. For $^{87}Sr/^{86}Sr$, the p value was 0.348. To further investigate translocation, Wilcoxon signed rank tests were performed on the same heartwood and sapwood datasets for concentrations of Sr, Ca, Mg, K, P, and Na, and $^{87}Sr/^{86}Sr$ values. The statistical difference between the heartwood and sapwood groups was large enough to point to translocation in $^{87}Sr/^{86}Sr$ ratios, Sr, Mg, Na, and P (Table 12). The results of the Wilcoxon signed rank tests indicated that there was a statistically significant difference between the heartwood and sapwood concentrations (or values, in the case of $^{87}Sr/^{86}Sr$ data) for $^{87}Sr/^{86}Sr$, Na, Mg, P, and Sr. There was not a statistically significant difference between the groups in K concentrations or Ca concentrations. The results of the two tests were compared. Based on the p values (results where $p < 0.05$), heartwood-sapwood shifts in Sr, Ca Mg, Na, and P are consistent with these elements being affected by translocation processes. Based on the Wilcoxon rank tests, heartwood-sapwood shifts in $^{87}Sr/^{86}Sr$, Sr, Mg, P, and Na are consistent with these elements being affected by translocation processes. Time series for elements Sr, Ca, Mg, K, P, and Na can be found for all analyzed trees in Figure 15.

5. Discussion

5.1. Preparation of tree cores for dendrochronology and dendrochemistry

Traditional methods of tree core preparation and handling for dendrochronology introduce contaminants that may obscure the results of dendrochemistry. Contamination from the mounting process and adhesive (in this case, Elmer's School Glue), was observed in our bald cypress tree cores. A series of experiments determined that the relatively high $^{87}Sr/^{86}Sr$ ratio overprint of the adhesive could not be removed from within the pores of the wood via ultrasonication, soaking in water, or physical removal of the glue. The reproducibility among glued samples was significantly lower than the reproducibility of samples prepared using the methods developed in this study. Trace elements found in adhesives, even when concentrations are below 1 ppm, may influence the chemical composition of wood outside of analytical uncertainty. The trace element and $^{87}Sr/^{86}Sr$ data of Elmer's School Glue are provided in Supplementary Tables 2 and 3. It is our recommendation that cores anticipated for use in dendrochemistry do not come into contact with adhesives or sandpaper. However, mixing calculations reveal that the adhesive alone accounts for only about 7% of the contamination, while the remaining 93% must come from another source or from a reaction between sources (Supp. Fig.5). We hypothesize that an interaction between the adhesive and the mounting wood may account for the high $^{87}Sr/^{86}Sr$ values found in cores prepared using traditional methods. Sanding and polishing also introduce contaminants to cores. The heat produced from sanding can volatilize organic compounds in wood (Balouet, et al., 2007). Additionally, sanding introduces the risk of cross-contamination by dispersing dust from various rings throughout the core (Pearson et al., 2005; Sheppard & Witten, 2005).

The core preparation methods developed in this study were designed to minimize contamination by replacing adhesives, sandpaper, and polishing with cleaner alternatives. These methods achieve the same result as traditional preparation methods (i.e., the flat, polished surface required for dating), with negligible contamination. See *section 7.1, Contamination advisory* below prior to utilizing methods outlined in this study to prevent contamination from specific elements.

5.2. Impacts of interstitial water on dendrochemistry

While most wood contains extractives held in interstitial pore water and xylem sap at only about 5% of its dry mass, these extractives can interfere with dendrochemical signals (Lehr et al., 2021). The high moisture content of the heartwood and sapwood of bald cypress trees (Cutter and Guyette, 1993) results in significant interstitial water remaining in the cores after collection. This interstitial water reflects the chemistry of modern water absorbed by the tree and may obscure the analytical results of the composition of the tree cellulose. In this study, residual water and extractives were flushed from the wood pores by soaking in deionized water for 24 hours, followed by ultra-sonification for 2 hours. Other solutions exist for flushing wood extractives, but Pettersen (1984) concluded that there is no solvent known to remove all extraneous material held interstitially. Water is known to gently extract inorganic salts, gums, and starches while diethyl ether extracts fats, resins, terpenes, and sterols (Pettersen, 1984). Ethanol/benzene or toluene extracts organics that are insoluble in water and have been used to treat cores before analyzing for N concentrations (Pettersen, 1984; Sheppard and Thompson, 2000). Previous studies have recommended soaking cores to 1) un-twist cores twisted during collection (Phipps, 1985), 2) replace the sapwood moisture lost while coring to determine original sapwood moisture content (Chan et al., 2010), and 3) soften the core for ease of splitting

(Gartner et al., 2015). To our knowledge, it is not common practice to flush cores of their interstitial water in preparation for dendrochemical analysis. The extraction of the interstitial water is a crucial part of core preparation if the analytical goal is to reconstruct the chemical composition of the wood cellulose alone.

In this study, soaking and ultra-sonification in deionized water were sufficient to remove the modern water overprint. This was determined based on the significant decrease observed in the concentration of cations after soaking in water for 24 hours (Fig. 6; Supp. Table 4). The greatest percent differences between soaked and unsoaked wood were seen in K, Na, Rb, and B (42-777%). Calcium and strontium yielded very similar results between the soaked and unsoaked procedures, indicating similarities in the way they migrate through tree xylem (Fig. 6).

5.3. $^{87}Sr/^{86}Sr$ variations in Waller Creek and Onion Creek watersheds

Tree cores from Waller Creek and Onion Creek watersheds analyzed in 5-year increments have $^{87}Sr/^{86}Sr$ ratios that reflect the values found in their respective environmental surroundings. The significantly higher values found in Waller Creek trees are consistent with the higher $^{87}Sr/^{86}Sr$ values found in the streamwater and soils of the Waller Creek watershed. Waller Creek streamwaters spanning 2001-2023 (n = 110) have an average $^{87}Sr/^{86}Sr$ of 0.7088 and range from 0.7081 to 0.7094 (Christian et al., 2011; Beal et al., 2020). The $^{87}Sr/^{86}Sr$ ratios of Onion Creek trees are significantly lower, by comparison, and fall almost entirely within the range of Onion Creek streamwater and soils. Onion Creek tree ratios are very close to or within the range of Sr isotope values of Cretaceous carbonate bedrock (n = 44; 0.7074-0.7080, mean = 0.7076; Mauceri and Banner, 2023; Beal et al., 2020; Christian et al., 2011). These trends between watersheds are consistent with the inference that Waller Creek, the more highly urbanized watershed, likely contains a significantly higher proportion of municipal water at baseflow than

Onion Creek (Christian et al., 2011; Banner et al., 2024). The high $^{87}Sr/^{86}Sr$ values of municipal water, in the form of irrigation or direct leakage into the stream, likely influence the chemical composition of soils, streamwater, and trees in the Waller Creek watershed (Mauceri and Banner, 2023; Christian et al., 2011; Manlove, 2020).

Our initial hypothesis predicted a temporal increase in the $^{87}Sr/^{86}Sr$ ratios of Waller Creek tree rings, consistent with the increased addition of municipal water to the stream as urbanization expanded and aging infrastructure failed. However, $^{87}Sr/^{86}Sr$ ratios in trees from the Waller Creek watershed have remained within a relatively narrow range, with little to no temporal trend observed within individual trees (Fig. 10). A similar narrow temporal $^{87}Sr/^{86}Sr$ range is seen in trees from Onion Creek watershed. In Onion Creek tree core OC3, however, the $^{87}Sr/^{86}Sr$ ratios of tree samples dating earlier than 1890 (n = 3) are significantly lower than the 10 younger samples of the same core. Tree OC3 is located within the Onion Creek soccer complex, suggesting a potential shift in water quality around 1890. Trees downstream of OC3 do not reflect the low $^{87}Sr/^{86}Sr$ ratios prior to 1890. We may infer that there was potentially some degree of municipal input into the stream downstream of OC3 prior to 1890. These results pose the paired questions: 1) are bald cypress trees accurately recording the historical evolution of streamwater chemistry in these streams, or 2) is the temporal environmental signal in the trees obscured by the translocation of elements across the heartwood-sapwood boundary? The relatively unchanging $^{87}Sr/^{86}Sr$ values over time in Waller Creek and Onion Creek trees raises important questions about the accuracy of bald cypress trees as recorders of historical streamwater chemistry evolution. Question 1, above, is addressed through the history of Austin's water infrastructure and chemical patterns observed within individual trees (Section 5.5, below). Question 2 is addressed based on a literature review of translocation and our own geochemical observations (Section 5.4, below), where we consider the potential influence of translocation of elements across the heartwood-sapwood boundary on environmental signals.

5.4. Trace elements and translocation in trees

Lepp (1975) identified the main pathways for vegetation to absorb trace elements: the foliage, roots, and bark. The founding principle in dendrochemistry is that the chemical composition of any individual growth ring will, to some degree, reflect the chemical environment during which it was formed (Cutter and Guyette, 1993). However, irregular movement of elements both radially and longitudinally throughout a tree complicates the ability to reconstruct a dendrochemical times series. This movement of elements is termed "translocation" (Cutter and Guyette, 1993; Symeonides, 1979; Stewart, 1965; Panshin and de Zeeuw, 1980). Radial translocation, which occurs across ring boundaries, depends on the characteristics of the xylem. The anatomical, chemical, and physical changes that occur within the xylem of the species of interest are integral to understanding the influence of translocation on the chemical makeup of the tree (Cutter and Guyette, 1993; Stewart, 1965). Research has determined the heartwood-sapwood boundary to be the focal point of understanding translocation. The potential extent of radial translocation can be determined by a number of xylem structural properties that change across the sapwood-heartwood boundary including: cell density, concentration of tannins, and internal moisture content (Cutter and Guyette, 1993; Stewart, 1965). The heartwood forms with the death of parenchyma cells (cells that compose the majority of living xylem) and is entirely composed of these dead cells (Stewart, 1965). Living xylem (sapwood) exists between the heartwood and the actively growing cambial layer (Fig. 18), and is a few to many growth rings wide, depending on the species and other environmental factors (Stewart, 1965). Jacquiot (1947) observed that cambial productivity is inhibited, even stopped entirely, by tannins present near the growing zone (Stewart, 1965). Toxic extraneous materials and tannins must be either 1) detoxicated, then accumulated and stored, or 2) translocated away from the cambial layer so growth may proceed. Tannin concentrations are at their lowest near the cambial growing layer and increase moving outward toward the bark and inward toward the heartwood (Stewart et al., 1965). Toxins will be translocated from the cambial layer, decreasing in concentration moving away from that layer and outward to their highest concentrations in the bark and heartwood (Stewart et al., 1965; Hasegawa and Shiroya 1966). These toxins will be translocated toward the sapwood-heartwood boundary where the permeability of the heartwood may decrease between 8 and 100+ times relative to the sapwood, as observed in North American conifers (Comstock, 1970; Stewart, 1965; Cutter and Guyette, 1993). Toxins will accumulate at this boundary until they reach a deadly concentration, thus killing all living parenchyma cells in their vicinity, which will then become a part of the heartwood (Stewart, 1965). Heartwood will form only when trees absorb compounds that are toxic or elements in high enough concentrations to become toxic, and the heartwood will move outward from the pith as these toxins accumulate (Stewart et al., 1965). Radial translocation is most effectively prevented in trees with low radial permeability, few sapwood rings, and low heartwood moisture content (Cutter and Guyette, 1993). The width of the sapwood zone is dependent upon species, hormonal and water stress, and a variety of other genetic and environmental factors (Hemingway and Hillis, 1970). However, the number of sapwood rings is crucial to understanding the temporal integrity of ring compositions. The temporal certainty of the chemical composition of an individual ring is limited by the number of sapwood rings at its time of formation. For example, 20 years of sapwood rings at the time of ring formation means that translocation is possible throughout the 19 other sapwood rings. This highlights the importance of selecting the oldest possible trees for dendrochemical studies. The temporal chemical trend of a tree with 200 growth rings will be less impacted by 20-year uncertainty than a 50-year-old tree will be. Even if translocation is occurring in the bald cypress trees used in this study, the temporal trend in chemistry will only be as uncertain as the number of sapwood rings (approximated for each tree in Table 10).

Studies of conifers including bald cypress, Scots pine, and Norway spruce conclude that the total number of active sapwood rings in mature trees increases with a tree's age (Edvardsson et al., 2022; Longuetaud et al., 2007; Tucker et al., 2019). Therefore, the number of sapwood rings today is likely the maximum number experienced over the lifetime of these trees. To reflect the temporal uncertainty due to possible translocation, Figure 19 displays horizontal error bars on each $^{87}Sr/^{86}Sr$ value spanning the number of sapwood rings. The heartwood-sapwood boundaries are based on the current number of sapwood rings observed in our cores today and, thus, the uncertainty as expressed by these error bars are likely overestimates in older analyses. While the high resolution of the 5-year sample increments may be lost, the overall trend through time is preserved. According to the combined results from the t-tests and Wilcoxon signed rank tests, there is evidence for the translocation of Sr, Mg, P, and strontium isotopes. This is based on the statistically significant difference between concentrations of these elements in the heartwood versus the concentrations of these elements in the sapwood. While translocation may be occurring in these elements, it is likely only obscuring the results as many years as the number of sapwood rings in each tree. Thus, consistency displayed by the narrow range of Sr isotope ratios within each watershed indicates that the $^{87}Sr/^{86}Sr$ values have preserved their environmental surroundings throughout the lives of the sampled trees.

In the Waller Creek watershed, tree 3920 has the smallest quantity of sapwood rings (6 sapwood rings). If the number of sapwood rings has remained consistent through this tree's life, then the younger extent of the temporal error bar (approximately 1957) is the oldest known $^{87}Sr/^{86}Sr$ ratio that could be assigned to the tree and to the overall watershed. This ratio falls well within the range of the ratios seen throughout the Waller Creek watershed. Therefore, it can be interpreted that Waller Creek water chemistry has remained relatively temporally stable and close to the oldest value (0.70863) at least back to 1957. This study originally hypothesized that a temporal increase in $^{87}Sr/^{86}Sr$ values would be observed in tree rings, ranging from the low values representative of Lower Cretaceous bedrock to the higher values of the Colorado River water. If the chemical composition of Waller Creek streamwater has remained the same since at least 1957, then either 1) baseflow has been significantly influenced by municipal water leakage since at least 1957, or 2) there are contributions to the $^{87}Sr/^{86}Sr$ ratio of the stream and/or the trees that are not yet constrained. Option 1 is supported in Section 5.5, below.

5.5. Historical baseflow in Waller Creek and Onion Creek watersheds

Water-related infrastructure in the Waller Creek watershed was initiated in 1919, leaving approximately 20 years between the original construction and the oldest Waller Creek bald cypress trees dated and analyzed in this study (austintexas.gov, n.d.). The city of Austin has prioritized the expansion of water-related infrastructure but have neglected the maintenance and replacement of already-existing infrastructure in state water plans (TWDB, 2022). To question 1 above, it is thus possible that the baseflow of Waller Creek was already altered by the influence of municipal water by the 1940s, when the trees began growing alongside Waller Creek. This inference is consistent with the tree-ring chronologies developed by Banner et al., 2024, where

Waller Creek ring widths display evidence for municipal input into the hydrologic system as far back as the 1930s.

The $^{87}Sr/^{86}Sr$ results from the two cores from the same Waller Creek tree (Tree ID 3924) may be evidence for these trees' ability to accurately reflect their direct water source. The upstream side of the tree has no direct, visible point source contributions of municipal or wastewater until approximately 75 meters upstream. During regular baseflow conditions, it is likely that the upstream side of the tree would have been exposed to a mixture of natural stream water and municipal water. Contrarily, the downstream side of the tree has several pipes extending outward to directly above the roots. While these pipes were not observed to be flowing over the course of this study, they likely would have dispensed municipal or wastewater if flowing in the past. The transport of water through the xylem is known, in some cases, to be constrained to the side of the tree from which roots have directly taken up that water (Nadezhdina et al., 2008; Zimmerman et al., 1975). For example, Zimmerman et al. (1975) document trees with approximately half of their root system extending into a ditch while the other half lies outside of the ditch. When the ditch flooded with intruding saltwater, only half of each individual tree was killed - the side in which roots extended into the ditch (Zimmerman et al., 1975). Tree 3924 is evidence that bald cypress trees may have the ability to retain water chemistry, at least in the signal of $^{87}Sr/^{86}Sr$, without the signal being transported circumferentially throughout the tree. This suggests that translocation in bald cypress trees is radially constrained to migration of elements within the sapwood rings and does not occur across the tree.

Urban streamwaters have been found to contain certain diagnostic ions in higher concentrations when compared with rural streamwaters in the Austin area. Wastewater contains heightened concentrations of SO_4, Cl, Ca, HCO_3, and Na, which are translated via infrastructure leakage into natural streams in urban watersheds (Christian et al., 2011). High $^{87}Sr/^{86}Sr$ ratios and increased impervious surface cover have been correlated with higher concentrations of these ions in streamwaters (Christian et al., 2011). Concentrations of SO_4, Cl, and Na increase at a threshold of approximately 20% urbanization of Austin watersheds, while Ca and HCO_3 concentrations have been observed to increase with as little as 10% impervious cover (Christian et al., 2011). Sodium was measured in all bald cypress samples and resulted in temporal concentration decreases in Waller Creek and Onion Creek trees (Fig. 15). This could be interpreted as either 1) translocation processes moving Na toward the heartwood, 2) a higher concentration of wastewater entering Onion and Waller Creeks prior to 1995 in Waller Creek and 1900 in Onion Creek, or 3) sodium concentrations alone are potentially not as diagnostic as we would expect in these watersheds without the analyses of SO_4, Cl, and HCO_3. Because trees from both watersheds experience the same temporal trend over different time scales, the more likely interpretation is that translocation of Na is occurring. Calcium concentrations in Waller Creek watershed trees decrease and converge in the young tree rings to within a relatively small concentration range (600-900 ppm) in 7 out of the 9 cores. However, trees 4172, 4164, and 3920 have Ca concentrations at their highest in young rings. These three trees span the Waller Creek bald cypress tree stand, and there is no visible difference water source, soil, number of sapwood rings, or bedrock. In Onion Creek trees, Ca and Sr concentrations are highly correlated (Fig. 16), indicating that they are likely translocated to the same degree toward the heartwood.

5.6. Soil complexity in Onion and Waller Creek watersheds

Bedrock in Austin area watersheds are overlain by soils 0.25 to several meters thick (Christian et al., 2011; Werchan et al., 1974). Previous studies have hypothesized that high

$^{87}Sr/^{86}Sr$ ratios in streams may be due to the weathering of soils with naturally high $^{87}Sr/^{86}Sr$ values (Christian et al., 2011). A complex aspect of Waller and Onion Creek watersheds that bears on addressing both questions 1 and 2 above is the potential for weathering of soils with high $^{87}Sr/^{86}Sr$ ratios to have a larger influence on stream chemistry than the low $^{87}Sr/^{86}Sr$ ratios of the carbonate bedrock. Soil thickness has been shown to correspond to $^{87}Sr/^{86}Sr$ ratios, and thicker soils have higher $^{87}Sr/^{86}Sr$ (Mauceri and Banner, 2023). According to Mauceri and Banner (2023), soil thickness is the main natural factor that is correlated with $^{87}Sr/^{86}Sr$ ratios, with thicker soils having higher values. Disturbed soil beds may have been eroded down from their original thickness, leading to heightened ratios in shallow beds. Factors including soil series, mineralogy, and soil thickness are not shown to impact the range of most soils in Austin watersheds. That is, most soils' $^{87}Sr/^{86}Sr$ values are bounded on the low end by Cretaceous carbonates and on the high end by municipal water (Mauceri and Banner, 2023).

The Onion Creek watershed trees retain low $^{87}Sr/^{86}Sr$ ratios that are representative of both the soils and the streamwater of the Onion Creek watershed (Figure 11). The $^{87}Sr/^{86}Sr$ values of the soils and water are similar to the values found in lower Cretaceous marine carbonate bedrock, which is influenced by the seawater from which they were deposited (mean seawater = 0.7076; Christian et al., 2011; Musgrove and Banner, 2004; Mauceri and Banner, 2023). The low $^{87}Sr/^{86}Sr$ ratios from Onion Creek trees and waters indicate that the Onion Creek watershed is not experiencing significant municipal water contribution to baseflow and is chemically dominated by the carbonate bedrock and soils.

Waller Creek watershed contains some unirrigated soils that have $^{87}Sr/^{86}Sr$ values higher than that of Austin's municipal water (Mauceri and Banner, 2023). Soil samples collected from the Waller Creek watershed are generally higher than those collected from Onion Creek watershed, but several outliers (n = 3) have $^{87}Sr/^{86}Sr$ ratios exceeding Waller Creek soils irrigated with municipal water (Figure 12). Mauceri and Banner (2023) find that $^{87}Sr/^{86}Sr$ values of unirrigated soils in Austin watersheds correlate with silicate mineral concentration, thus leading to the interpretation that silicates may be playing a part in soils' $^{87}Sr/^{86}Sr$ ratios. Irrigated soil samples from the same watersheds correlated weakly with silicate concentrations, indicating that the municipal water contribution to soils is stronger than the signal retained from the mineralogy (Mauceri and Banner, 2023). The Waller Creek trees reflect the $^{87}Sr/^{86}Sr$ values of the streamwater and the range of soils, excluding the high-$^{87}Sr/^{86}Sr$ outliers. Which leads us to conclude that any high $^{87}Sr/^{86}Sr$ values from silicates in surrounding soils are overridden by the municipal water contribution to the stream and soils.

5.7. Streamwater endmembers

Austin-area streams display elemental and isotopic differences due to interactions with the carbonate bedrock and contribution from municipal tap and wastewater, which originate from the Colorado River. Distinct $^{87}Sr/^{86}Sr$ and elemental signatures between urban and rural watersheds, which are influenced by soils bedrock, groundwater, and municipal water, can be used to trace water sources. Municipal supply water in the Austin area has a high $^{87}Sr/^{86}Sr$ ranging from 0.7088-0.7095 (mean = 0.7091, Christian et al., 2011) relative to the local rural water (Fig. 2). The high $^{87}Sr/^{86}Sr$ signature is influenced by the Precambrian granites and Lower Paleozoic units underlying parts of the Colorado River upstream of Austin. Rural springs and streamwaters in the area, collected between 2001 and 2023, have a mean $^{87}Sr/^{86}Sr$ of 0.7079 (Christian et al., 2011), similar to that of the local Cretaceous carbonate bedrock (0.7074-0.7080, mean = 0.7076; Mauceri and Banner, 2023; Beal et al., 2020; Christian et al., 2011). Wastewater Sr concentrations range from 0.12 to 0.40 mg/L (Beal et al., 2020; Christian et al., 2011). In municipal supply, the average Sr concentration ranges from 0.11 to 0.13 mg/L (Beal et al., 2020).

5.8. Soils, bedrock, and rainwater

Mauceri and Banner (2023) find that the $^{87}Sr/^{86}Sr$ ratio of irrigated soils in Austin-area watersheds are higher than that of unirrigated soils within the same watersheds. In Waller Creek watershed, soil $^{87}Sr/^{86}Sr$ values ranged from 0.7086 to 0.7099 for irrigated samples and 0.7084-0.7107 for unirrigated soils (Fig. 11). Onion Creek, which has the lowest soil $^{87}Sr/^{86}Sr$ values in Austin-area watersheds, has soils ranging from 0.70797 to 0.70848 (Fig. 11; Mauceri and Banner, 2023). Densely urbanized watersheds (defined here as ≥55% impervious cover) were found to have $^{87}Sr/^{86}Sr$ that were overall higher (mean = 0.7089) than soils from the more rural watersheds (mean = 0.7084). Rainwater in the Austin area contains an average Sr concentration of 0.006 mg/L (Christian et al., 2011) which is negligible relative to the other sources of Sr (i.e., groundwater, bedrock, soil, municipal supply, and wastewater).

6. Summary and Conclusions

This study reconstructs a historical time series of $^{87}Sr/^{86}Sr$ ratios and trace elements preserved in bald cypress tree rings. These time series are used to interpret past environmental conditions within Austin's Waller Creek and Onion Creek watersheds. Significant contamination is introduced to cores using traditional core preparation procedures. Therefore, a novel method of tree core preparation was developed to minimize contamination introduced through traditional core preparation methods. Methods for wood digestion and analysis were also optimized and used to collect reproducible, high-resolution data in tree rings at 5-year intervals. Among these methods, it was found that soaking tree cores in deionized water after extraction mobilizes interstitial water and promotes accurate analysis of wood material. We better constrain our time series through an evaluation of translocation processes occurring within bald cypress trees. Using statistical analyses, we determine that, while translocation may be occurring for elements Sr, Mg, P, Na, and Sr isotopes, it is obscuring a given result within an approximately 22-year interval in Waller Creek trees and an approximately 35-year interval in Onion Creek trees. The consistency in the narrow range of $^{87}Sr/^{86}Sr$ values within each watershed indicates that the $^{87}Sr/^{86}Sr$ values have relatively accurately preserved their environmental surroundings through time. We infer from the Sr isotope time series that the baseflow of Waller Creek and Onion Creek has not been significantly geochemically altered over the life spans of these trees (i.e., since approximately 1945 for Waller Creek and 1840 for Onion Creek). This result is consistent with the installation of the wastewater infrastructure network established in 1919 in the Waller Creek watershed, which may have started degrading prior to 1940 (City of Austin, n.d.). These results are also consistent with the Waller Creek trees' missing response to the 1950s Drought of Record, as is observed in Onion Creek trees (Banner et al.,, 2024). Bald cypress trees are inferred to be accurate recorders of their environmental surroundings through time, limited by the number of sapwood rings present at the time of ring formation.

7. Future work

The findings of this project could be better understood through further analysis. Two the oldest bald cypress trees growing along Waller Creek (trees #2954 and 2956) date back to the early 1940s. Preliminary analyses in preparation for this project, conducted by Larry Mack in 2007, indicated a temporal increase in the $^{87}Sr/^{86}Sr$ values in these trees. The University of Texas at Austin Urban Forestry Department asked that we avoid coring these trees again in 2023 due to their display of signs of disease. If these trees become healthy and are able to be cored in the future, the results of this project may benefit from their addition to the dataset.

A curiosity that remains prominent upon the completion of this thesis is the $^{87}Sr/^{86}Sr$ range observed between trees of the same watershed for the same time increments. The $^{87}Sr/^{86}Sr$ range in trees within either watershed could potentially be accounted for by 1) significant heterogeneity of the streamwater, as observed in Waller Creek by Christian et al., 2011 (Fig. 10), or 2) contribution from localized environmental influences such as pipes discharge, soils, or bedrock. To rule out the second of the options, I suggest an analysis of environmental conditions specific to, at minimum, the trees on opposite ends of a range (e.g., trees #4204 and 3924 in Waller Creek; Fig. 10). A more comprehensive understanding might include an analysis of all potential pipes contributing to an individual tree's chemical composition. Future questions include: 1) How much of the variation in tree chemistry can be accounted for by pipes turning on and off? 2) What fraction of municipal water in either creek would have had to be delivered to a tree to account for the elevated or decreased $^{87}Sr/^{86}Sr$ values?

To further understand the influence a point source input of municipal supply or wastewater may have on any given tree, the pipes beside Waller Creek tree #3924 should continue to be monitored and investigated for their source and potential history of flow (Fig. 13). Irrigation patterns should also be further investigated, specifically for those trees on the west side of Waller Creek. Irrigation input may potentially be contributing to the high $^{87}Sr/^{86}Sr$ values observed in some of the trees. However, we do still discern that the streamwater would be the primary source of water intake for the trees analyzed in this study.

There is little to no information published regarding sapwood fluctuations through time in bald cypress trees. Constraining this factor would allow us to potentially re-evaluate our temporal geochemical records with smaller error bars on the time axis. Future questions that arise include 1) why do cores taken from the same bald cypress tree on the same day have different numbers of sapwood rings? 2) Is there a correlation between water quality, ring width, and/or the quantity of sapwood rings (i.e., the creation of new heartwood)?

7.1. Contamination advisory

If dendrochemistry is to be done with the intention of reconstructing iron or tungsten, there is a risk of contamination that may be introduced by the increment borer (Sheppard and Witten, 2005). Additionally, the stainless steel razor blade used in planing the cores in this study potentially introduces iron, nickel, and chromium to cores (Sheppard and Witten, 2005; Lula, 1986).

8. Acknowledgements

We acknowledge support from the NSF Environmental Engineering, Hydrologic Sciences,and Environmental Sustainability Programs (2055536) and from the Jackson School of Geosciences at the University of Texas at Austin. We would like to thank Jennifer Hrobar and the rest of the University of Texas at Austin Urban Forestry Department for granting us access to the bald cypress trees located on campus. We would also like to extend thanks to the City of Austin, Department of Parks and Recreation and Texas Parks and Wildlife for issuing our tree coring permits (permit no. *2023-Brandt-001* and permit no. *08-23*, respectively). We acknowledge Staci Loewy, Nathan Miller, and Aaron Satkoski from the University of Texas at Austin, Department of Earth and Planetary Sciences for lab analyses and geochemical insight. We thank Bryan Black from the University of Arizona for completing the dendrochronology on all cores. Thanks to Ari Brant and Sneha Nachimuthu for field assistance.

9. Tables

Table 1: The hydrogeologic and urbanization characteristics of watersheds in this study.

Water-shed	**2003 Impervious Cover[1] (%)**	**2019 Impervious Cover[2,3] (%)**	**Population Density (person/km)[3]**	**Primary Bedrock Units[4]**	**Area (km^2)[3]**	**Bald cypress age range[3]**
Waller Creek	43	58	2,363	Austin Chalk	15	1933-2023
Onion Creek	6.2	9.5	59	Glen Rose Fm., Edwards Limestone	547	1844-2023

[1] *Impervious cover calculations from the City of Austin, Texas, Watershed Protection Department (WPD, 2003). The City of Austin defines impervious cover as surfaces that cause water to run off into drainage systems. We modify this definition to exclude above-ground and in-ground pools, compacted soils, courtyards, golf courses, gravel/sandpits, open spaces, quarries, unpaved athletic fields, and paved ditches.*
[2] *Impervious cover calculations from the City of Austin, Texas, Watershed Protection Department (WPD, 2019).*
[3] *Data reported in Banner et al. (2024).*
[4] *Bedrock units are from the Bureau of Economic Geology, The University of Texas at Austin.*

Table 2: Filtered vs unfiltered (indicated using F and UF, respectively) streamwater sample concentration comparisons and percent differences. Detection limits are listed below each cation in parts per billion. Samples were collected from the same site on the same day and analyzed via ICP-MS.

Water-shed	**Site ID**	**Sample Date**	**F/ UF**	**Na** (ppm)	**Na** (% diff)	**Mg** (ppm)	**Mg** (% diff)	**K** (ppm)	**K** (% diff)	**Ca** (ppm)	**Ca** (% diff)	**Sr** (ppm)	**Sr** (% diff)
Detection limits (ppb)				**1.5**		**0.3**		**2.0**		**0.2**		**0.05**	
Waller	P40	4/16/22	F	38.0	0.6	14.1	5.5	8.5	3.4	103.0	0.7	0.4	1.1
			UF	37.8		14.9		8.8		102.4		0.4	
Waller	WW	4/16/22	F	58.4	0.1	10.0	4.7	25.2	7.1	109.4	0.3	0.5	0.7
			UF	58.4		9.5		4.2		127.6		0.5	
Waller	DSRS	4/16/22	F	27.6	0.5	4.9	0.5	3.9	3.5	127.2	0.2	0.4	0.3
			UF	27.4		4.9		2.2		99.8		0.4	
Waller	SHIPE	4/16/22	F	54.4	0.5	7.8	0.2	2.5	1.4	13.3	0.5	0.6	0.5
			UF	54.7		7.7		2.5		13.4		0.6	
Waller	DSP40	4/16/22	F	56.1	0.7	9.9	2.1	4.4	2.3	123.8	0.3	0.5	1.7
			UF	55.7		9.6		4.3		123.4		0.5	
Waller	DSRS	4/13/23	F	23.2	0.5	4.5	1.7	1.7	12.9	108.2	1.5	0.5	1.1
			UF	23.3		4.6		1.8		110.0		0.5	
Waller	WW	4/13/23	F	58.8	1.6	10.7	1.5	4.2	0.0	133.1	2.2	0.5	2.2
			UF	59.7		10.8		4.2		136.0		0.5	
Onion	US MCK	5/4/23	F	20.2	4.8	8.0	4.1	3.1	6.4	65.5	3.3	0.6	2.3
			UF	19.3		7.7		3.3		63.3		0.6	
Onion	TCK	7/5/23	F	27.6	2.8	7.0	1.3	3.2	13.4	50.8	0.4	0.6	0.6
			UF	26.8		6.9		3.6		50.6		0.6	

Table 3: Tree core analyses completed in this study, including watershed, increment dates, the date of core extraction, and the digestion method.

Watershed	Tree Number	Increment Years	Collection Date	Digestion Method
Waller	4172	1950-1954	4/8/23	Ashing
Waller	4172	1984-1987	4/8/23	Ashing
Waller	4172	2019-2023	4/8/23	Ashing
Onion	10	1870-1874	6/9/23	Ashing
Onion	10	1943-1947	6/9/23	Ashing
Onion	10	2017-2023	6/9/23	Ashing
Waller	4164	1955-1960	4/8/23	Ashing
Waller	4164	1983-1988	4/8/23	Ashing
Waller	4164	2017-2023	4/8/23	Ashing
Waller	3924	1950-1954	6/29/23	Ashing
Waller	3924	1983-1987	6/29/23	Ashing
Waller	3924	2017-2023	6/29/23	Ashing
Waller	3924	1953-1957	6/29/23	Ashing
Waller	3924	1985-1989	6/29/23	Ashing
Waller	3924	2017-2023	6/29/23	Ashing
Waller	4036	1951-1955	6/30/23	Ashing
Waller	4036	1985-1989	6/30/23	Ashing
Waller	4036	2017-2023	6/30/23	Ashing
Onion	6	1878-1882	6/9/23	Ashing
Onion	6	1948-1952	6/9/23	Ashing
Onion	6	2017-2023	6/9/23	Ashing
Onion	14	1855-1859	6/9/23	Ashing
Onion	14	1937-1941	6/9/23	Ashing
Onion	14	2017-2023	6/9/23	Ashing
Waller	4161	1970-1975	4/8/23	Ashing
Waller	4161	1993-1997	4/8/23	Ashing
Waller	4161	2017-2022	4/8/23	Ashing
Waller	4204	1990-1994	4/8/23	Ashing
Waller	4204	2003-2007	4/8/23	Ashing
Waller	4204	2016-2021	4/8/23	Ashing
Waller	3920	1948-1953	6/29/2023	Ashing
Waller	3920	1985-1990	6/29/2023	Ashing

Waller	3920	2016-2021	6/29/2023	Ashing
Waller	3920	1948-1953	6/29/2023	Microwave
Waller	4161	2017-2023	4/8/23	Microwave
Waller	4171	2019-2023	6/29/23	Ashing
Waller	4171	2014-2018	6/29/23	Microwave
Waller	4171	2009-2013	6/29/23	Microwave
Waller	4171	2004-2008	6/29/23	Microwave
Waller	4171	1999-2003	6/29/23	Microwave
Waller	4171	1994-1998	6/29/23	Microwave
Waller	4171	1989-1993	6/29/23	Microwave
Waller	4171	1982-1986	6/29/23	Ashing
Waller	4171	1977-1981	6/29/23	Microwave
Waller	4171	1972-1976	6/29/23	Microwave
Waller	4171	1967-1971	6/29/23	Microwave
Waller	4171	1962-1966	6/29/23	Microwave
Waller	4171	1957-1961	6/29/23	Microwave
Waller	4171	1950-1954	6/29/23	Ashing
Waller	4171	1945-1949	6/29/23	Microwave
Onion	3	1840-1849	7/6/23	Microwave
Onion	3	1850-1859	7/6/23	Microwave
Onion	3	1860-1869	7/6/23	Microwave
Onion	3	1870-1879	7/6/23	Microwave
Onion	3	1880-1889	7/6/23	Microwave
Onion	3	1890-1899	7/6/23	Microwave
Onion	3	1900-1909	7/6/23	Microwave
Onion	3	1910-1919	7/6/23	Microwave
Onion	3	1920-1929	7/6/23	Microwave
Onion	3	1930-1939	7/6/23	Microwave
Onion	3	1940-1944	7/6/23	Microwave
Onion	3	1945-1949	7/6/23	Microwave
Onion	3	1950-1954	7/6/23	Microwave
Onion	3	1955-1959	7/6/23	Microwave
Onion	3	1960-1964	7/6/23	Microwave
Onion	3	1965-1969	7/6/23	Microwave
Onion	3	1970-1974	7/6/23	Microwave
Onion	3	1975-1979	7/6/23	Microwave
Onion	3	1980-1984	7/6/23	Microwave
Onion	3	1985-1989	7/6/23	Microwave
Onion	3	1990-1994	7/6/23	Microwave

Onion	3	1995-1999	7/6/23	Microwave
Onion	3	2000-2004	7/6/23	Microwave
Onion	3	2005-2009	7/6/23	Microwave
Onion	3	2010-2014	7/6/23	Microwave
Onion	3	2015-2019	7/6/23	Microwave
Onion	3	2019-2023	7/6/23	Microwave

Table 4: Cation concentrations and percent differences between replicates for streamwater.

Water-shed	**Site ID**	**Sample Date**	**Na** (ppm)	**Mg** (ppm)	**K** (ppm)	**Ca** (ppm)	**Sr** (ppm)	**Percent Difference Range** (%)
Detection limit (ppb)			**1.5**	**0.3**	**2.0**	**0.2**	**0.05**	
Waller	P40	4/16/22	37.8	14.9	8.8	102.4	0.4	0.8 – 3.4
Waller	P40	4/16/22	38.1	15.1	9.2	104.8	0.4	
Waller	P40	9/14/22	47.6	18.2	9.7	68.1	0.3	0.3 – 3.5
Waller	P40	9/14/22	46.9	17.6	9.5	67.9	0.3	
Onion	TCK	10/23/22	18.4	6.8	4.1	61.2	0.7	0.0 – 8.8
Onion	TCK	10/23/22	18.5	6.8	3.8	55.8	0.7	
Waller	P40	12/3/22	40.1	17.3	7.3	62.2	0.2	1.7 – 3.0
Waller	P40	12/3/22	41.0	17.8	7.2	64.0	0.3	
Onion	McK	12/15/22	29.9	10.1	4.8	80.8	0.6	0.2 – 26.7
Onion	McK	12/15/22	30.0	10.1	6.0	83.1	0.6	
Waller	P40	2/13/23	45.2	19.0	7.7	76.7	0.3	0.2 – 2.0
Waller	P40	2/13/23	45.3	19.0	7.6	78.0	0.3	
Onion	McK	3/7/23	25.7	9.2	3.3	74.4	0.8	0.2 – 2.6
Onion	McK	3/7/23	25.9	9.2	3.2	76.3	0.8	
Waller	P40	4/13/23	50.9	16.4	11.3	139.2	0.5	0.0 – 1.4
Waller	P40	4/13/23	50.9	16.4	11.1	139.7	0.5	
Waller	WW	6/19/23	26.9	5.3	3.4	74.7	0.3	0.0 – 1.7
Waller	WW	6/19/23	27.2	5.3	3.4	75.9	0.3	

Table 5: Anion concentrations and percent differences between replicates for streamwater. BDL indicates that the concentration is below the limit of detection.

Water-shed	**Site ID**	**Sample Date**	**F** (ppm)	**Cl** (ppm)	**NO_3** (ppm)	**SO_4** (ppm)	**HCO_3** (ppm)	**Percent Difference Range** (%)
Detection limits (ppm)			**0.04**	**0.2**	**0.2**	**0.2**		
Waller	P40	4/16/22	0.5	64.0	14.4	83.4	252.5	0.1 – 0.7
Waller	P40	4/16/22	0.5	63.9	14.4	83.5	253.2	
Waller	P40	9/14/22	0.8	77.9	0.9	159.8	125.7	0.1 – 22.1
Waller	P40	9/14/22	0.8	77.9	1.2	158.5	119.6	
Onion	TCK	10/23/22	BDL	17.0	BDL	60.5	169.6	0.0 – 2.9
Onion	TCK	10/23/22	BDL	16.9	BDL	60.5	164.7	
Waller	P40	12/3/22	BDL	67.0	4.2	114.9	104.9	0.0 – 12.1
Waller	P40	12/3/22	BDL	67.1	3.7	115.2	100.0	
Onion	McK	12/15/22	BDL	45.1	3.6	49.9	134.7	0.1 – 32.4
Onion	McK	12/15/22	BDL	45.0	BDL	49.9	178.4	
Waller	P40	2/13/23	0.7	88.9	16.7	59.4	92.7	1.0 – 61.8
Waller	P40	2/13/23	0.7	89.8	17.1	96.2	104.9	
Onion	McK	3/7/23	0.3	39.3	BDL	133.7	136.6	0.3 – 5.4
Onion	McK	3/7/23	0.3	39.4	BDL	134.2	129.3	
Waller	P40	4/13/23	0.6	92.6	42.5	BDL	172.5	0.7 – 2.8
Waller	P40	4/13/23	0.7	93.4	42.8	161.6	176.4	
Waller	WW	6/19/23	0.3	37.0	3.3	39.8	185.4	0.0 – 7.7
Waller	WW	6/19/23	0.3	37.3	3.3	39.8	187.9	

Table 6a: Anion concentrations in streamwater field blanks. BDL indicates that the concentration is below the limit of detection.

Water-shed	**Sample Date**	**F** (ppm)	**Cl** (ppm)	**NO_2** (ppm)	**Br** (ppm)	**NO_3** (ppm)	**SO_4** (ppm)	**PO_4** (ppm)
Detection limits		**0.04**	**0.2**	**0.2**	**0.2**	**0.2**	**0.2**	**0.4**
Waller	4/16/22	BDL	BDL	BDL	BDL	BDL	0.3	BDL
Onion	10/23/22	BDL	BDL	BDL	BDL	BDL	BDL	BDL
Waller	12/3/22	BDL	BDL	BDL	BDL	BDL	BDL	BDL
Onion	12/15/22	BDL	BDL	BDL	BDL	BDL	BDL	BDL
Waller	2/13/23	BDL	BDL	BDL	BDL	BDL	BDL	BDL
Onion	3/7/23	BDL	BDL	BDL	BDL	BDL	3.1	BDL
Waller	4/13/23	BDL	BDL	BDL	BDL	BDL	BDL	BDL

Table 6b: Sample-to-blank ratio ranges for SO_4 concentrations for two sampling events. The ranges represent the sample-to-blank ratio calculated for each analyzed Waller Creek sample collected in the sampling event.

Watershed	**Sample Date**	**Creek Sites Sampled**	**SO_4** Sample/Blank
Waller	4/16/22	7	114 - 273
Onion	3/7/23	4	44 - 56

Table 7a: Cation concentrations in streamwater field blanks. BDL indicates that the concentration is below the limit of detection.

Water-shed	**Sample Date**	**Na** (ppm)	**Mg** (ppm)	**K** (ppm)	**Ca** (ppm)	**Sr** (ppm)
Detection limits (ppb)		**1.5**	**0.3**	**2**	**0.2**	**0.05**
Waller*	4/16/22	BDL	BDL	0.06	BDL	BDL
Onion	10/23/22	0.40	BDL	BDL	BDL	BDL
Waller	12/3/22	0.20	BDL	0.74	BDL	BDL
Onion	12/15/22	BDL	BDL	BDL	0.29	BDL
Waller	2/13/23	0.36	BDL	0.02	BDL	BDL
Onion	3/7/23	0.41	BDL	0.02	BDL	BDL
Waller	4/13/23	0.86	0.02	0.04	0.10	BDL

*The Waller Creek blank data presented here is from an unfiltered blank sample. All other blank samples above were filtered.

Table 7b: Sample-to-blank ratio ranges for Waller Creek and Onion Creek field blank concentrations. The ranges represent the sample-to-blank ratio calculated for each analyzed Waller Creek sample collected in the sampling event.

Water-shed	**Sample Date**	**Creek Sites Sampled**	**Na** Sample/ Blank	**Mg** Sample/ Blank	**K** Sample/ Blank	**Ca** Sample/ Blank
Waller	4/16/22	7	BDL	BDL	34 - 142	BDL
Onion	10/23/22	2	47 - 183	BDL	BDL	BDL
Waller	12/3/22	6	109 - 258	BDL	5 - 10	BDL
Onion	12/15/22	2	BDL	BDL	BDL	242 - 284
Waller	2/13/23	7	68 - 183	BDL	102 - 374	BDL
Onion	3/7/23	4	53 - 66	BDL	127 - 134	BDL
Waller	4/13/23	6	27 - 69	286 – 1039	46 - 312	1012 - 1365

Table 8: $^{87}Sr/^{86}Sr$ in streamwaters analyzed for this study.

Watershed	**Sample Site**	**Sample Date**	**$^{87}Sr/^{86}Sr$**	**2σ**
Waller	WW	4/13/23	0.708919	0.000012
Waller	WW	6/19/23	0.708858	0.000012
Waller	WW	8/18/23	0.708922	0.000015
Waller	WW	10/18/23	0.708865	0.000016
Onion	OCSC	3/7/23	0.708108	0.000010
Onion	OCSC	5/4/23	0.708123	0.000013
Onion	McK	5/4/23	0.708120	0.000007

Table 9: Bald cypress sample replicates analyzed for $^{87}Sr/^{86}Sr$ using TIMS.

Number of Replicate Analyses	**Replicate 1**	**Replicate 2**	**Replicate 3**	**Replicate 4**	**Replicate 5**	**Variab-ility**
3	0.708618	0.708634	0.708642			0.00002
5	0.708792	0.708729	0.708752	0.708750	0.708750	0.00006

Table 10: Ages and estimated heartwood-sapwood boundaries in cores collected in 2023.

Watershed	**Core ID**	**Tree Age**	**Heartwood – Sapwood Boundary**	**Number of Sapwood Rings**
Waller	4172	1950	1996	27
Waller	4164	1955	1996	27
Waller	3924A	1950	2005	18
Waller	3924B	1953	2003	20
Waller	4036	1951	1991	32
Waller	4161	1970	1991	32
Waller	4204	1990	2005	18
Waller	3920	1948	2017	6
Waller	4171	1945	2003	20
Onion	14	1855	1964	59
Onion	6	1878	1990	33
Onion	10	1847	1977	46
Onion	3	1840	1994	29

Table 11: The p-value here here represents the statistical significance in the difference between the concentrations (and $^{87}Sr/^{86}Sr$ ratios) found in the heartwood and in the sapwood. The coefficient of variance was used to determine whether to use an equal variance or an unequal variance test.

Element	Heartwood or Sapwood	Coefficient of Variation (%)	P Value
Sr $n = 75$	Heartwood	53	0.001
	Sapwood	37	
Ca $n = 75$	Heartwood	96	0.023
	Sapwood	74	
K $n = 75$	Heartwood	71	0.224
	Sapwood	95	
Mg $n = 75$	Heartwood	47	0.000
	Sapwood	29	
Na $n = 75$	Heartwood	62	0.027
	Sapwood	89	
P $n = 75$	Heartwood	87	0.000
	Sapwood	31	
$^{87}Sr/^{86}Sr$ $n = 60$	Heartwood	0.04	0.348
	Sapwood	0.04	

Table 12: Results of the Wilcoxon signed rank tests used to determine statistically significant differences between elements and $^{87}Sr/^{86}Sr$ ratios in cores' heartwood and sapwood. For each element, the null hypothesis (N_0) was that the concentrations (or values, in the case of $^{87}Sr/^{86}Sr$) were equivalent between the sapwood and the heartwood.

	$^{87}Sr/^{86}Sr$	Na	Mg	K	Ca	Sr	P
Sample Size	11	13	13	13	13	13	13
Test Statistic	9	0	0	35	32	7	0
Critical Value ($\alpha = 0.05$)	10	17	17	17	17	17	17
Reject N_0?	Yes	Yes	Yes	No	No	Yes	Yes

10. Figures

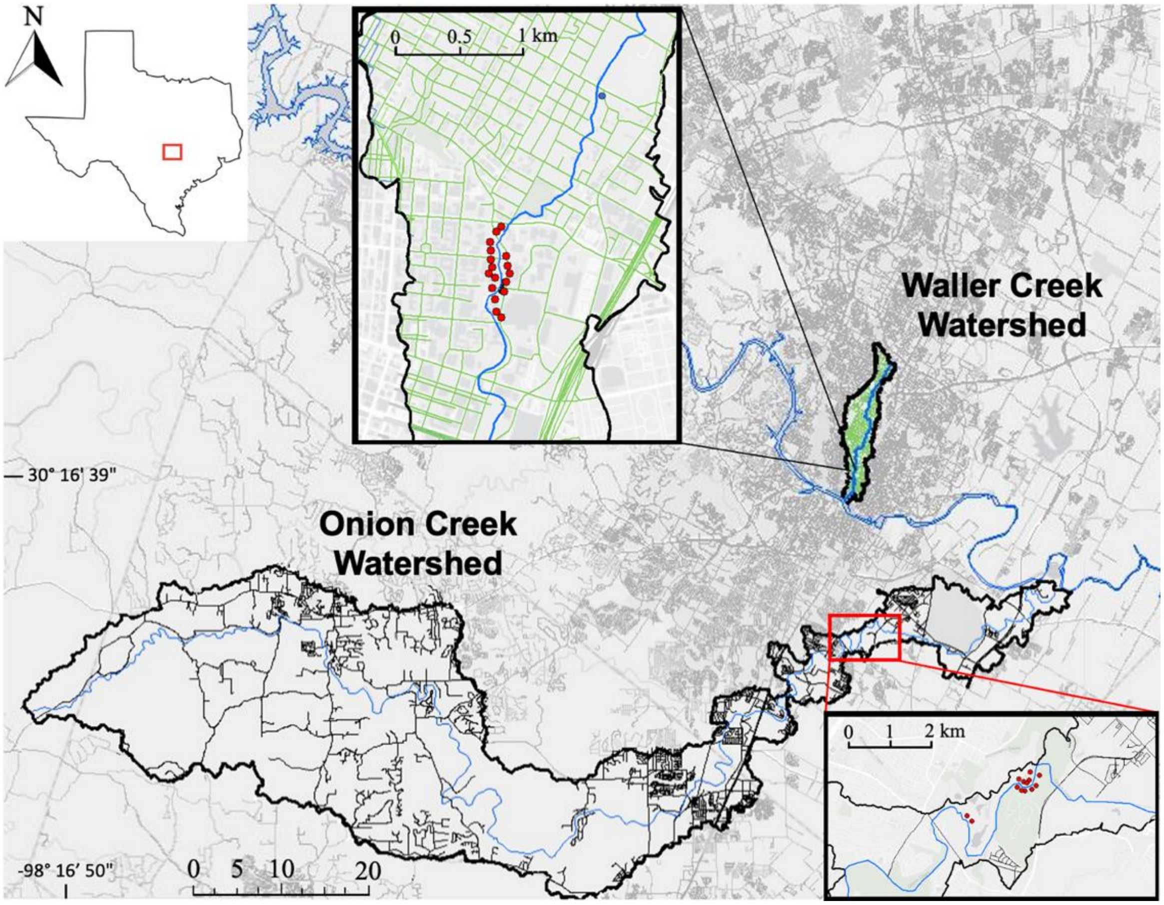

Figure 1: **Austin-area road densities and sampled trees** highlighting Waller Creek and Onion Creek watersheds. Sampled trees from this study are indicated by red circles. The inset box in the top left corner shows the location of these two watersheds within the state of Texas. GIS data for watershed boundaries and streams are from the City of Austin (2016) (http://data.austintexas.gov, Accessed July 2023) and road densities are from the Texas Department of Transportation (2020) (https://gis-txdot.opendata.arcgis.com).

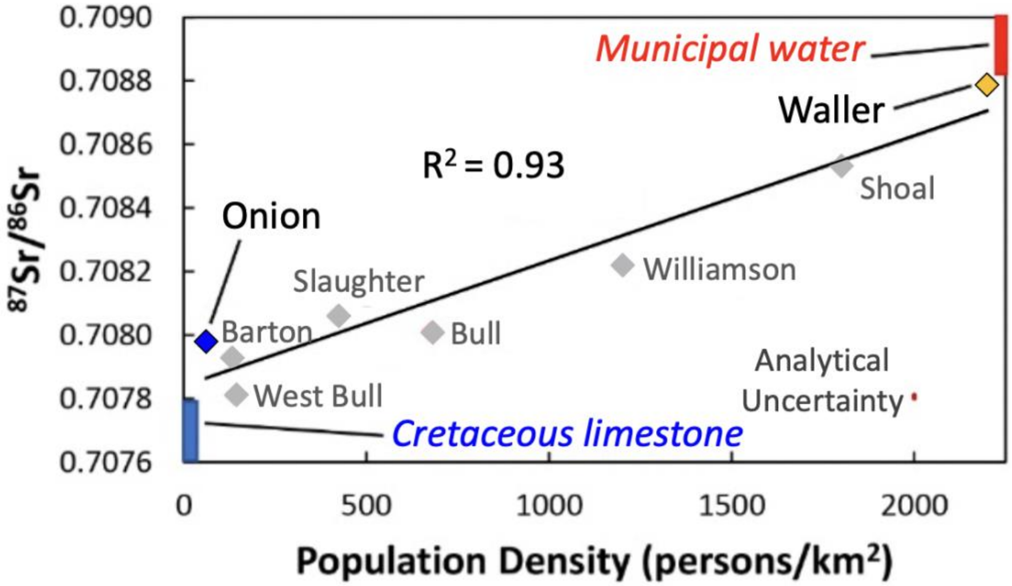

Figure 2: **Variation in stream water $^{87}Sr/^{86}Sr$ ratios with population density. Streamwater** data was collected between 2001 and 2011 by the Banner Research Group and population density for eight Austin-area watersheds comes from the City of Austin (2011). The $^{87}Sr/^{86}Sr$ range of municipal (i.e., tap and wastewater) collected from within these watersheds is represented by the red bar. The $^{87}Sr/^{86}Sr$ ratio range of Cretaceous limestone samples collected from these watersheds is represented by the blue bar. This figure is modified from Christian et al., 2011 to emphasize Waller Creek and Onion Creek streamwater data.

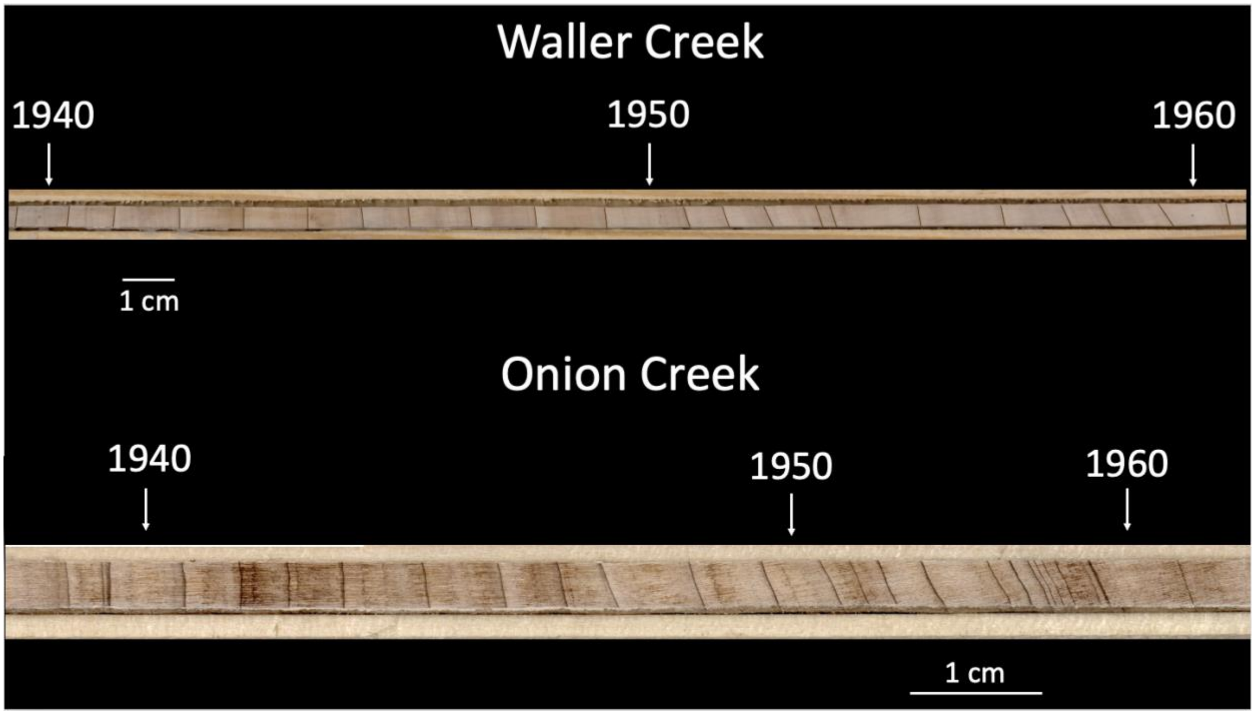

Figure 3: **Drought of the 1950s, displayed in Waller and Onion Creek tree rings**. The top image is a bald cypress tree core from Waller Creek watershed and the bottom image is an Onion Creek watershed bald cypress tree core. Growth rings shown include those from the drought of the 1950s (1949-1957) are shown. Onion Creek trees are more prone to respond to climate fluctuations due to the lack of municipal input during drought conditions, leading to thinner growth rings during drought conditions (Banner et al., 2024).

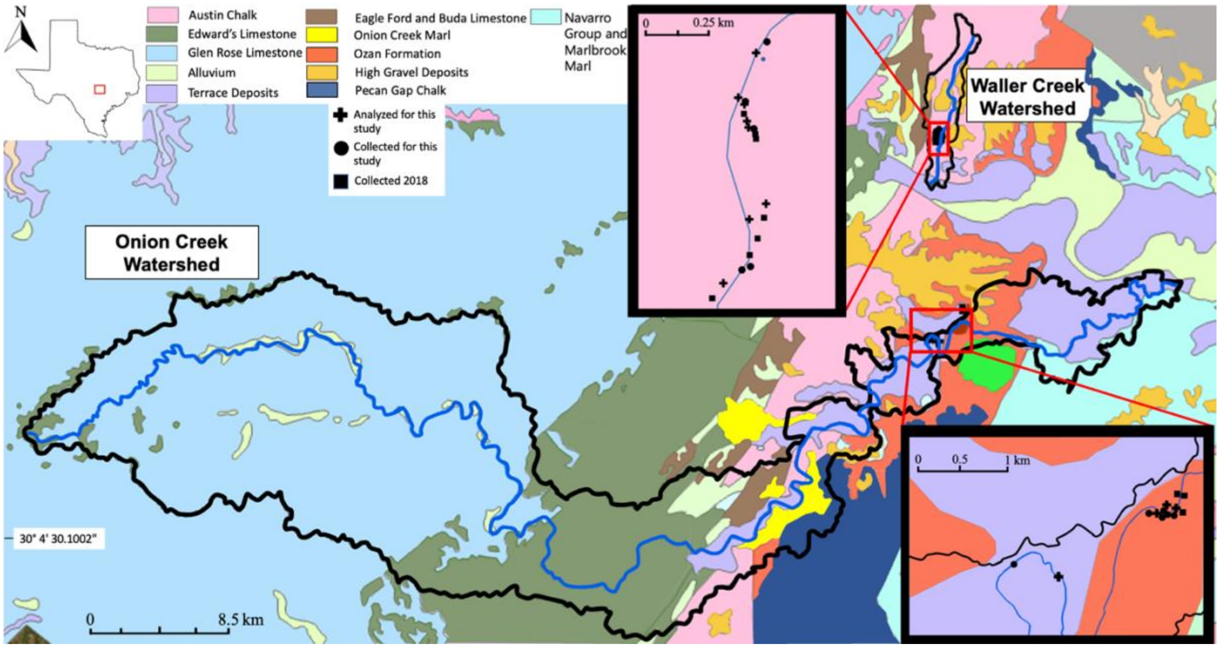

Figure 4: **Geologic map of the Austin area.** Waller Creek and Onion Creek watershed boundary and stream GIS data from the City of Austin (http://data.austintexas.gov). Geologic data are from the Bureau of Economic Geology, The University of Texas at Austin (Bureau of Economic Geology; 1:62,500 scale). The major Cretaceous units impacting these watersheds include the Navarro Group and the Marlbrook Marl, the Pecan gap chalk, the Ozan Formation, the Austin Chalk, the Eagle Ford Formation and the Buda Limestone, the Del Rio Clay and the Georgetown Limestone, the Edwards Limestone, the Fredericksburg Group, and the Glen Rose Limestone. Quaternary units include alluvium, terrace deposits, the Onion Creek Marl, and the High gravel deposits.

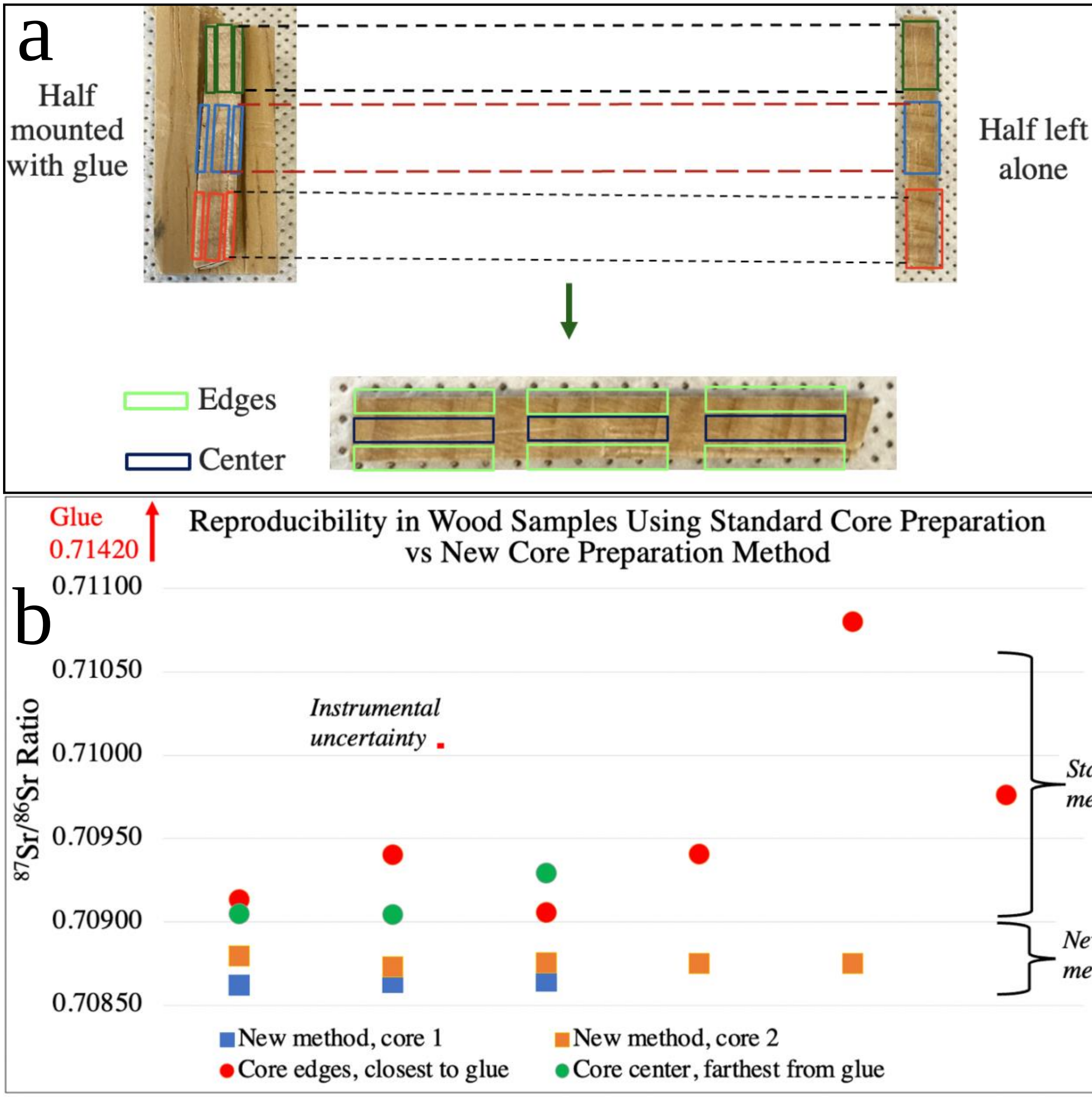

Figure 5: **Glue contamination and method reproducibility test.** a) A core segment containing 6 annual growth rings was split vertically in two halves. One half was mounted (left) and the corresponding half was not (right). The edge pieces of mounted wood, in direct contact with the glue (green rectangles), were analyzed separately from the center pieces (black rectangles) to determine infiltration of the glue into the pores of the wood. b) $^{87}Sr/^{86}Sr$ ratios found in bald cypress cellulose prepared and mounted the standard way, using Elmer's glue (circles). These values are compared to ratios found in 2 sets of samples prepared without glue (blue and orange squares). All samples were digested using the methods developed in this project and analyzed using TIMS (analytical uncertainty is +/-0.000017). These analyses were done on a core taken from a Waller Creek bald cypress tree (tree ID #2987).

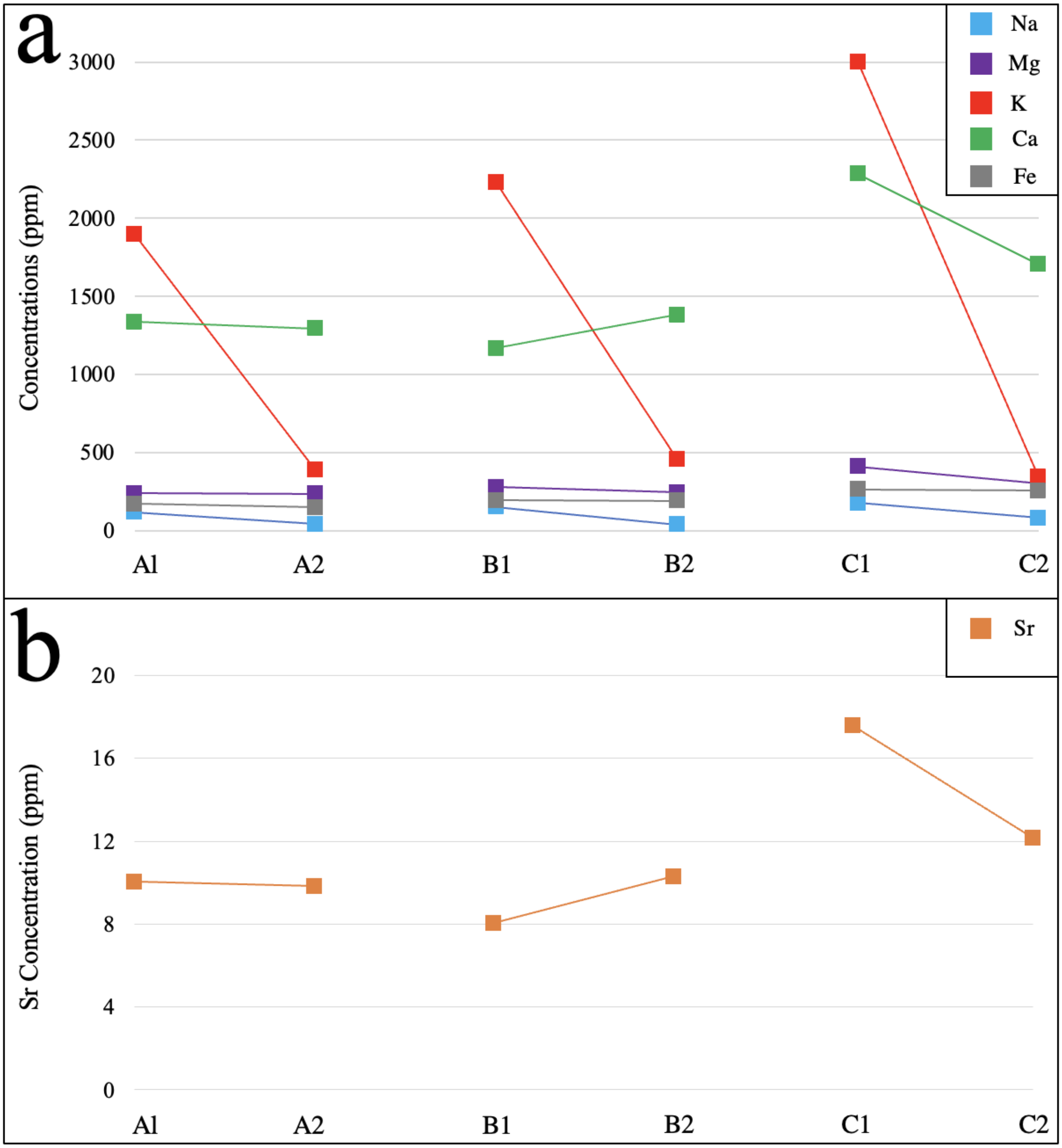

Figure 6: **Interstitial water extraction results**. a) Major cation concentration differences between soaked (A2, B2, and C2) and not soaked (A1, B1, and C1) bald cypress halves. b) Sr concentration differences between the same segments with a different y-axis for ease of interpretation. The data points in a and b are larger than or equal to the size of the error bars.

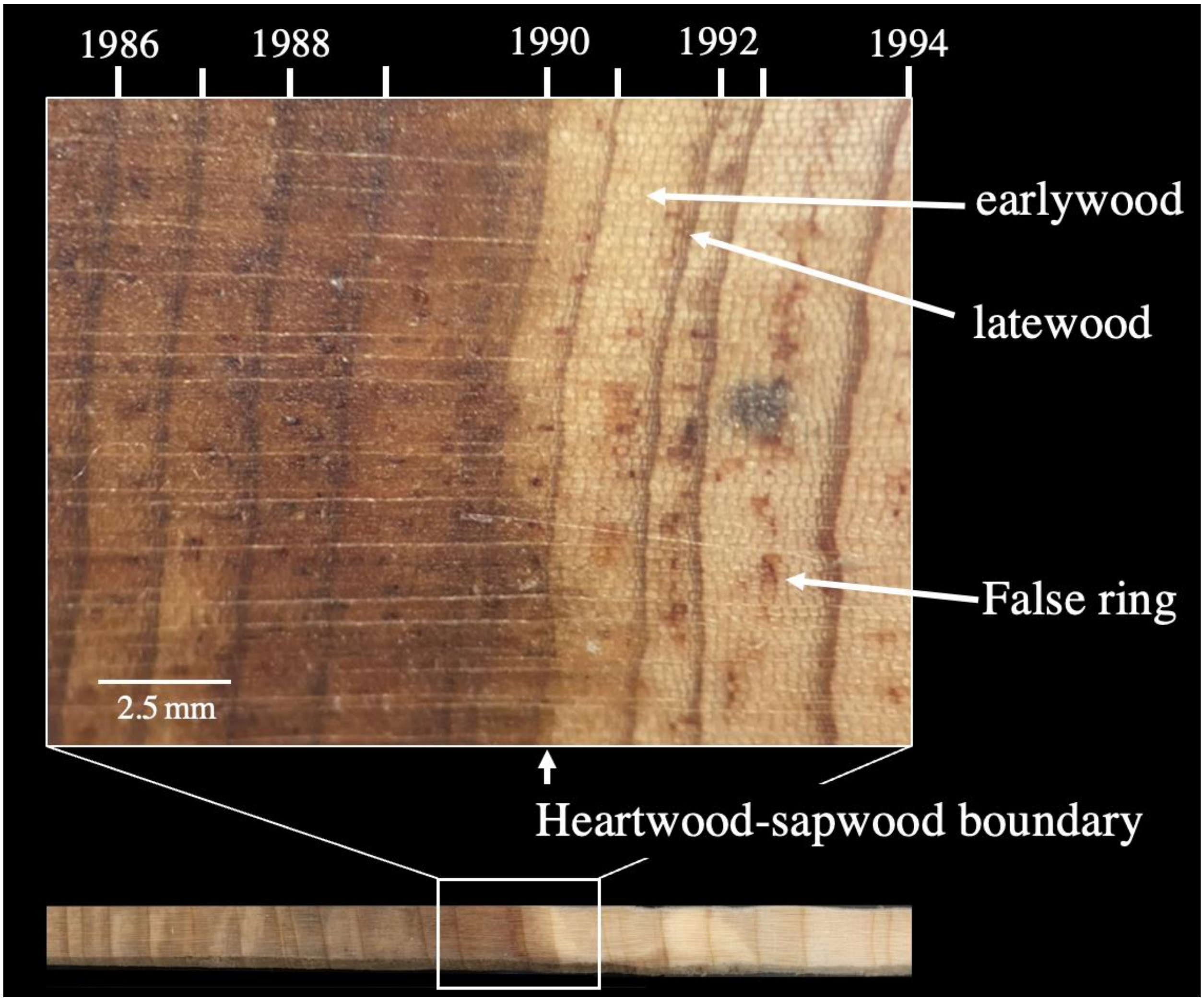

Figure 7: **A bald cypress heartwood-sapwood boundary**. Bald cypress core wood sliced with an ethanol-cleaned, stainless steel razor blade to produce a flat surface that was dated using dendrochronology. Cores were scanned at 2600 dpi. Growth rings displayed here are 1978 – 1999 (left to right) in Onion Creek core 4171. The drastic color change from brown to tan (observed in all cores) was used to help determine the heartwood-sapwood boundary.

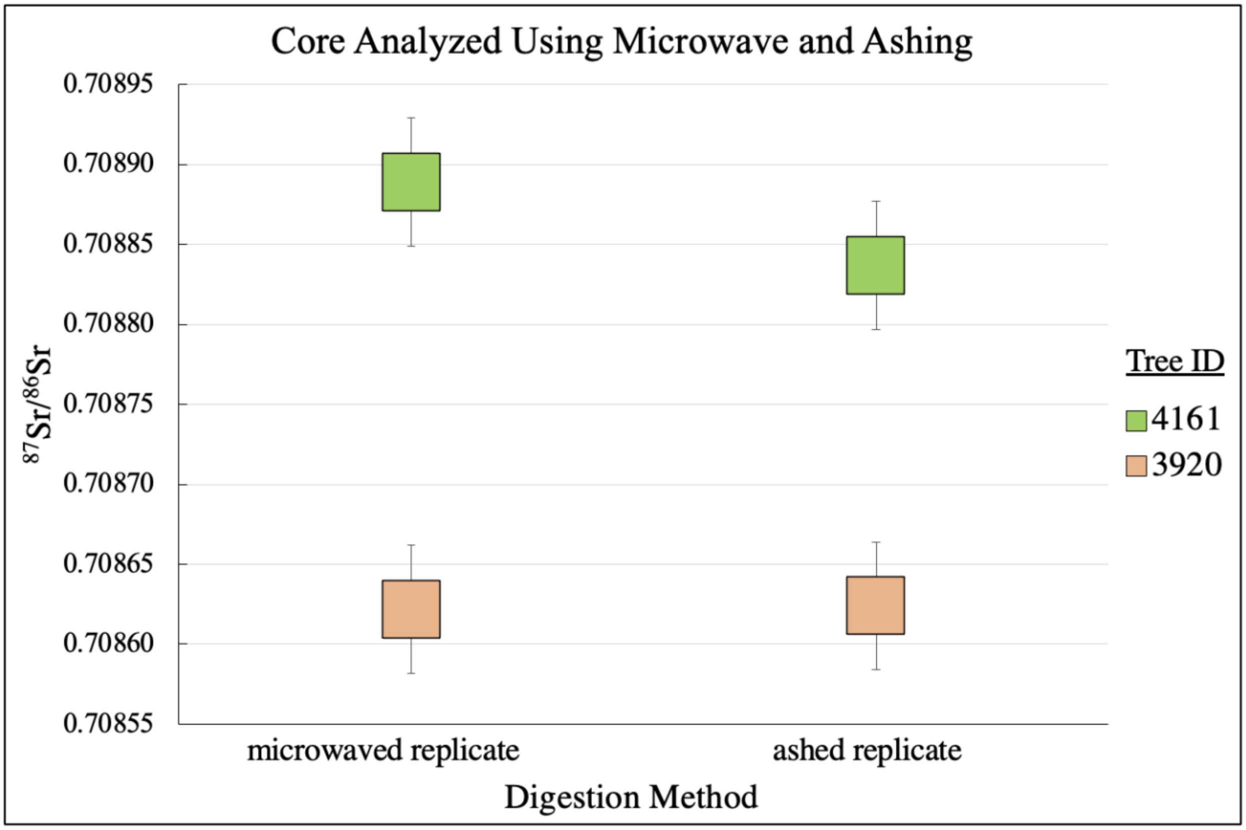

Figure 8: **Comparison of wood digestion methods.** A comparison of replicate core increments using different methods of digestion (i.e., microwave and ashing). The size of the markers is the size of the analytical uncertainty (+/0.000017), indicating that Waller Creek tree #3920 reproduces within analytical uncertainty between the two methods. The visible error bars represent the variation found within a replicate analysis of the same sample using the uncertainty represented by the ashing method (+/-0.00004).

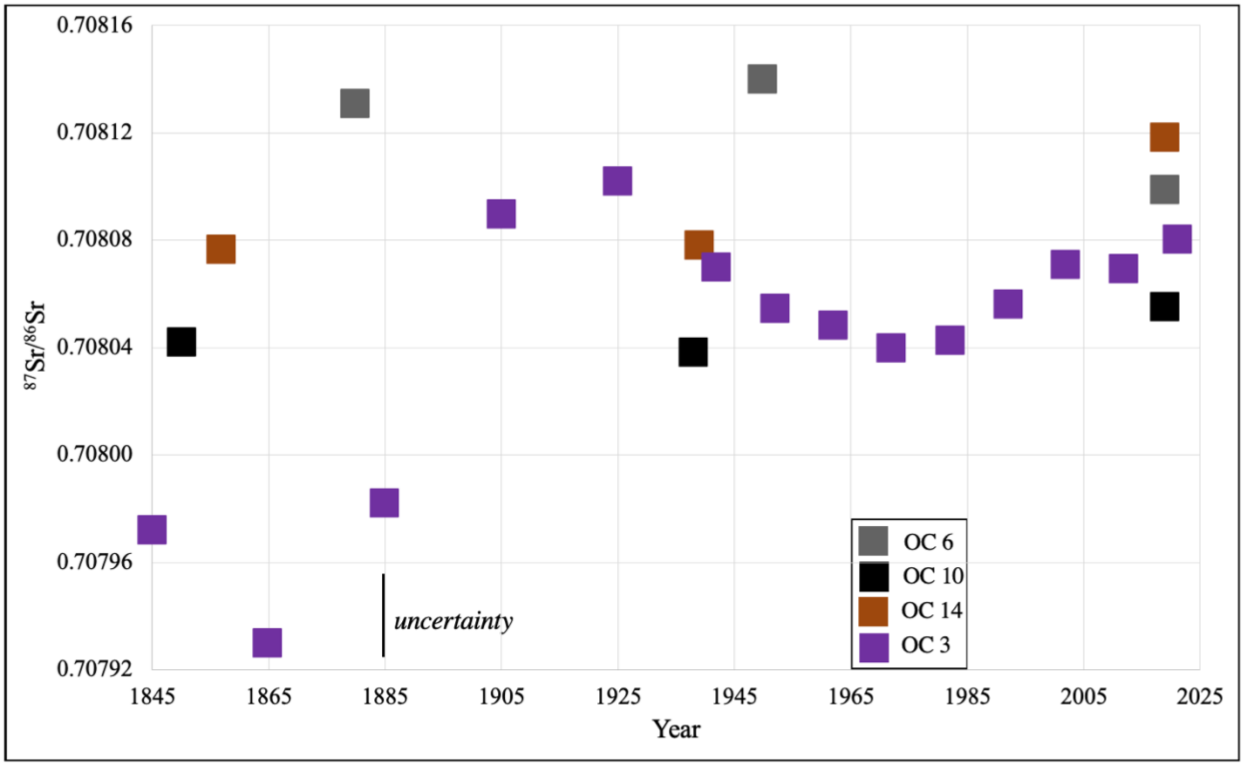

Figure 9: **Temporal $^{87}Sr/^{86}Sr$ ratios in Onion Creek trees.** The horizontal length of the squares is the 5-year time span covered by each analyzed set of growth rings. The $^{87}Sr/^{86}Sr$ ratios for Tree OC 6 and Tree OC 10 follow a similar pattern with an overall increase between the oldest and youngest points while the ratio decreases over time for Tree OC 6. The uncertainty is +/- 0.000017.

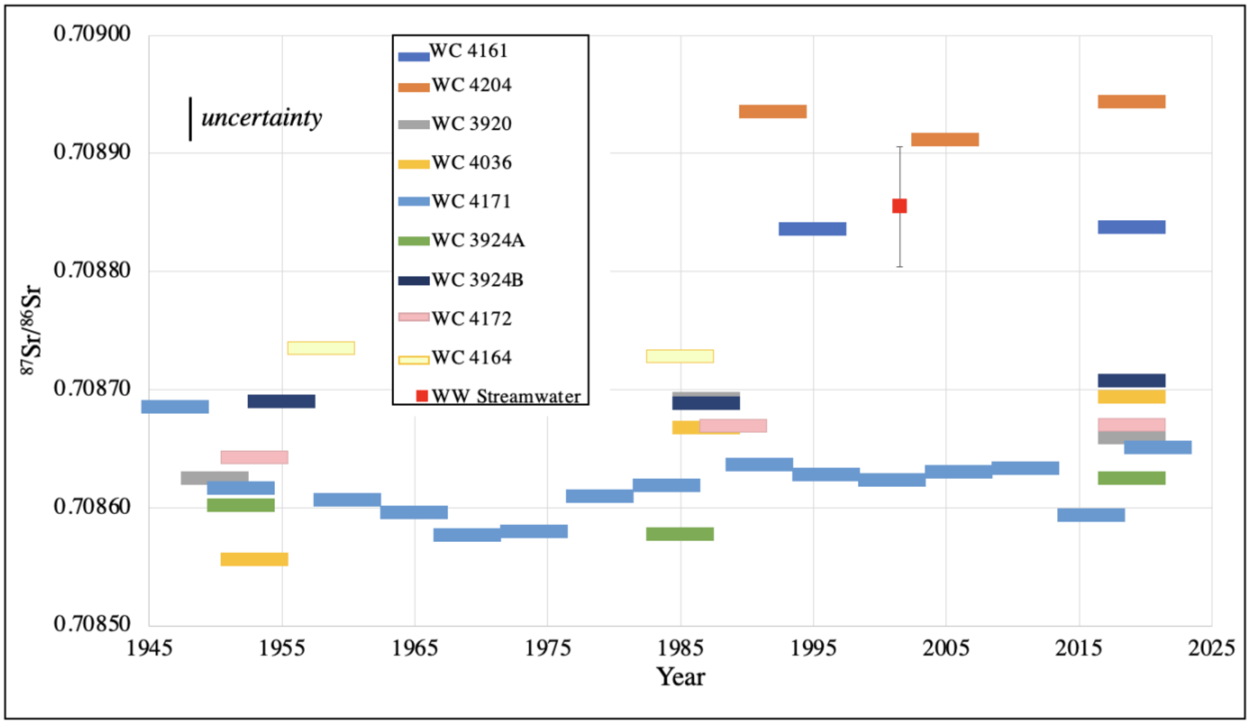

Figure 10: **Temporal $^{87}Sr/^{86}Sr$ ratios in Waller Creek trees.** The horizontal length of the rectangles is the 5-year time span covered by each analyzed increment. The red square and error bar are the average $^{87}Sr/^{86}Sr$ ratio and one standard deviation of the mean of Waller Creek streamwater collected from the same site each week for one year (Christian et al., 2011). The $^{87}Sr/^{86}Sr$ ratios through time are within the variability of one year of streamwater data, aside from trees 4171 and 4036, which both show significant fluctuations. The uncertainty is +/-0.000017.

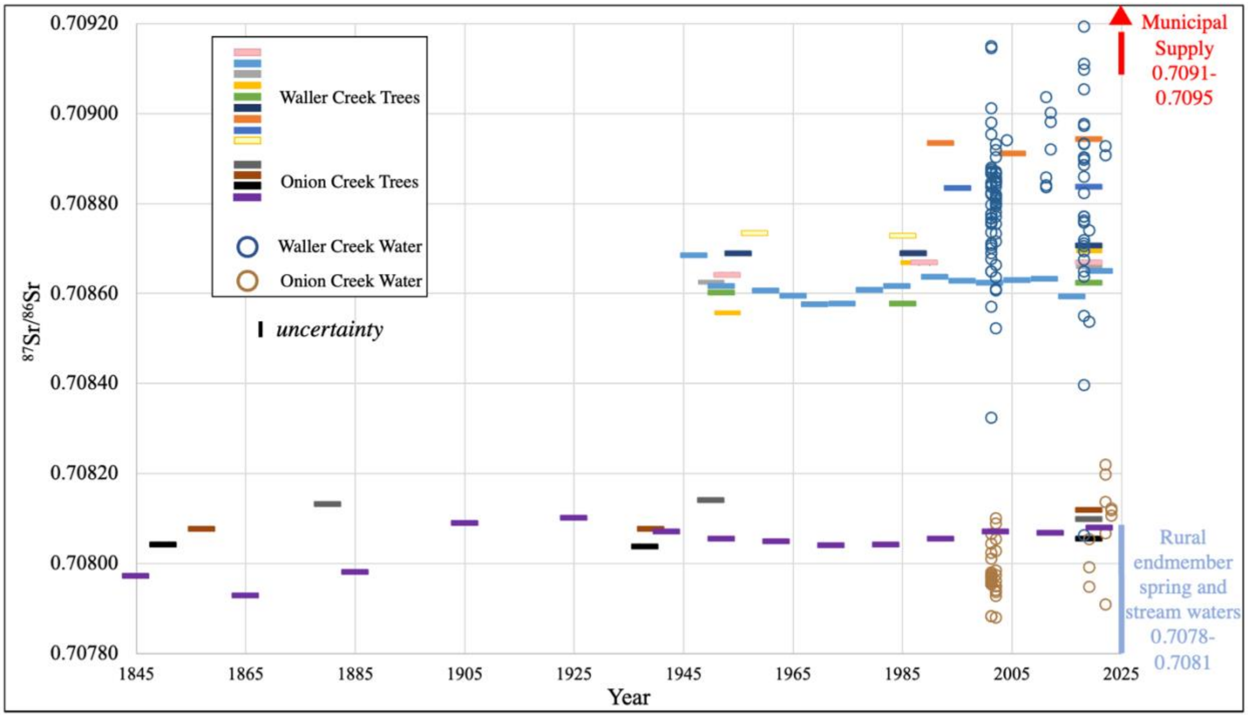

Figure 11: **Temporal $^{87}Sr/^{86}Sr$ ratios in all trees and streamwaters**. Bald cypress $^{87}Sr/^{86}Sr$ ratios in Waller Creek and Onion Creek tree rings over time (5-year increments) plotted alongside streamwater samples from the same streams. In Waller Creek trees, variation within individual tree cores (n = 9) ranges from 0.000001 to 0.000137 and averages 0.000049. In Onion Creek trees, variation within individual trees (n = 4) ranges from 0.000017 to 0.00017 and averages 0.000068. In each watershed, the range of all analyzed streamwater Sr isotopes encapsulates the full range of tree data over time.

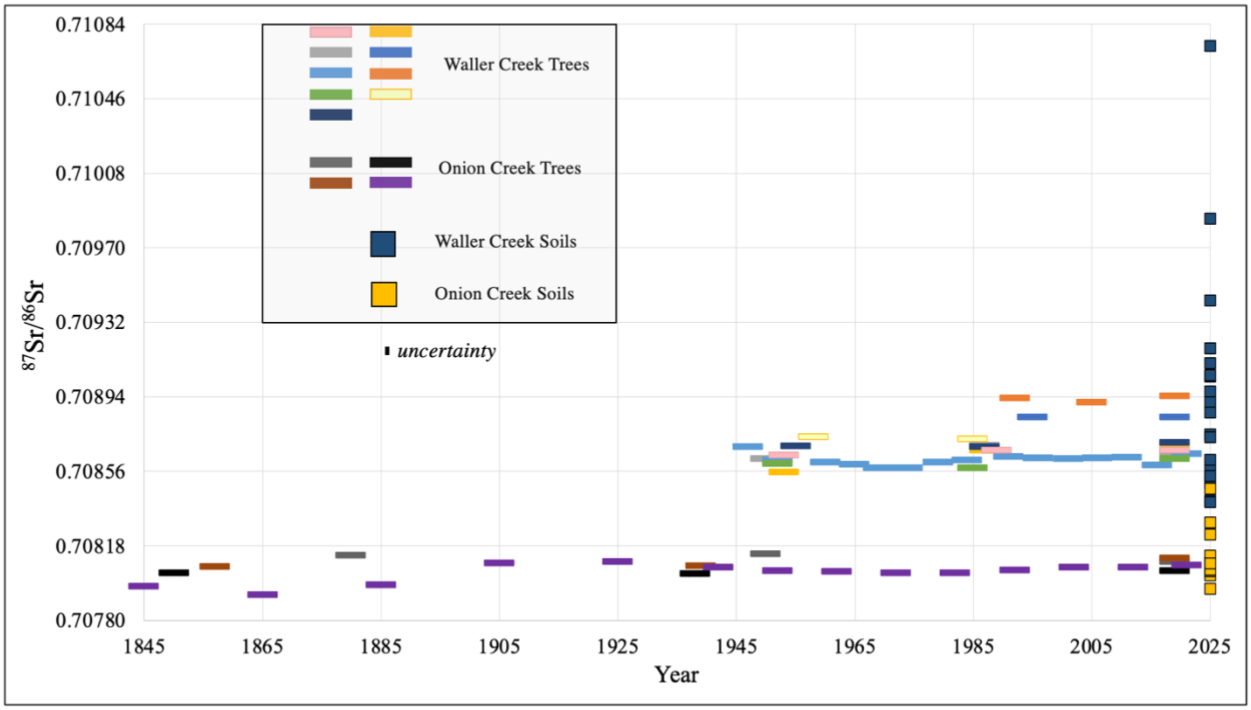

Figure 12: **Temporal $^{87}Sr/^{86}Sr$ ratios in all trees and soils.** Bald cypress $^{87}Sr/^{86}Sr$ ratios in Waller Creek and Onion Creek tree rings over time (5-year increments) compared with the range of irrigated and unirrigated soil ratios in each watershed (Mauceri & Banner, 2023; Beal et al., 2020; Christian et al., 2011). Onion Creek soils (n = 11) range from 0.70797 to 0.70848 (yellow squares) and Waller Creek soils (n = 19) range from 0.70840 to 0.71073 (blue squares). The range of Sr isotope ratios of trees within each watershed fall within the range of $^{87}Sr/^{86}Sr$ ratios found within soils and waters from each watershed. Analytical uncertainty is +/-0.000017.

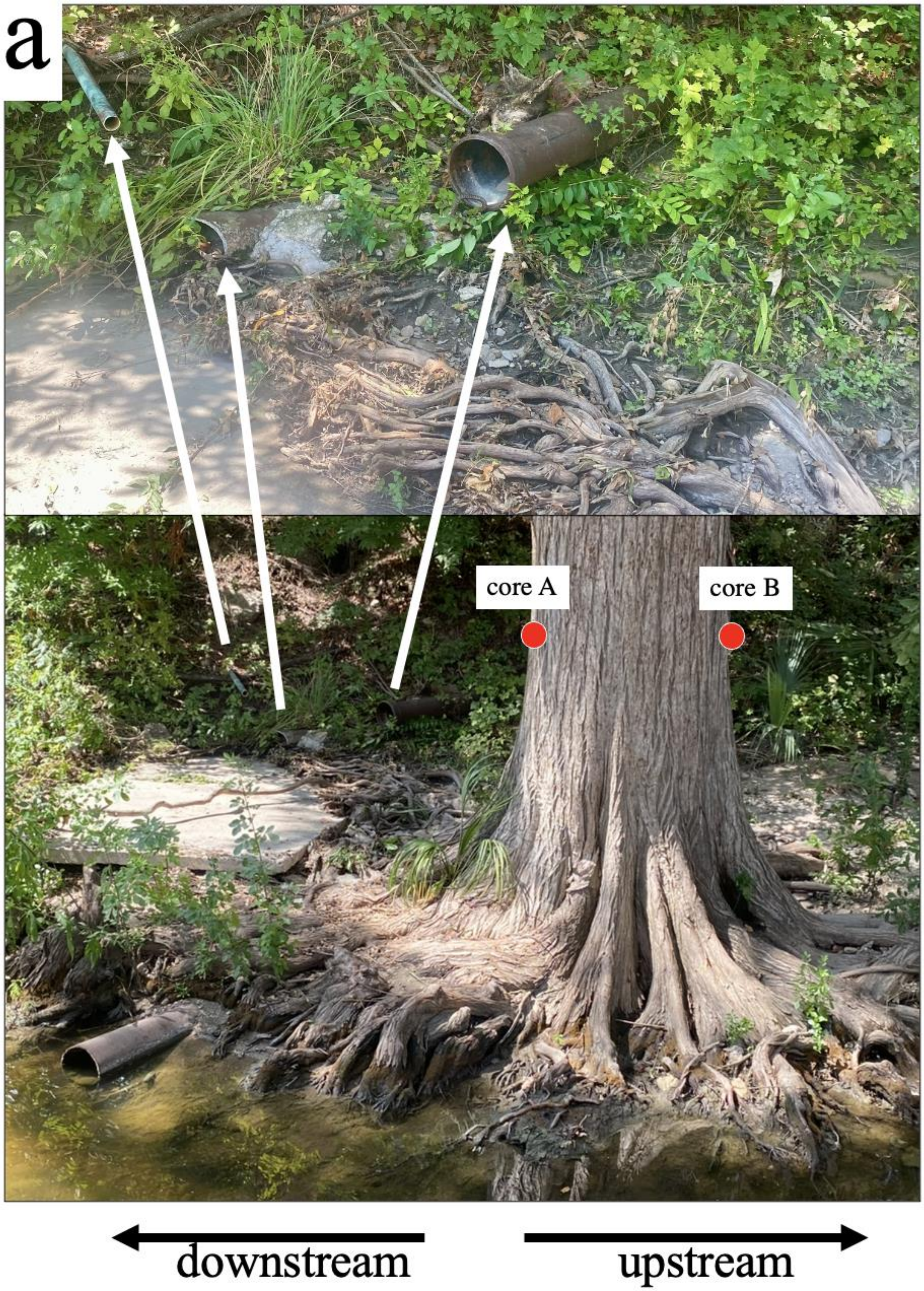
a
core A
core B
downstream
upstream

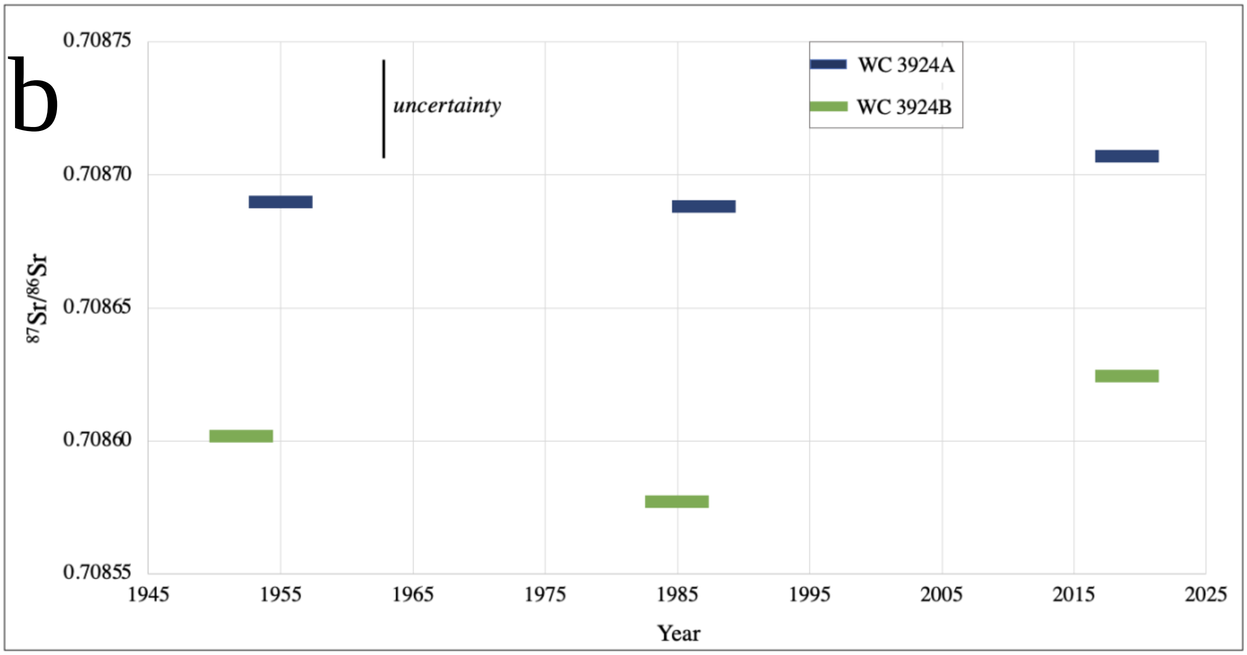

Figure 13: **$^{87}Sr/^{86}Sr$ ratios in two cores taken from the same tree.** a) A photograph of Waller Creek tree 3924 with a zoomed-in photograph of the pipes on the downstream side of the tree. Core 'A' was taken from the upstream side of the tree (the right side of this photo) while core 'B' was collected from the downstream side of the tree (the left side in this photo). There are 3 pipes that, if flowing, would allow water to flow across the roots on the downstream side of the tree. These pipes have not been observed to be flowing during this study. b) The $^{87}Sr/^{86}Sr$ ratios of two cores taken from the same tree (Waller Creek 3924). Analytical uncertainty is 0.000017.

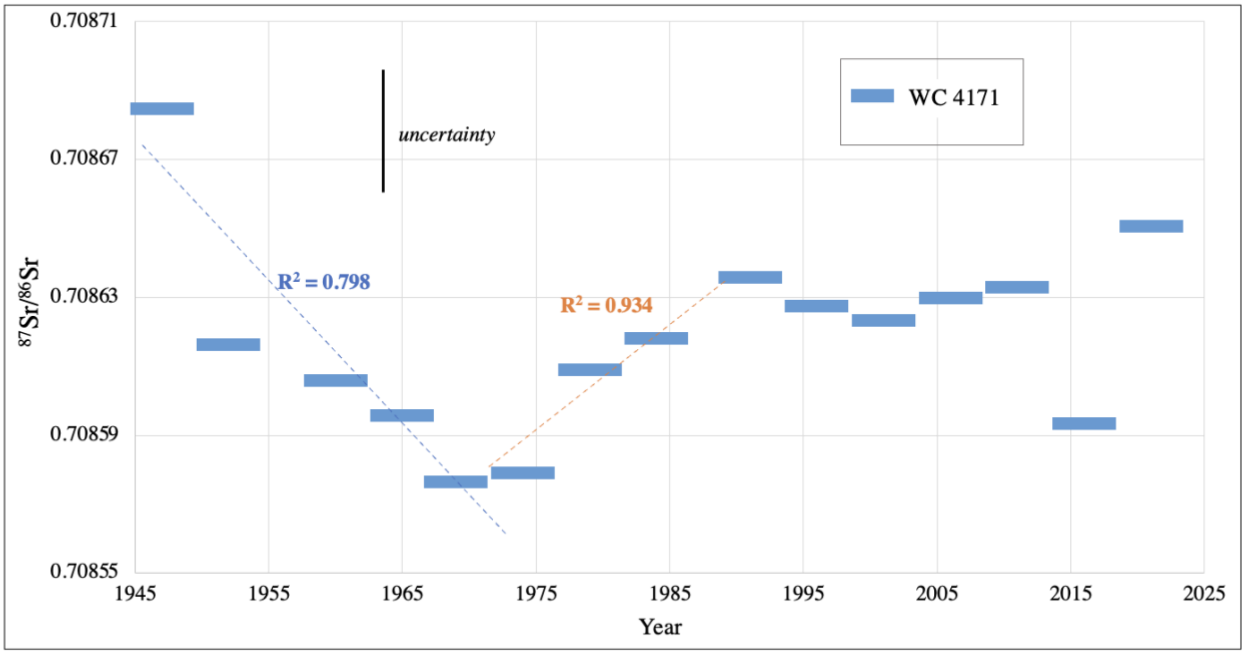

Figure 14: **$^{87}Sr/^{86}Sr$ ratios in 5-year segments of a full core.** The temporal trend of $^{87}Sr/^{86}Sr$ in one core (Waller Creek 4171) from pith to bark in 5-year segments. There is a strong linear decrease in the $^{87}Sr/^{86}Sr$ values between 1945 to 1971 followed by a strong linear increase in $^{87}Sr/^{86}Sr$ between 1971 and 1993. Analytical uncertainty shown is +/-0.000017.

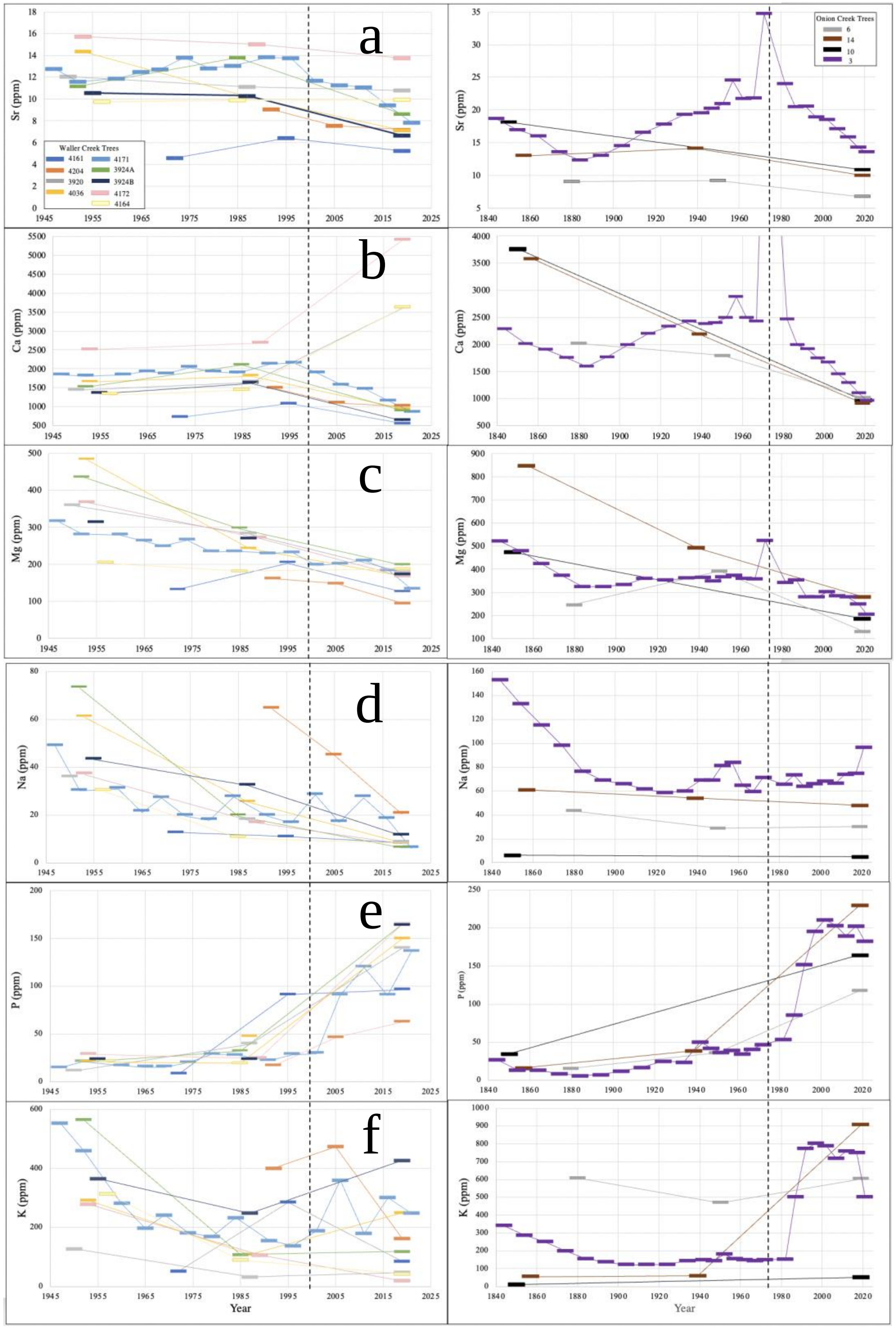
a
b
c
d
e
f
Sr (ppm)
Ca (ppm)
Mg (ppm)
Na (ppm)
P (ppm)
K (ppm)
Year
Waller Creek Trees
4161
4171
4204
3924A
3920
3924B
4036
4172
4164
Onion Creek Trees
6
14
10
3

Figure 15: **Temporal trends of trace elements in tree cores.** The temporal trend of major cations and strontium in all Waller Creek and Onion Creek cores. The black dashed line represents the average location of the heartwood-sapwood boundary from each dataset (i.e., Waller Creek and Onion Creek trees). R^2 values for each element within each watershed is presented in Supp. Table 1).

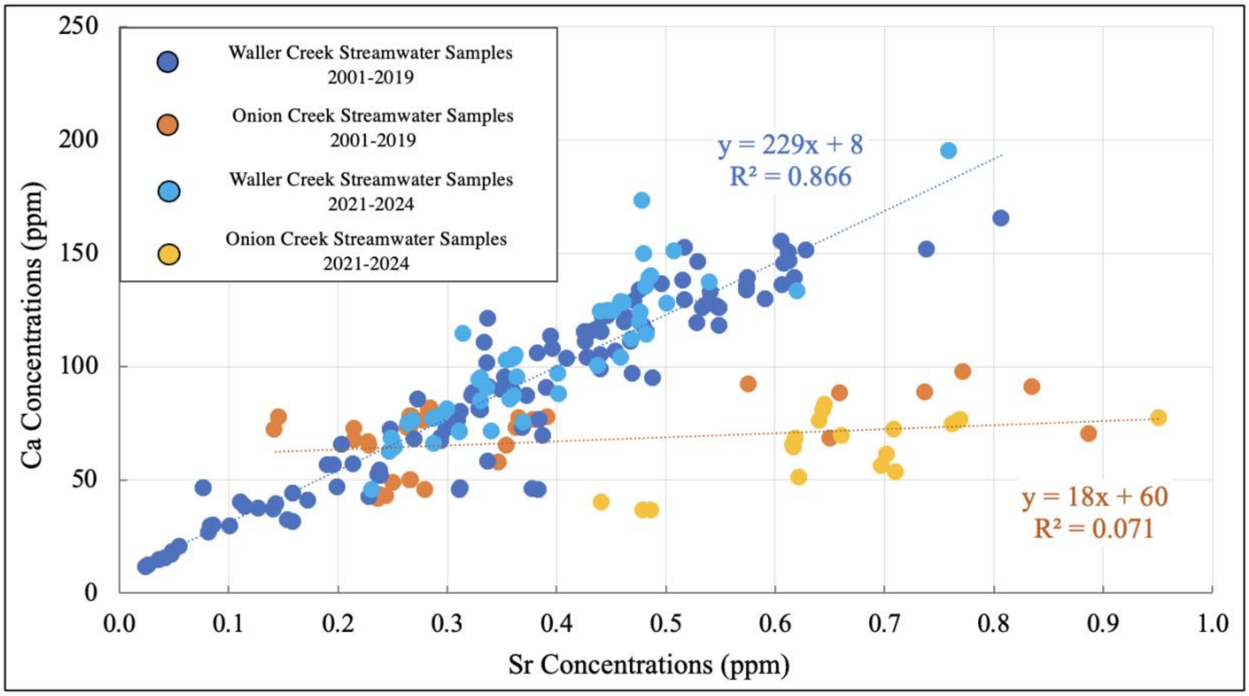

Figure 16: **Elemental ratios (Sr and Ca) in streamwaters**. Strontium and calcium in all Waller Creek and Onion Creek streamwaters with trendlines displaying the trends between the two watersheds. Data is from Christian et al., 2011, Beal et al., 2020, and this study.

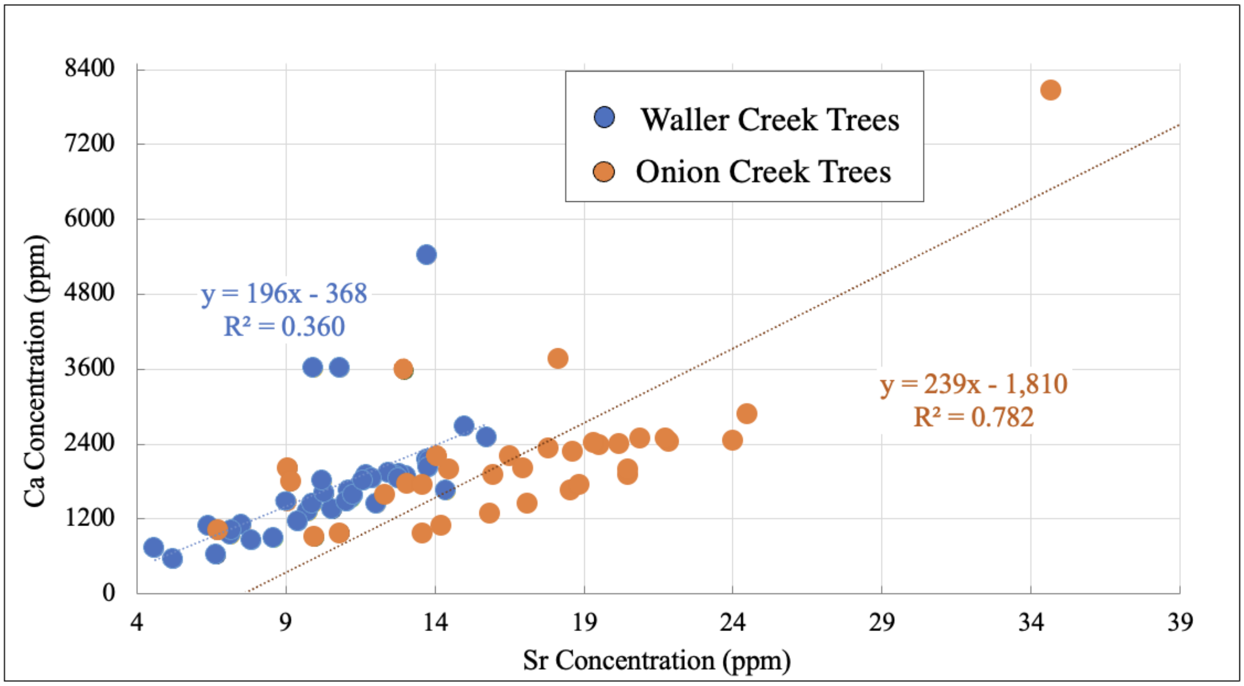

Figure 17: **Elemental ratios (Sr and Ca) in trees.** Strontium and calcium in Waller and Onion Creek tree cores using the same color scheme as Figure 16 to best display the watershed differences. Removing the Onion Creek outlier decreases the R^2 to 0.275 and changes the slope to 80. This figure is available with different colors used to differentiate individual trees in Supplementary Figure 3.

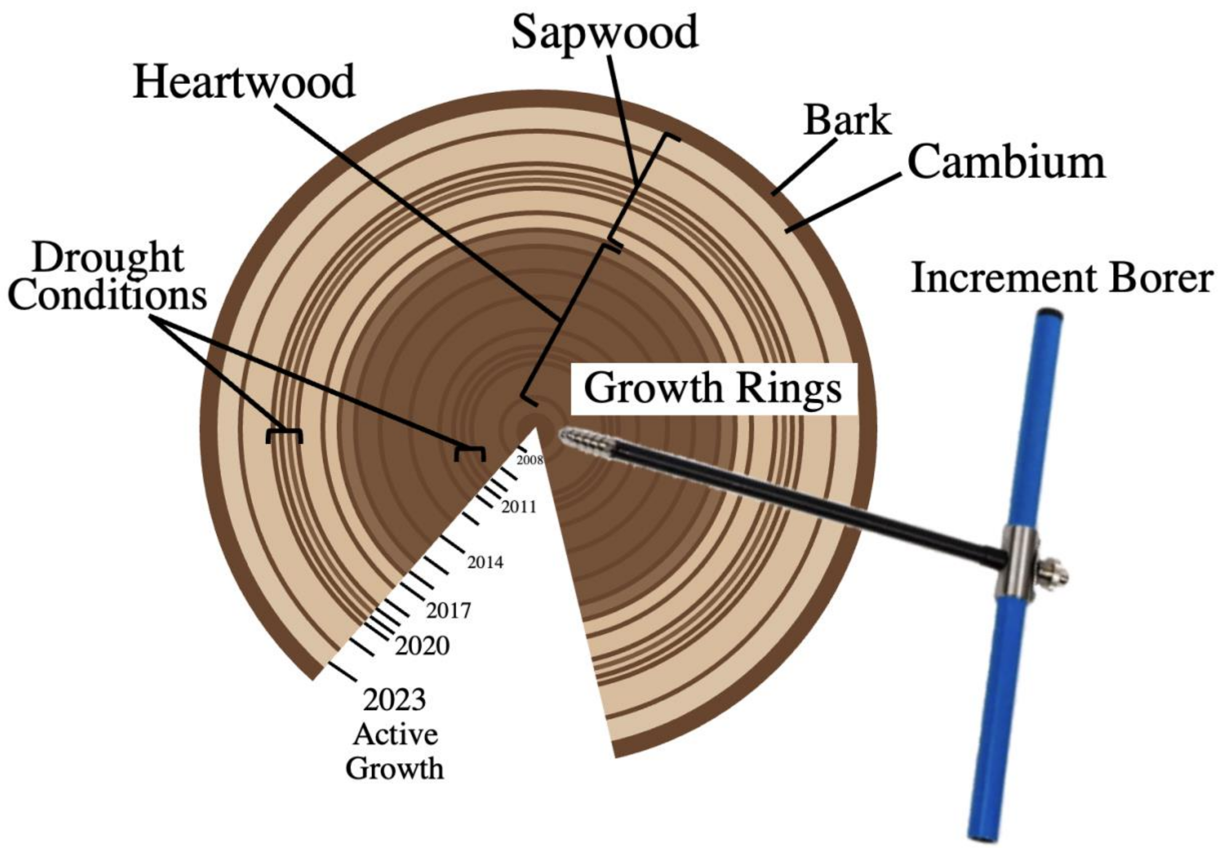

Figure 18: **Anatomy of a tree trunk and dendro methods** showing the position of the cambium relative to the heartwood and sapwood. The increment borer illustrates how a tree core is collected.

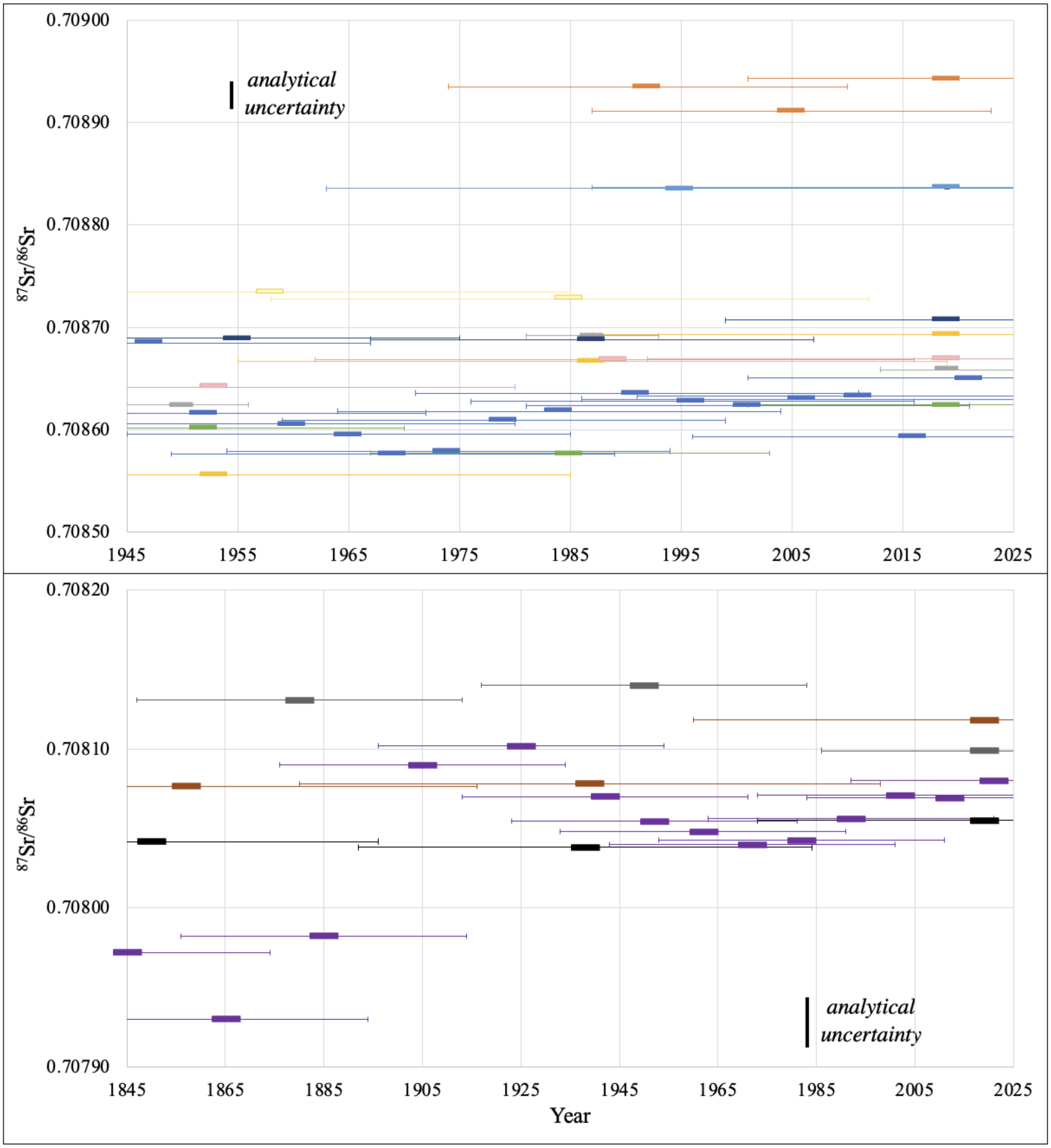

Figure 19: **^{87}Sr/^{86}Sr temporal uncertainty based on number of sapwood rings.** Sr isotope values in trees through time with horizontal error bars representing the number of sapwood rings in each tree. The analytical uncertainty is +/-0.000017.

11. Appendix

11.1. Supplementary tables

Supp. Table 1: The R^2 values corresponding to Figure 15 temporal element trends.

Element	R^2 in Waller Creek trees	R^2 in Onion Creek trees (all data)	R^2 in Onion Creek trees, excluding outlier samples*
Sr	0.214	0.007	0.005
Ca	0.002	0.004	0.061
Mg	0.586	0.173	0.394
Na	0.396	0.092	0.110
K	0.139	0.290	0.312
P	0.647	0.632	0.653

*Outlier samples include 1) the 1975-1979 increment of tree OC3, and 2) the 1936-1940 increment of tree OC10.

Supp. Table 2: Trace element concentrations found in Elmer's School Glue with concentrations >1 ppm. $^{87}Sr/^{86}Sr$ ratio also listed in the left most column. Trace element concentrations in ppm.

$^{87}Sr/^{86}Sr$ ratio	B	Na	Mg	Si	P	K	Ca	Fe	Zn	Sn
0.714204	6.8	594.6	4.8	5.1	22.5	143.3	5.4	0.3	0.3	0.1

Supp. Table 3: Trace Element concentrations in Elmer's School Glue with concentrations <1 ppm. Concentrations in ppb.

Ti	Cr	Mn	Cu	Rb	Sr	Zr	Ba
22.3	3.3	17.3	21.0	17.7	36.5	4.8	20.4

Supp. Table 4: Trace elements analyzed in bald cypress wood via ICP-MS, comparing soaked cores to their corresponding unsoaked halves. The percent difference indicates the percent increase or percent decrease.

	A1 (Not Soaked)	A2 (Soaked)	Percent Difference (%)	B1 (Not Soaked)	B2 (Soaked)	Percent Difference (%)	C1 (Not Soaked)	C2 (Soaked)	Percent Difference (%)
B	4	2	-101	3	2	-42	6	2	-194
Na	116	39	-194	149	37	-301	173	81	-115
Mg	238	237	0	276	242	-14	410	302	-36
Si	7	20	66	3	18	82	4	18	76
P	36	44	20	32	48	33	51	51	0
K	1895	388	-387	2231	458	-386	3001	342	-777
Ca	1336	1292	-3	1166	1382	16	2283	1705	-34
Ti	0	0	35	0	0	43	0	0	4
V	0	BDL	N/A	0	0	-30	0	0	9
Cr	1	1	-40	2	1	-40	2	3	31
Mn	1	1	4	1	1	27	1	1	2
Fe	170	148	-15	192	188	-2	261	255	-3
Co	0	0	91	0	0	86	0	0	88
Ni	0	0	6	0	0	16	1	1	40
Cu	BDL	BDL	N/A	BDL	BDL	N/A	0	BDL	N/A
Zn	4	5	22	3	4	37	6	6	-5
As	0	BDL	N/A	BDL	BDL	N/A	BDL	BDL	N/A
Rb	1	0	-333	1	0	-383	1	0	-748
Sr	10	10	N/A	8	10	22	18	12	-44
Zr	0	0	-23	0	0	22	0	0	4
Mo	1	0	-61	2	1	-242	1	1	-36
Cd	BDL	BDL	N/A	BDL	BDL	N/A	0	BDL	N/A
Ba	9	6	-44	4	6	31	9	8	-23
Pb	0	0	-41	0	0	43	0	0	-159

Supp. Table 5: Stream water chemical data collected over the duration of this study.

Water-shed	Sample Name/Description	QC	Collection DateTime	Filtered or Unfiltered	Flow Condition	Conductivity (uS)	pH	Temp (deg C)
Waller	DSHG		12/16/21	0.45	Baseflow	897.2	7.53	21.4
Waller	DELL (15th)		12/16/21	0.45	Baseflow	841.4	7.95	22.7
Waller	DSRS		12/16/21	0.45	Baseflow	678.6	7.86	22.1
Waller	DSP40		12/16/21	0.45	Baseflow	848.5	7.97	21.1
Waller	WW		12/16/21	0.45	Baseflow	888.1	7.53	21.2
Waller	WW		2/11/22	0.45	Baseflow	1007	8.3	18.4
Onion	1826 Bridge		3/4/22	0.45	Baseflow	610.4	7.54	17.4
Onion	US McKinney Falls		3/4/22	0.45	Baseflow	643.5	7.51	17.9
Onion	Twin Creek Rd		3/4/22	0.45	Baseflow	577.3	7.65	17.5
Onion	FM 1626 Bridge		3/4/22	0.45	Baseflow	263.9	8.71	18.4
Onion	US McKinney Falls		3/4/22	0.45	Baseflow	643.5	7.51	17.9
Onion	Twin Creek Rd		3/4/22	0.45	Baseflow	577.3	7.65	17.5
Waller	DSRS	Filt Rep	4/16/22	0.45	Baseflow	653.3	6.43	21.6
Waller	DSRS	UF Rep	4/16/22		Baseflow	653.3	6.43	21.6
Waller	P40	Filt Rep	4/16/22	0.45	Baseflow	791.2	7.22	21.8
Waller	P40	UF Rep	4/16/22		Baseflow	791.2	7.22	21.8
Waller	P40 Rep	Filt Rep	4/16/22	0.45	Baseflow	792.9	7.48	21.7
Waller	P40 Rep	UF Rep	4/16/22		Baseflow	792.9	7.48	21.7
Waller	DSP40	Filt Rep	4/16/22	0.45	Baseflow	932.6	7.47	22
Waller	DSP40	UF Rep	4/16/22		Baseflow	932.6	7.47	22
Waller	DELL (15th)	Filt Rep	4/16/22	0.45	Baseflow	877.4	6.74	22.6
Waller	DELL (15th)	UF Rep	4/16/22		Baseflow	877.4	6.74	22.6
Waller	WW	Filt Rep	4/16/22	0.45	Baseflow	941.7	6.84	22.3

Supp. Table 5 (cont.)

Water-shed	Sample Name/Description	QC	Collection DateTime	Filtered or Unfiltered	Flow Condition	Conductivity (uS)	pH	Temp (deg C)
Waller	WW	UF Rep	4/16/22		Baseflow	941.7	6.84	22.3
Waller	SHIPE	Filt Rep	4/16/22	0.45	Baseflow	1379	6.31	22.1
Waller	SHIPE	UF Rep	4/16/22		Baseflow	1379	6.31	22.1
Waller	DSHG	Filt Rep	4/16/22	0.45	Baseflow	854	7.03	22.4
Waller	DSHG	UF Rep	4/16/22		Baseflow	854	7.03	22.4
Waller	P40		9/14/22	0.45	Baseflow	765	7.54	27.2
Waller	DSRS		9/14/22	0.45	Baseflow	593	7.2	26
Waller	DSHG		9/14/22	0.45	Baseflow	658.5	7.29	28.6
Waller	SHIPE		9/14/22	0.45	Baseflow	1837	7.01	29.7
Waller	DSP40		9/14/22	0.45	Baseflow	729.4	7.74	26.8
Waller	WW		9/14/22	0.45	Baseflow	743.1	7.22	26.4
Waller	DELL (15th)		9/14/22	0.45	Baseflow	727	7.48	28.6
Onion	US McKinney Falls		10/23/22	0.45	Baseflow	862.1	6.35	23.1
Onion	Twin Creek Rd		10/23/22	0.45	Baseflow	424.3	6.3	21.3
Onion	Blank		10/23/22	0.45	Baseflow	(Blanks)	(Blanks)	(Blanks)
Waller	DSP40		12/3/22	0.45	Baseflow	762.5	7.95	16.3
Waller	DSRS		12/3/22	0.45	Baseflow	592.2	7.55	16.9
Waller	P40		12/3/22	0.45	Baseflow	651.2	7.94	16.8
Waller	DSHG		12/3/22	0.45	Baseflow	990	7.65	16
Waller	DELL (15th)		12/3/22	0.45	Baseflow	832.4	7.83	16.2
Waller	WW		12/3/22	0.45	Baseflow	880.3	7.54	16.3
Onion	Twin Creek Rd		12/15/22	0.45	Baseflow	442	7.59	16.7
Onion	US McKinney Falls		12/15/22	0.45	Baseflow	584.2	7.69	18.2

Supp. Table 5 (cont.)

Water-shed	Sample Name/Description	QC	Collection DateTime	Filtered or Unfiltered	Flow Condition	Conductivity (uS)	pH	Temp (deg C)
Waller	DSRS		2/13/23	0.45	Baseflow	640.5	7.84	16.3
Waller	SHIPE		2/13/23	0.45	Baseflow	934.7	7.41	16.9
Waller	DSHG		2/13/23	0.45	Baseflow	830.4	8.06	16.2
Waller	WW		2/13/23	0.45	Baseflow	919.5	7.99	15.5
Waller	P40		2/13/23	0.45	Baseflow	775.9	8.02	17
Waller	DSP40		2/13/23	0.45	Baseflow	857.9	8.09	17.4
Waller	DELL (15th)		2/13/23	0.45	Baseflow	796.8	8.08	16.5
Onion	US McKinney Falls		3/7/23	0.45	Baseflow	563.4	7.9	21.2
Onion	OC-20		3/7/23	0.45	Baseflow	556.6	7.85	21.8
Onion	OCSC		3/7/23	0.45	Baseflow	558.5	8.09	22.5
Onion	Twin Creek Rd		3/7/23	0.45	Baseflow	562	7.87	22.5
Waller	DSRS		4/13/23	0.45	Baseflow	660.4	7.76	20.8
Waller	DSHG		4/13/23	0.45	Baseflow	857.8	8.13	23.5
Waller	WW		4/13/23	0.45	Baseflow	1001	8	20.4
Waller	P40		4/13/23	0.45	Baseflow	1049	8.34	19.9
Waller	DSP40		4/13/23	0.45	Baseflow	1004	8.12	20.4
Waller	DELL (15th)		4/13/23	0.45	Baseflow	843.8	8.28	23.1
Onion	Twin Creek Rd		5/4/23	0.45	Baseflow	536.1	8.04	23.7
Onion	OC-20		5/4/23	0.45	Baseflow	504.1	7.92	24.1
Onion	US McKinney Falls		5/4/23	0.45	Baseflow	488.4	8.38	25.8
Waller	DSRS		6/19/23	0.45	Baseflow	566.4	7.92	28.5
Waller	DSHG		6/19/23	0.45	Baseflow	537.7	8.2	30.1
Waller	WW		6/19/23	0.45	Baseflow	521.9	8.08	27.5

Supp. Table 5 (cont.)

Water-shed	Sample Name/Description	QC	Collection DateTime	Filtered or Unfiltered	Flow Condition	Conductivity (uS)	pH	Temp (deg C)
Waller	P40		6/19/23	0.45	Baseflow	792	8.4	25.5
Waller	DSP40		6/19/23	0.45	Baseflow	689.1	8.24	26.4
Waller	DELL (15th)		6/19/23	0.45	Baseflow	556.4	8.09	28.9
Onion	US McKinney Falls		7/6/23	0.45	Baseflow			
Onion	Twin Creek Rd		7/6/23	0.45	Baseflow			
Onion	OC-20		7/6/23	0.45	Baseflow			
Onion	OCSC		7/6/23	0.45	Baseflow			
Waller	DSHG		8/18/23	0.45	Baseflow	604.5	7.92	30.5
Waller	WW		8/18/23	0.45	Baseflow	856.8	8.1	30.2
Waller	P40		8/18/23	0.45	Baseflow	1228	8.41	26.6
Waller	DSP40		8/18/23	0.45	Baseflow	901.4	8.32	29.3
Waller	DELL (15th)		8/18/23	0.45	Baseflow	1228	7.84	29.4
Waller	DSHG		8/31/23	0.45	Baseflow	740.6	7.53	26.5

Supp. Table 6: Sr Isotope data for Waller and Onion Creek watershed tree samples.

Water-shed	Tree ID	Core ID	Ring Sample Years	Digestion Method	$^{87}Sr/^{86}Sr$	2σ	Instrument
Onion	10	A	1848-1852	Ashing	0.708042	0.000006	TIMS
Onion	10	A	1936-1940	Ashing	0.708038	0.000006	TIMS
Onion	10	A	2017-2023	Ashing	0.708055	0.000009	TIMS
Onion	6	A	1878-1882	Ashing	0.708131	0.000014	ICP
Onion	6	A	1948-1952	Ashing	0.708140	0.000013	ICP
Onion	6	A	2017-2023	Ashing	0.708099	0.000012	TIMS
Onion	14	A	1855-1859	Ashing	0.708077	0.000016	ICP
Onion	14	A	1937-1941	Ashing	0.708078	0.000013	ICP
Onion	14	A	2017-2023	Ashing	0.708118	0.000013	ICP
Onion	3	A	2019-2023	Microwave	0.708080	0.000013	ICP
Onion	3	A	2010-2014	Microwave	0.708069	0.000014	ICP
Onion	3	A	2000-2004	Microwave	0.708071	0.000014	ICP
Onion	3	A	1990-1994	Microwave	0.708056	0.000014	ICP
Onion	3	A	1980-1984	Microwave	0.708043	0.000015	ICP
Onion	3	A	1970-1974	Microwave	0.708040	0.000015	ICP
Onion	3	A	1960-1964	Microwave	0.708048	0.000014	ICP
Onion	3	A	1950-1954	Microwave	0.708055	0.000013	ICP
Onion	3	A	1940-1944	Microwave	0.708070	0.000013	ICP
Onion	3	A	1920-1929	Microwave	0.708102	0.000015	ICP
Onion	3	A	1900-1909	Microwave	0.708090	0.000012	ICP
Onion	3	A	1880-1889	Microwave	0.707982	0.000011	ICP
Onion	3	A	1860-1869	Microwave	0.707930	0.000012	ICP
Onion	3	A	1840-1849	Microwave	0.707972	0.000015	ICP

Water-shed	Tree ID	Core ID	Ring Sample Years	Digestion Method	$^{87}Sr/^{86}Sr$	2σ	Instrument
Waller	4172	A	1950-1955	Ashing	0.708642	0.000007	TIMS
Waller	4172	A	1987-1991	Ashing	0.708668	0.000007	TIMS
Waller	4172	A	2017-2023	Ashing	0.708669	0.000006	TIMS
Waller	4164	A	1955-1960	Ashing	0.708734	0.000007	TIMS
Waller	4164	A	1983-1988	Ashing	0.708728	0.000007	TIMS
Waller	4164	A	2017-2023	Ashing			
Waller	3924	A	1950-1954	Ashing	0.708602	0.000016	ICP
Waller	3924	A	1983-1987	Ashing	0.708577	0.000014	ICP
Waller	3924	A	2017-2023	Ashing	0.708624	0.000009	TIMS
Waller	3924	B	1953-1957	Ashing	0.708690	0.000017	ICP
Waller	3924	B	1985-1989	Ashing	0.708688	0.000033	TIMS
Waller	3924	B	2017-2023	Ashing	0.708707	0.000008	TIMS
Waller	4036	B	1951-1955	Ashing	0.708555	0.000012	
Waller	4036	B	1985-1989	Ashing	0.708667	0.000021	ICP
Waller	4036	B	2017-2023	Ashing	0.708693	0.000016	ICP
Waller	4161	A	1970-1975	Ashing			
Waller	4161	A	1993-1997	Ashing	0.708835	0.000009	TIMS
Waller	4161	A	2017-2022	Ashing	0.708837	0.000010	TIMS
Waller	4204	A	1990-1994	Ashing	0.708935	0.000006	TIMS
Waller	4204	A	2003-2007	Ashing	0.708911	0.000008	TIMS
Waller	4204	A	2016-2021	Ashing	0.708943	0.000009	TIMS
Waller	3920	B	1948-1953	Ashing	0.708624	0.000008	TIMS
Waller	3920	B	1985-1990	Ashing	0.708692	0.000011	TIMS
Waller	3920	B	2016-2021	Ashing	0.708658	0.000008	TIMS
Waller	4171	B	2019-2023	Ashing	0.708650	0.000015	ICP
Waller	4171	B	2014-2018	Microwave	0.708593	0.000012	ICP

Waller	4171	B	2009-2013	Microwave	0.708633	0.000011	ICP
Waller	4171	B	2004-2008	Microwave	0.708630	0.000014	ICP
Waller	4171	B	1999-2003	Microwave	0.708623	0.000014	ICP
Waller	4171	B	1994-1998	Microwave	0.708627	0.000017	ICP
Waller	4171	B	1989-1993	Microwave	0.708636	0.000012	ICP
Waller	4171	B	1982-1986	Ashing	0.708618	0.000017	ICP
Waller	4171	B	1977-1981	Microwave	0.708609	0.000014	ICP
Waller	4171	B	1972-1976	Microwave	0.708579	0.000012	ICP
Waller	4171	B	1967-1971	Microwave	0.708576	0.000012	ICP
Waller	4171	B	1962-1966	Microwave	0.708596	0.000014	ICP
Waller	4171	B	1957-1961	Microwave	0.708606	0.000013	ICP
Waller	4171	B	1950-1954	Ashing	0.708616	0.000017	ICP
Waller	4171	B	1945-1949	Microwave	0.708685	0.000015	ICP

Supp. Table 7: Cation data for Waller and Onion Creek tree core samples, analyzed via ICP-Q-MS.

Water-shed	Tree ID	Core ID	Ring Sample Years	Sr	Ca	Mg	Na	K	P
Onion	10	A	1848-1852	18.1	3765.4	475.0	6.5	10.3	34.8
Onion	10	A	1936-1940	50.3	14820.5	1099.4	21.7	9.8	53.7
Onion	10	A	2017-2023	10.8	969.7	186.3	4.9	51.1	165.0
Onion	6	A	1878-1882	9.1	2015.1	248.1	43.3	608.0	15.8
Onion	6	A	1948-1952	9.2	1796.7	392.1	29.1	469.2	36.3
Onion	6	A	2017-2023	6.7	1013.7	133.0	30.3	602.3	117.8
Onion	14	A	1855-1859	13.0	3584.6	847.1	61.0	55.6	16.2
Onion	14	A	1937-1941	14.1	2189.7	492.1	54.3	59.1	39.0
Onion	14	A	2017-2023	10.0	905.4	281.7	48.0	906.9	230.5
Onion	3	A	2019-2023	13.6	959.9	206.5	96.8	504.6	182.7
Onion	3	A	2015-2019	14.2	1095.5	249.8	75.2	748.3	202.9
Onion	3	A	2010-2014	15.8	1292.6	278.2	74.1	759.7	189.8
Onion	3	A	2005-2009	17.1	1450.0	285.0	66.4	716.4	203.2
Onion	3	A	2000-2004	18.5	1661.9	302.1	68.2	788.2	210.6
Onion	3	A	1995-1999	18.9	1743.2	279.8	66.1	801.4	195.9
Onion	3	A	1990-1994	20.5	1913.2	279.0	63.8	773.1	151.7
Onion	3	A	1985-1989	20.5	1991.8	353.0	73.6	504.0	85.5
Onion	3	A	1980-1984	24.0	2461.7	343.3	65.7	152.8	53.7
Onion	3	A	1975-1979	51.5	12546.3	630.7	83.9	171.2	42.4
Onion	3	A	1970-1974	34.7	8058.2	521.9	71.4	149.3	47.1
Onion	3	A	1965-1969	21.8	2428.8	358.8	59.5	143.6	40.8
Onion	3	A	1960-1964	21.7	2492.1	361.0	65.0	148.9	35.1
Onion	3	A	1955-1959	24.5	2879.8	373.7	84.0	155.6	39.9

Water-shed	Tree ID	Core ID	Ring Sample Years	Sr	Ca	Mg	Na	K	P
Onion	3	A	1950-1954	20.9	2491.3	366.1	81.5	179.6	37.0
Onion	3	A	1945-1949	20.2	2403.6	348.7	69.0	144.2	42.1
Onion	3	A	1940-1944	19.5	2380.1	363.7	69.2	147.9	50.4
Onion	3	A	1930-1939	19.3	2423.3	362.3	60.3	143.2	23.8
Onion	3	A	1920-1929	17.8	2327.0	351.9	58.7	125.4	25.3
Onion	3	A	1910-1919	16.5	2197.8	360.7	62.0	121.7	16.8
Onion	3	A	1900-1909	14.5	1987.7	332.9	66.0	122.4	12.3
Onion	3	A	1890-1899	13.1	1765.5	325.5	69.0	136.0	7.8
Onion	3	A	1880-1889	12.3	1591.0	323.8	76.7	157.1	6.4
Onion	3	A	1870-1879	13.6	1751.0	372.4	98.4	198.9	8.8
Onion	3	A	1860-1869	16.0	1901.0	424.2	115.6	250.5	13.2
Onion	3	A	1850-1859	16.9	2014.5	478.1	133.0	288.4	13.5
Onion	3	A	1840-1849	18.6	2281.3	521.3	153.0	340.9	27.4
Waller	4172	A	1950-1955	15.8	2503.4	367.3	36.8	278.7	28.6
Waller	4172	A	1987-1991	15.0	2679.3	270.1	16.6	105.9	24.6
Waller	4172	A	2017-2023	13.8	5409.9	167.1	7.9	19.4	164.8
Waller	4164	A	1955-1960	9.8	1305.3	202.8	30.0	314.5	20.5
Waller	4164	A	1983-1988	9.9	1437.1	182.1	10.5	89.2	19.3
Waller	4164	A	2017-2023	9.9	3613.1	186.7	8.1	43.2	149.4
Waller	3924	A	1950-1954	11.2	1520.0	436.4	73.1	564.9	20.6
Waller	3924	A	1983-1987	13.8	2098.0	295.7	19.5	108.1	32.1
Waller	3924	A	2017-2023	8.6	889.9	196.7	6.3	119.7	164.6
Waller	3924	B	1953-1957	10.6	1339.5	312.2	43.2	365.6	23.3
Waller	3924	B	1985-1989	10.3	1618.7	267.3	32.3	248.3	23.0
Waller	3924	B	2017-2023	6.7	625.1	173.0	11.3	427.1	163.4
Waller	4036	B	1951-1955	14.4	1647.3	481.9	60.9	292.1	21.0

Waller	4036	B	1985-1989	10.2	1808.1	242.1	25.5	109.2	47.4
Waller	4036	B	2017-2023	7.1	944.6	167.9	8.5	250.1	149.0
Waller	4161	A	1970-1975	4.6	724.7	131.4	12.8	51.7	8.0
Waller	4161	A	1993-1997	6.4	1082.8	202.7	11.0	284.3	91.1
Waller	4161	A	2017-2022	5.2	557.8	124.4	8.4	84.8	96.0
Waller	4204	A	1990-1994	9.0	1472.3	161.0	64.4	400.0	16.9
Waller	4204	A	2003-2007	7.5	1104.2	148.2	45.0	473.8	46.0
Waller	4204	A	2016-2021	7.2	1006.1	94.9	20.3	163.8	62.6
Waller	3920	B	1948-1953	12.0	1431.1	359.2	35.6	128.3	11.2
Waller	3920	B	1985-1990	11.1	1640.5	281.9	17.8	32.8	39.1
Waller	3920	B	2016-2021	10.8	3609.5	178.6	8.3	47.7	139.9
Waller	4171	B	2019-2023	7.9	857.1	132.0	6.0	248.1	136.5
Waller	4171	B	2014-2018	9.4	1151.0	183.9	18.1	300.7	90.5
Waller	4171	B	2009-2013	11.1	1465.7	210.0	27.2	179.1	119.8
Waller	4171	B	2004-2008	11.3	1580.7	201.6	17.0	360.4	90.9
Waller	4171	B	1999-2003	11.7	1889.1	197.3	28.4	188.5	29.4
Waller	4171	B	1994-1998	13.8	2149.0	231.0	16.7	138.8	28.2
Waller	4171	B	1989-1993	13.8	2120.9	229.6	19.5	156.5	22.4
Waller	4171	B	1982-1986	13.0	1885.0	235.0	27.5	233.2	28.0
Waller	4171	B	1977-1981	12.8	1920.4	233.4	17.7	168.3	29.0
Waller	4171	B	1972-1976	13.8	2028.0	264.3	19.4	182.4	20.0
Waller	4171	B	1967-1971	12.7	1875.8	249.2	27.1	241.4	15.1
Waller	4171	B	1962-1966	12.5	1930.9	262.1	21.1	197.0	15.1
Waller	4171	B	1957-1961	11.9	1848.8	279.1	30.7	281.5	16.7
Waller	4171	B	1950-1954	11.6	1804.5	280.6	30.2	460.1	20.9
Waller	4171	B	1945-1949	12.8	1836.5	315.9	48.7	553.1	14.7

11.2. Supplementary figures

Supp. Figure 1: New core preparation method. The wooden vise-like device created for this study and used to hold tree cores in place without adhesive while a flat surface is planed with a stainless steel razor blade.

Supp. Figure 2: New mounting process, composed of string wrapped around a core to hold it into a mount.

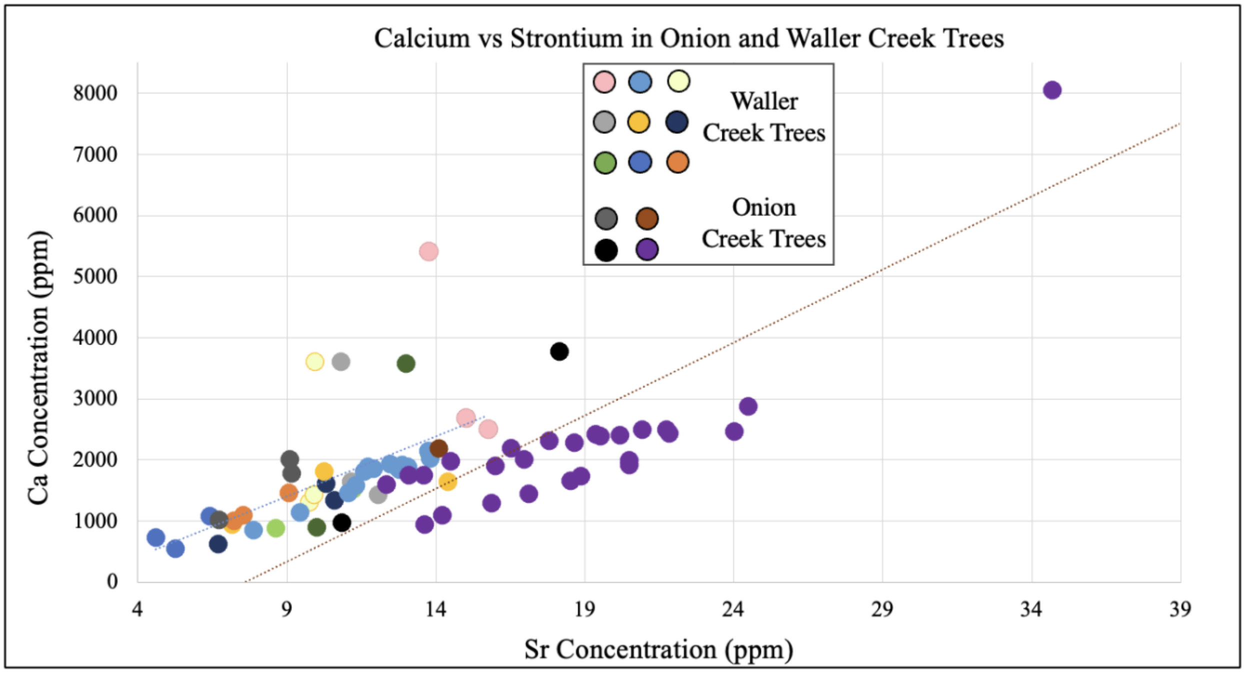

Supp. Figure 3: Strontium and calcium found in all Waller Creek and Onion Creek tree cores with trendlines displaying the trends between the two watersheds. This data is the same as in Figure 16, but individual trees are represented using different colors. The R^2 for Waller Creek trees (blue dotted line) is 0.360 and the R^2 for Onion Creek trees (red dotted line) is 0.782.

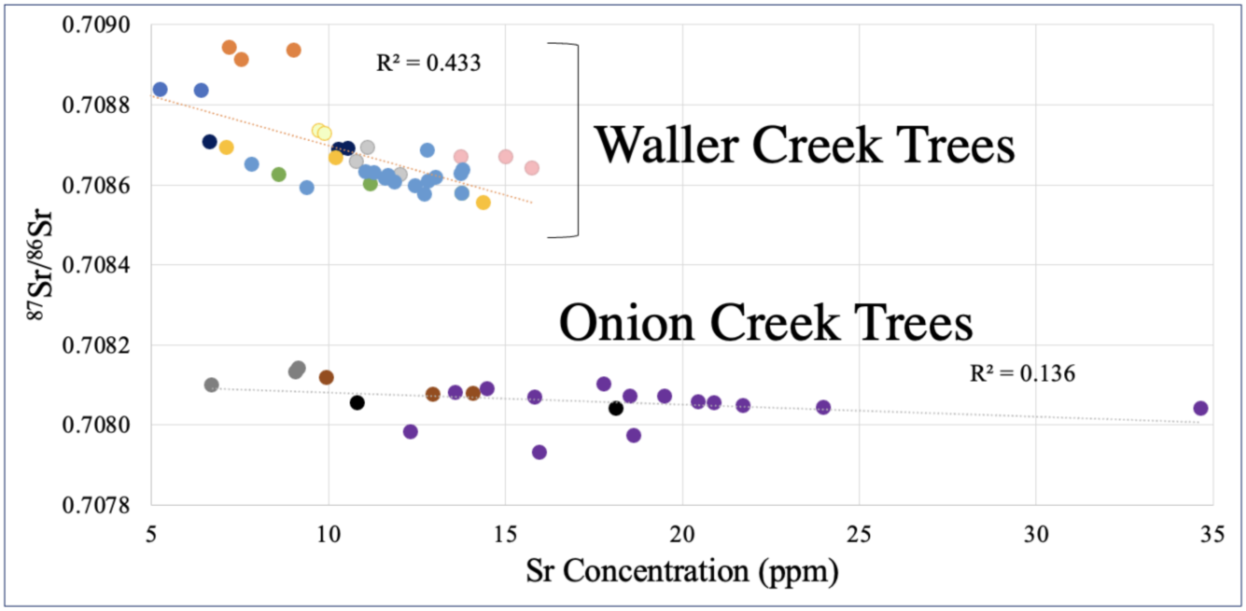

Supp. Figure 4: Sr and $^{87}Sr/^{86}Sr$ in Waller and Onion Creek trees.

Elmer's Glue Contamination

Components:

Sr concentration in Elmer's Glue = **0.09 ppm**

$^{87}Sr/^{86}Sr$ in Elmer's Glue = **0.714204**

Average Sr concentration in bald cypress wood = **8.05 ppm**

$^{87}Sr/^{86}Sr$ in pure bald cypress wood = **0.708679**

$^{87}Sr/^{86}Sr$ in bald cypress wood with glue = **0.7089435**

General mixing equation:

$$\left[\frac{87Sr}{86Sr}\right]_{mix} = \frac{X_A[Sr]_A\left(\frac{87Sr}{86Sr}\right)_A + (1 - X_A)[Sr]_B\left(\frac{87Sr}{86Sr}\right)_B}{X_A[Sr]_A + (1 - X_A)[Sr]_B}$$

A = bald cypress wood

B = Elmer's glue

$$0.709435 = \frac{X_A(8.05_{ppm})(0.708679) + (1 - X_A)(0.09_{ppm})(0.714204)}{X_A(8.05_{ppm}) + (1 - X_A)(0.09_{ppm})}$$

Weight fractions of components A and B:

$\mathbf{X_A = 0.06656}$

$\mathbf{X_B = 0.93344}$

Supp. Figure 5:Elmer's glue mixing equation in mounted bald cypress wood.

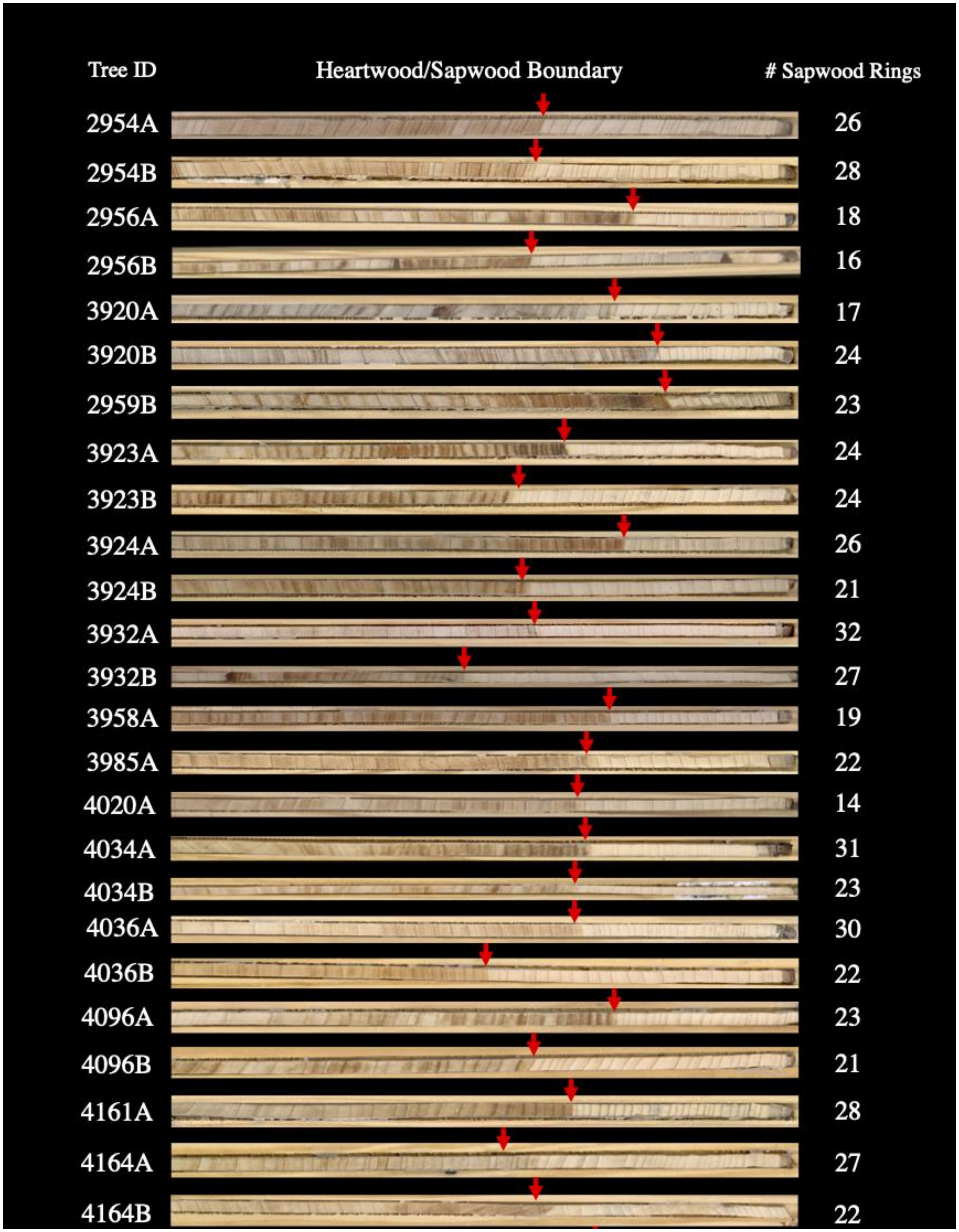
Tree ID
Heartwood/Sapwood Boundary
Sapwood Rings
2954A 26
2954B 28
2956A 18
2956B 16
3920A 17
3920B 24
2959B 23
3923A 24
3923B 24
3924A 26
3924B 21
3932A 32
3932B 27
3958A 19
3985A 22
4020A 14
4034A 31
4034B 23
4036A 30
4036B 22
4096A 23
4096B 21
4161A 28
4164A 27
4164B 22

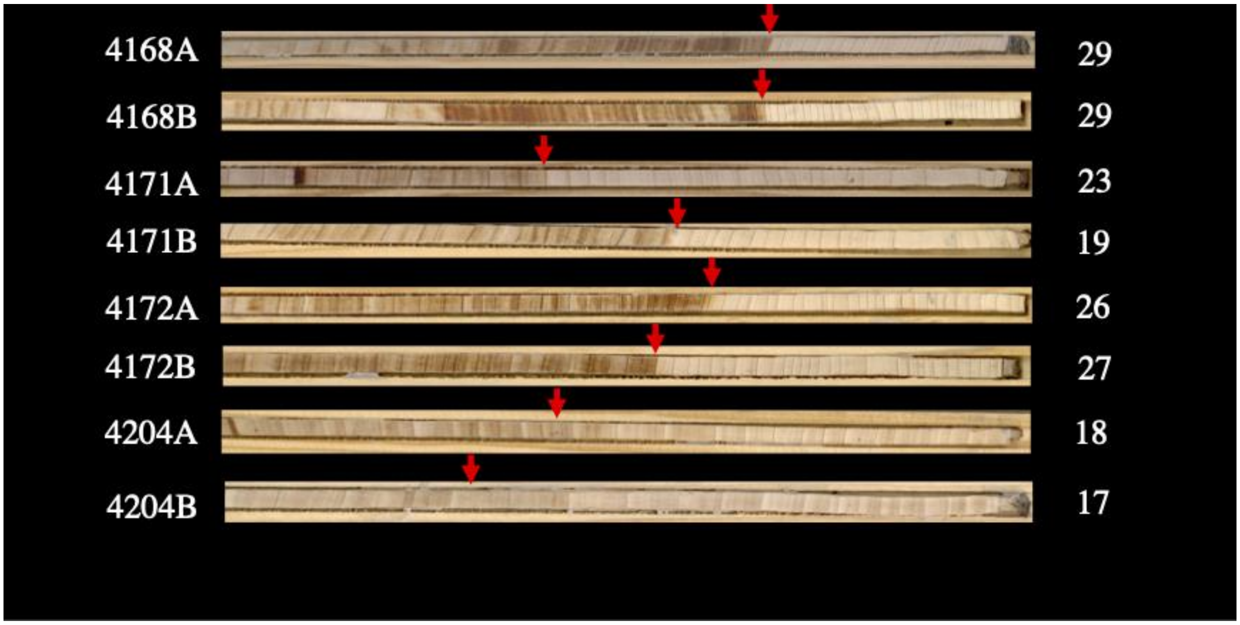

Supp. Figure 6: Heartwood-sapwood boundaries in Waller Creek trees collected in 2018.

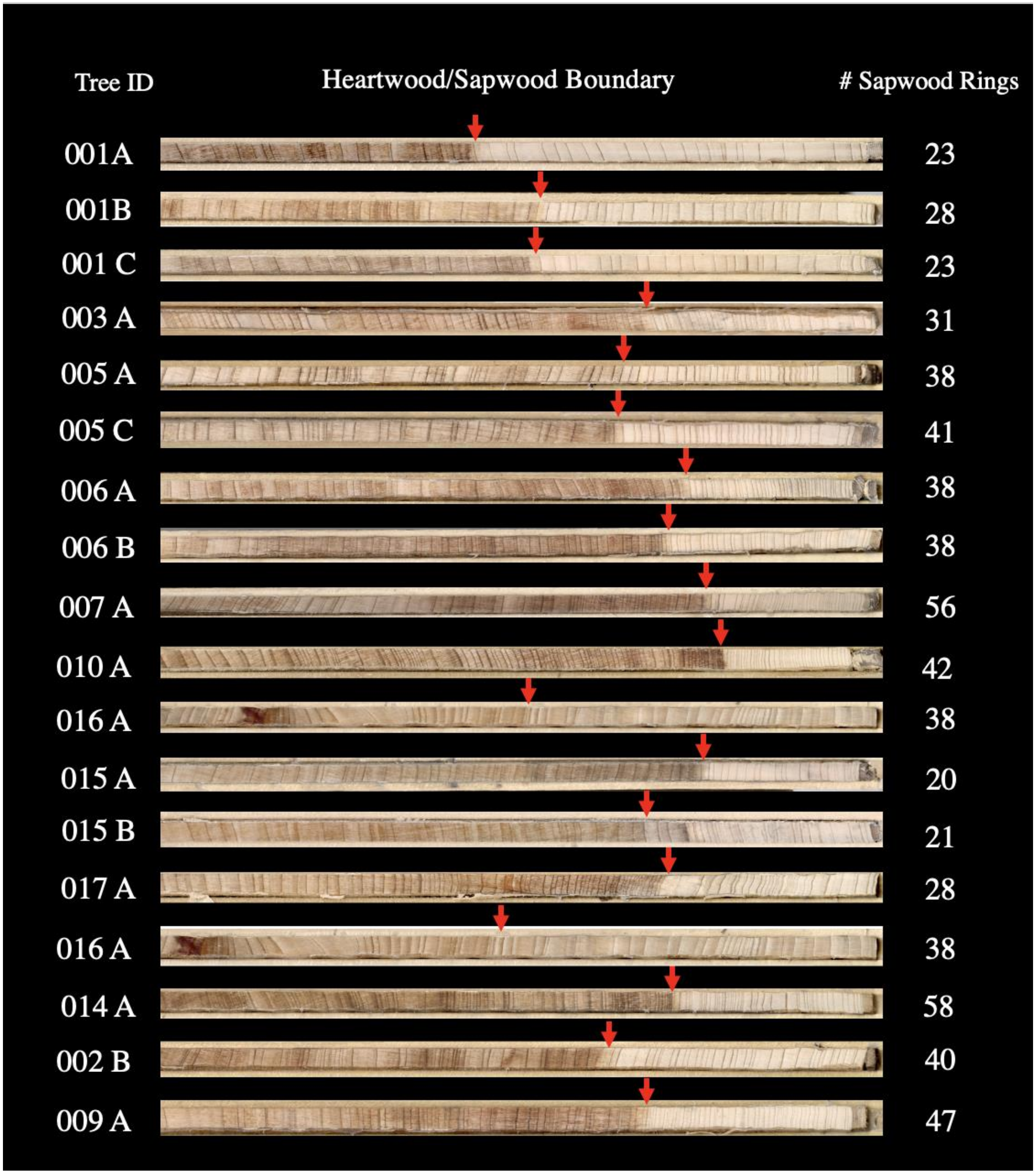

Supp. Figure 7: Heartwood-sapwood boundaries in Onion Creek trees collected in 2018.

12. References

Åberg, G., Jacks, G., Wickman, T., and Hamilton, P.J., 1990. Strontium isotopes in trees as indicators for calcium availability, Catena, 17(1), pp. 1-11.

AustinTexas.gov, n.d. Austin Water History, https://www.austintexas.gov/

AustinTexas.gov, 2017. Watershed Overview, www.austintexas.gov/Watershed/Slaughter_2016.pdf

Balouet, J.C., Oudijk, G., Smith, K.T., Petrisor, I., Grudd, H., and Stocklassa, B., 2007. Applied dendroecology and environmental forensics. Characterizing and age dating environmental releases: fundamentals and case studies, Environmental Forensics, 8(1-2).

Banner, J.L, Black., B., and Tremaine, D., 2024. Positive unintended consequences of urbanization for climate-resilience of stream ecosystems, npj Urban Sustainability, http://dx.doi.org/10.21203/rs.3.rs-2587818/v1.

Banner, J.L. and Kaufman, J., 1994. The isotopic record of ocean chemistry and diagenesis preserved in non-luminescent brachiopods from Mississippian carbonate rocks, Illinois and Missouri. GSA Bulletin, 106(8), pp. 1074-1082.

Banner, J.L., Musgrove, M., and Capo, R.C., 1994. Tracing groundwater evolution in a limestone aquifer using Sr isotopes: Effects of multiple sources of dissolved ions and mineral-solution reactions. Geology, 22, pp. 687-690.

Beal, L., Senison, J., Banner, J., Musgrove, M. L., Yazbek, L., Bendik, N., Herrington, C., and Reyes, D., 2020. Stream and spring water evolution in a rapidly urbanizing watershed, Austin, TX. Water Resources Research, 56(4). https://doi.org/10.1029/2019WR025623

Chan, J.M., 2010. Effects of moisture content and temperature on acoustic velocity and dynamic MOE of radiata pine sapwood boards, Wood Science and Technology, 45, pp. 609-626.

Christian, L.N., Banner, J.L., and Mack, L.E., 2011. Sr isotopes as tracers of anthropogenic influences on stream water in the Austin, Texas, area, Chemical Geology, 282, pp. 84-97.

City of Austin 2023 Watershed boundaries [Shapefile], accessed July 2022 at https://data.austintexas.gov/Locations-and-Maps/Watershed-Boundaries/yfaf-uvsu

City of Austin, Watershed Protection Department, 2016. Watershed profile. https://services.austintexas.gov/watershed_protection/publications/document.cfm?id=269891

Comstock, G.L., 1970. Directional permeability of softwoods, Wood and Fiber Science, 4.

Cook, E.R. and Kairiukstis, L.A., 2013. Methods of dendrochronology: Applications in the environmental sciences. Chapter by Pilcher, J.R. Springer Science & Business Media, pp. 40.

Cutter, B.E. and Guyette, R.P., 1993. Anatomical, chemical, and ecological factors affecting tree species choice in dendrochemistry studies, Journal of Environmental Quality, 22, pp. 611-619.

DeMott, L.M., Banner, J.L., and Christian, L., 2006. Recent travertine deposits as records of groundwater processes in urbanizing environments, Geological Society of America Annual Meeting Abstract Paper No. 116-2

Drouet, T, Herbauts, J., and Demaiffe, D., 2005. Long-term records of strontium isotopic composition in tree rings suggest changes in forest calcium sources in the early 20th century, Global Change Biology, 11(11), pp. 1926-1940.

Edvardsson, J., Rognvaldsson, K., Helgadottir, E., Linderson, H., and Hrafnkelsson, B., 2022. A statistical model for the prediction of the number of sapwood rings in Scots pine (*Pinus sylvestris* L.), Dendrochronologia, 74

English, N.B., Betancourt, J.L., Dean, J.S., and Quade, J., 2001. Strontium isotopes reveal distant sources of architectural timber in Chaco Canyon, New Mexico, Proc. Natl. Acad. Sci., 98(21), pp. 11891-11896. www.pnas.orgycgiydoiy10.1073ypnas.211305498

Frauendorfer, R., Liemberger, R., and Bank, A.D., 2010. The issues and challenges of reducing non-revenue water, Asian Development Bank, Mandaluyong City.

Galicki, S.J., Davidson, G.R., and Threlkeld, S.T., 2008. Element mobility in bald cypress xylem, Tree-Ring Research, 64(1), pp. 39-46.

Garcia-Fresca, B. and Sharp, J.M., 2005. Hydrogeologic considerations of urban development: urban-induced recharge, Humans as Geologic Agents, by Judy Ehlen et al., 16, Geological Society of America, pp. 123-36

Garner, L.E., Ruppel, S.C., and Seni, S.J., 1993. An introduction to the geology of state parks near Austin, Texas, Austin Geological Society. UT Libraries http://dx.doi.org/10.26153/tsw/4974

Gärtner, H., Lucchinetti, S., and Schweingruber, F.H., 2015. A new sledge microtome to combine wood anatomy and tree-ring ecology, IAWA Journal, 36(4), pp. 452-459.

Graustein, W.C., 1989. $^{87}Sr/^{86}Sr$ ratios measure the sources and flow of strontium in terrestrial ecosystems, Stable Isotopes in Ecological Research, 68, pp. 491-512.

Graustein, W.C. and Armstrong, R.L., 1983. The use of strontium-87/strontium-86 ratios to measure atmospheric transport into forested watersheds, Science, 219, pp. 289-292.

Harrington, G.A. and Herczeg, A.L., 2003 The importance of silicate weathering of a sedimentary aquifer in arid Central Australia indicated by very high $^{87}Sr/^{86}Sr$ ratios, Chemical Geology, 199(3-4), pp. 281-292.

Hasegawa, M. and Shiroya, M., 1966. Translocation and transformation of sucrose in the wood of Prunus yefoensis, Botanical Magazine, Tokyo, 79, pp. 595-601.

Hemingway, R.W. and Hillis, W.E., 1970. Heartwood formation in living stumps of Douglas-fir, Wood Science and Technology, 4, pp. 246-254.

Hesse, I.D., Day, J.W., and Doyle, T.W., 1998. Long-term growth enhancement of Baldcypress (*Taxodium distichum*) from municipal wastewater application, Environmental Management, 22(1), pp. 119-127.

Holmes, R.L., 1983. Computer-assisted quality control in tree-ring dating and measurement, Tree-Ring Bulletin, 43, pp. 69-78.

Hovorka, S.D., 1998. Facies and diagenesis of the Austin Chalk and controls on fracture intensity – a case study from North Central Texas: The University of Texas at Austin, Bureau of Economic Geology, Geological Circular 98-2.

Hughes, M.K., Milsom, S.J., and Leggett, P.A., 1981. Sapwood estimates in the Interpretation of Tree-ring Dates, Journal of Archaeological Science, 8, pp. 381-390.

Humphrey, D.C., 1937. Austin- a history of the capital city, Library of Congress Cataloging-in-Publication Data.

Hunt, B.B., Broun, A.S., Wierman, D.A., Johns, D.A., and Smith, B.A., 2016. Surface-water and groundwater interactions along Onion Creek, Central Texas, Gulf Coast Association of Geological Societies Transactions, 66, pp. 261-282.

Jacquiot, C., 1947. Biologie vegetale- effet inhibiteur des tannins sur le developpement des cultures invitro du cambium de certains arbres forestiers, Comptes Rendus Hebdomadaires des Seances de L Academie des Sciences, 225(434).

Kagawa, A., Aoki, T., Okada, N., and Katayama, Y., 2002. Tree-ring strontium-90 and cesium-

137 as potential indicators of radioactive pollution, Journal of Environmental Quality, 31(6), pp. 2001-2007

Kloesel, K., Bartush, B., Banner, J.L., Brown, D., Lemory, J., Lin, X., Loeffler, C., McManus, G., Mullens, E., Nielsen-Gammon, J., Shafer, M., Sorensen, C., Sperry, S., Wildcat, D., and Ziolkowska, J., 2018. Ch. 23 Southern Great Plains. In Impacts risks, and adaptation in the United States: Fourth National Climate Assessment, 2, pp. 987–1035.

Latimer, S.D., Devall, M.S., Thomas, C., Ellgaard, E.G., Kumar, S.D., and Thien, L.B., 1996. Dendrochronology and heavy metal deposition in tree rings of baldcypress, Journal of Environmental Quality, 25(6), pp. 1411-1419.

Larsson, L., 2013. CooRecorder and Cdendro Programs of the Coorecorder/Cdendropackage Version 7.6, http://www.cybis.se/forfun/dendro/

LCRA, 2022. Water Use Summary. https://www.lcra.org/water/water-supply-planning/water-use-summary/

Legge, A.H., Kaufmann, H.C., and Winchester, J.W., 1984. Tree-ring analysis by pixe for a historical record of soil chemistry response to acidic air pollution, Nuclear Instruments and Methods in Physics Research Section B: Beam Interactions with Materials and Atoms, 3(1-3), pp.507-510.

Lehr, M., Miltner, M., and Friedl, A., 2021. Removal of wood extractives as pulp (pre-)treatment: a technological review, SN Applied Sciences, 3(886).

Lepp, N.W., 1975. The potential of tree-ring analysis for monitoring heavy metal pollution Patterns, Environmental Pollution (1970), 9(1), pp. 49-61.

Little, E. L. Jr., 1971. Atlas of United States trees, volume 1, conifers and important hardwoods. US Department of Agriculture Miscellaneous Publication 1146.

Longuetaud, F., Mothe, F., Leban, J.M., and Makela, A., 2007. Pices abies sapwood width: Variations within and between trees, Scandanavian Journal of Forest Research, 21(1), pp. 41-53.

Lula, R.A., 1986. Manganese stainless steels, Manganese Centre, Paris, 83.

Manlove, H.M., 2020. Geochemical evolution of municipal water in the natural hydrologic system. Master's thesis, The University of Texas at Austin. Repositories.lib.utexas.edu

Mauceri, A.A & Banner, J.L., 2023. Resetting of soil compositions by irrigation in urban watersheds. Evidence from Sr isotope variations in Austin, TX, Science of the Total Environment, 904.

Massey, H. F., 1972. pH and soluble Cu, Ni, and Zn in Eastern Kentucky coalmine spoil materials, Soil Science., 114, pp. 217-21.

McDonald, R.I., Green, P., Balk, D., Fekete, B.M., Revenga, C., Todd, M., and Montgomery, M., 2011. Urban growth, climate change, and freshwater availability. PNAS, 108(15), pp. 6312-6317.

Meyer, J. L., Paul, M. J., and Taulbee, K. W., 2005. Stream ecosystem function in urbanizing landscapes. Journal of the North American Benthological Society, 24(3), pp. 602–612.

Miles, D., 2013. The interpretation, presentation, and use of tree-ring dates, Vernacular Architecture, 28(1), pp. 40-56.

Miller, O.L., Solomon, D.K., Fernandez, D.P., Cerling, T.E., and Bowling, D.R., 2014. Evaluating the use of strontium isotopes in tree rings to record the isotopic signal of dust deposited on the Wasatch Mountains, Applied Geochemistry, 50, pp. 53-65. https://doi.org/10.1016/j.apgeochem.2014.08.004

Muller, A., Osterlund, H, Marsalek, J., and Viklander, M., 2020. The pollution conveyed by urban runoff: A review of sources, Science of the Total Environment, 709.

Musgrove, M., and Banner, J.L., 2004. Controls on the spatial and temporal variability of vadose dripwater geochemistry: Edward's aquifer, central Texas, Geochimica et Cosmochimica Acta, 68(5), pp. 1007-1020.

Nadezhdina, N., Ferreira, M.I., Silvia, R., and Pacheco, C.A., 2008. Seasonal variation of water uptake of a *Quercus suber* tree in Central Portugal, Plant and Soil, 305(1-2), pp. 105-119. DOI 10.1007/s11104-007-9398-y

Nielson-Gammon, J.W., Banner, J.L., Cook, B.I., Tremaine, D.M., Wong, C.I., Mace, R.E., Gao, H., Yang, Z.-L., Flores Gonzales, M., Hoffpauir, R., Gooch, T., and Kloesel, K., 2020. Unprecedented drought challenges for Texas water resources in a changing climate: what do researchers and stakeholders need to know? Earths Future, 8(8).

Panshin, A.J. and de Zeeuw, C., 1980. Textbook of wood technology. Part 1. Formation, anatomy, and properties of wood, 11, 404.

Paul, M. J., and Meyer, J. L., 2001. Streams in the urban landscape, Annual Review of Ecology and Systematics, 32(1), pp. 333–365. https://doi.org/10.1146/annurev.ecolsys.32.081501.114040

Pearson, C., Manning, S.W., Coleman, M., and Jarvis, K., 2005. Can tree-ring chemistry reveal absolute dates for past volcanic eruptions? Journal of Archaeological Science, 32(8), pp. 1265-1274. https://doi.org/10.1016/j.jas.2005.03.007

Pearson, K., 2012. Geologic models and evaluation of undiscovered conventional and continuous oil and gas resources- Upper Cretaceous Austin Chalk, U.S. Gulf Coast. United States Geological Survey Scientific Investigations Report, pp. 2012 – 5159.

Pettersen, R.C., 1984. The chemical composition of wood, The Chemistry of Solid Wood, 207, pp. 57-126.

Phipps, R.L., 1985. Collecting, preparing, crossdating, and measuring tree increment cores, U.S. Geological Survey Water Resources Investigations Report 85-4148.

Pu, J., Cao, M., Zhang, Y., Yuan, D., and Zhao, H., 2014. Hydrochemical indications of human impact on karst groundwater in a subtropical karst area, Chongqing, China, Environmental Earth Sciences, 72, pp. 1683-1695.

Rediske, J.H. and Selders, A.A, 1953. The absorption and translocation of strontium by plants, Plant Physiology, 28(4), pp. 594-605.

Reynolds, J.H., and Barrett, H.M., 2003. A review of the effects of sewer leakage on groundwater quality. Journal of the Institution of Water & Environmental Management, 17(1), pp. 34-39.

Senison, J., Banner, J., Reyes, D., and Bendik, N., 2013. Geochemical indicators of municipal water influx into streamwater in the Bull Creek watershed, Austin, TX, Geological Society of America Annual Meeting Abstract, 45(7), pp. 667.

Sheppard, P.R. and Thompson, T.L., 2000. Effect of extraction pretreatment on radial variation of nitrogen concentration in tree rings, Journal of Environmental Quality, 29(6).

Sheppard, P.R. and Witten, M.L., 2005. Laser trimming tree-ring cores for dendrochemistry of metals, Tree-Ring Research, 61(2), pp. 87-92.

Smith, K.A., 1971. The comparative uptake and translocation by plants of calcium, strontium, barium, and radium, Plant and Soil, 34, pp. 369-379.

Smith, K.T. and Shortle, W.C., 1996. Tree biology and dendrochemistry, Tree Rings, Environment and Humanity. Radiocarbon, pp. 629-635

Stahle, D.W. and Cleaveland, M.K., 1992. Reconstruction and analysis of spring rainfall over the Southeastern U.S. for the past 1000 years, Bulletin of the American Meteorological Society, 73(12), 1947-1961. doi: 10.1175/1520 0477(1992)073<1947:RAAOSR>2.0.CO;2

Stahle, D.W., Cleaveland, M.K., and Hehr, J.G.,1988. North Carolina climate changes reconstructed from tree rings: A.D. 372 to 1985, Science, 240(4858), pp. 1517-19.

Stahle, D.W., Edmondson, J.R., Howard, I.M., Robbins, C.R., Griffin, R.D., Carl, A., Hall, C.B., Stahle, D.K., Torbenson, M.C.A., 2019. Longevity, climate sensitivity, and conservation status of wetland trees at Black River, North Carolina, Environmental Research Communications, 1(4).

Stahle, D.W. and Cleaveland, M.K., 1998. Experimental dendroclimatic reconstruction of the southern oscillation, Bulletin of the American Meteorological Society, 79(10), pp. 2137-2152. https://doi.org/10.1175/1520-0477(1998)079<2137:EDROTS>2.0.CO;2

Stewart, C.M., 1965. Excretion and heartwood formation in living trees, Science, 153(3740), pp.1068-1074.

Stowell, J.F.W., 2011. Characterization of opening mode fracture systems in the Austin Chalk. Gulf Coast Assosication of Geological Societies Transactions, 51, pp. 313-319. https://doi.org/10.1306/8626cf9b-173b-11d7-8645000102c1865d

Swanson, C.A., 1957. Translocation in trees, The Ohio Journal of Science. 57(6), pp. 331-335.

Symeonides, C., 1979. Tree-ring analysis for tracing the history of pollution: application to a study in Northern Sweden, Journal of Environmental Quality, 8(4), pp. 482-486. https://doi.org/10.2134/jeq1979.00472425000800040009x

Tang, C., Chen, J., Shindo, S., Sakura, Y., Zhang, W., and Shen, Y., 2004. Assessment of groundwater contamination by nitrates associated with wastewater irrigation: a case study in Shijiazhuang region, China, Hydrological Processes, 18(12), pp. 2303-2312.

Texas Department of Transportation TxDOT Roadways [Feature Layer], accessed July 2022 at https://gis-txdot.opendata.arcgis.com/datasets/008906d83772435bb757cb76c9644e5d/explore?location=31.008846%2C-100.055172%2C6.58

Texas Water Development Board. Water for Texas: State Water Plan, Ch. 4 Future population and water demand, 2022. https://www.twdb.texas.gov/waterplanning/swp/2022/docs/SWP22-Water-For-Texas.pdf

Tucker, C.S., Harley, G.L., Oliver, J.S., and Baird, D., 2019. *Taxodium distichum* (baldcypress) growth rings reveal origins of an 18th century Jesuit plantation, New Orleans, Louisiana, USA., Dendrochronologia, 53, pp. 95-103.

United Nations, Department of Economic and Social Affairs, Population Division. World Urbanization Prospects: The 2018 Revision, Methodology. Report No. ESA/WP.252 (New York, NY, USA, 2018).

United States Geological Survey, 1993. Quaternary geologic map of the Austin 4° x 6° quadrangle, United States. 10.3133/i1420(NH14)

United States Geological Survey, 2016. Fact Sheet 042-00. https://pubs.usgs.gov/fs/old.2000/fs-042-00/fs042-00.htm

UT-Austin, 2022. Walking Waller Creek, A self-guided tour, Office of Sustainability, University of Texas at Austin. https://sustainability.utexas.edu/walking-waller-creek

Walsh, C.J., Roy, A.H., Feminella, J.W., Cottingham, P.D., Groffman, P.M., and Morgan II, R.P.M., 2005. The urban stream syndrome: current knowledge and the search for a cure, The North American Benthological Society, 24(3), pp. 706–723.

Watmough, S.A., 2013. Calcium, strontium, and barium biogeochemistry in a forested catchment and insight into elemental discrimination, Biogeochemistry, 118, pp. 357-369.

Wong, C.I., Mahler, B.J., Musgrove, M., and Banner, J.L, 2012. Changes in sources and storage in a karst aquifer during a transition from drought to wet conditions, Journal of Hydrology, 468–469, pp. 159–172.

Wong, C.I., Kromann, J.S., Hunt, B.B., Smith, B.S., and Banner, J.L., 2014. Investigating groundwater flow between Edwards and Trinity Aquifers in Central Texas, Groundwater, 52(4), pp. 624-639.

Yanosky, T.M., Hupp, C.R., and Hackney, C.T., 1995. Chloride concentrations in growth rings of Taxodium distichum in a saltwater-intruded estuary, Ecological Applications, 5(3), pp. 785-792. https://doi.org/10.2307/1941986

Young, K., 1977. Guidebook to the Geology of Travis County, The Student Geology Society, The University of Texas. https://repositories.lib.utexas.edu/bitstream/handle/2152/63760/Guidebook to the Geology of Travis County.pdf?sequence=2&isAllowed=y

Zhang, X., 2019. The history of pollution elements in Zhengzhou, China recorded by tree rings, Dendrochronologia, 54, pp. 71-77.

Zimmerman, M.H., Brown, C.L., and Tyree, M.T., 1975. Tree Structure and Function. Chapter 4, pp. 172-174.